OUTPUT FROM MOTOR CORTEX TO CONTRALATERAL AND IPSILATERAL HINDLIMB MUSCLES IN THE PRIMATE

By

William G Messamore

B.A., University of Kansas, 2006

Submitted to the graduate degree program in Molecular and Integrative Physiology and the Graduate Faculty of the University of Kansas School of Medicine in partial fulfillment of the requirements for the degree of Doctor of Philosophy

Dissertation Committee:

_____

Paul D. Cheney, Ph.D., Chairman

_____

Jules M. Nazzaro, M.D.

_____

Randolph J. Nudo, Ph.D.

_____

Thomas J. Imig, Ph.D.

_____

John A. Stanford, Ph.D.

_____

Dianne Durham, Ph.D.

Dissertation defended: 08/31/2012

The Dissertation Committee for William G Messamore

Certifies that this is the approved version of the following dissertation:

OUTPUT FROM MOTOR CORTEX TO CONTRALATERAL AND IPSILATERAL HINDLIMB MUSCLES IN THE PRIMATE

_____

Paul D. Cheney, Ph.D., Chairman

Date approved: 09/04/2012

ABSTRACT

Although corticospinal control of the forelimb has been heavily studied for several decades, relatively little is known about corticospinal control of the hindlimb despite its importance. The overall goal of this project is to investigate hindlimb corticospinal organization and function using methods that have been successfully used to investigate the forelimb. The first two specific aims are designed to evaluate the organization and characteristics of output from primary motor cortex (M1) to hindlimb muscles using spike triggered averaging (SpTA) of electromyography (EMG) recordings. Aim one is to determine whether postspike effects can be detected in averages of EMG activity of distal and proximal hindlimb muscles. This was done by isolating single neurons in the hindlimb representation of M1 and generating averages of EMG segments associated with the individual action potentials (spikes) of each cell. The second aim is to compare the properties of hindlimb postspike effects to forelimb postspike effects collected previously in the laboratory. The third aim is to determine the extent to which poststimulus effects, elicited by stimulus triggered averaging (StTA) in distal and proximal muscles match the postspike effects from a single cell recorded at the same cortical site.

Aim four is to evaluate the organization and characteristics of output from the ipsilateral M1 to hindlimb muscles using StTA of EMG activity. In this aim, we will document the properties of poststimulus effects in hindlimb muscles from ipsilateral cortex compared to those from the contralateral cortex.

Aim five is to evaluate the function of hindlimb M1 in voluntary movement by reversibly inactivating large portions of the M1 hindlimb representation using injections of the GABA-A agonist, muscimol.

Three-hundred-seventy-one neurons in the hindlimb representation of M1 were isolated and tested with spike triggered averaging of EMG activity from twenty-two hindlimb muscles including hip, knee, ankle, digit and intrinsic foot muscles. Despite the presence of monosynaptic connections from corticospinal neurons to hindlimb motoneurons and the fact that the density of corticospinal neurons in hindlimb M1 is similar to that of forelimb M1 (Cheney et al. 2004), the effects in hindlimb muscles from M1 differed substantially from those of forelimb M1. Although the fraction of cells producing a significant postspike effect was similar for forelimb and hindlimb M1, the number of muscles with postspike effects (muscle field) per cell was markedly lower for hindlimb. Another striking difference was the much higher incidence of synchronous and complex effects, compared to true postspike effects, from hindlimb neurons compared to forelimb.

To evaluate the strength of motor output from ipsilateral M1 cortex (Aim 4), microstimuli (120 μA) were applied a low rate (5 Hz) and served as triggers to construct stimulus triggered averages of EMG activity. Post-stimulus effects from ipsilateral M1 cortex were then compared to those from contralateral cortex obtained under the same conditions. The magnitudes of contralateral effects were far greater than the magnitudes of ipsilateral effects. In addition, there were fewer effects from ipsilateral cortex obtained at the same stimulus intensity. The organization of neurons was also quite different. For all muscles, the location of maximal output from M1 was shifted anterior and laterally in the ipsilateral cortex compared to contralateral M1. Surprisingly, the minimal onset latencies of effects from ipsilateral cortex were similar to those from contralateral cortex.

In conclusion, we were able to detect clear effects in spike triggered averages of EMG activity. The output effects from single neurons in hindlimb M1 differ from those from forelimb

M1 neurons in the number and strength of effects as well as the incidence of strong synchrony effects. We used stimulus triggered averaging of EMG activity to evaluate the ipsilateral connections from M1 to motoneurons. Effects from ipsilateral cortex are distinctly weaker than those from contralateral cortex. However, the onset latency of the shortest latency effects from ipsilateral cortex were similar to those from contralateral cortex suggesting that ipsilateral cortex has a minimal linkage that is as direct as that from contralateral cortex. This result suggests that at least some corticospinal neurons in ipsilateral cortex make monosynaptic connections with motoneurons in the spinal cord. We used stimulus triggered averaging data to construct maps of cortical output to different muscle groups. Comparing ipsilateral and contralateral maps revealed that the spatial distribution of neurons producing maximal output effects from ipsilateral cortex is not a mirror image of those in contralateral cortex. Rather, the best location for producing output to a particular muscle from ipsilateral cortex is substantially displaced relative to its position in contralateral cortex. This dissertation provides foundational data on the output properties of ipsilateral cortex in healthy, intact subjects. How these properties may change in relation to recovery of function following damage to contralateral M1 cortex is a question that remains for future studies.

TABLE OF CONTENTS

PAGE

LIST OF TABLES

TABLE PAGE

LIST OF FIGURES

FIGURE PAGE

LIST OF ABBREVIATIONS

M1 .....Primary Motor Cortex

SpTA ..... Spike Triggered Average

StTA..... Stimulus Triggered Average

ICMS ..... Intracortical Microstimulation

EMG .....Electromyography

PSpF .....Postspike Facilitation

PSpS .....Postspike Suppression

GRA .....Gracilis

ADB .....Adductor Brevis

GMAX .....Gluteus Maximus

TFL .....Tensor Fasciae Latae

BFL ..... Biceps Femoris (long head)

SEM ..... Semimembranosus

SET ..... Semitendinosus

RF .....Rectus Femoris

VL .....Vastus Lateralis

VM .....Vastus Medialis

SAR ..... Sartorius

PERL .....Peroneus Longus

TA .....Tibialis Anterior

LG ..... Lateral Gastrocnemius

MG ..... Medial Gastrocnemius

SOLd ..... Distal Soleus

SOLp ..... Proximal Soleus

FDL ..... Flexor Digitorum Longus

EDL .....Extensor Digitorum Longus

FHB ..... Flexor Hallucis Brevis

EDB ..... Extensor Digitorum Brevis

AH ..... Abductor Hallucis

MRI .....Magnetic Resonance Imaging

CHAPTER 1

INTRODUCTION

Studies of the organization and function of the human brain using electrophysiological methods began with the work of scientists over one hundred and fifty years ago. In the late 19th century Paul Broca, a French physician, and Hughlings Jackson, an English neurologist, both made clinical observations that provided mounting evidence for localization of function within the human brain. Broca in observing that a lesion in the left frontal lobe of one of his patients lead to aphasia, and Jackson in observing the patterns of activation of muscle groups of patients experiencing seizures were convinced of localization of function within the human brain (Jackson 1873; Broca 1999). With the understanding of localization of function, many scientists began to develop experimental models that would help to understand the structure and function of brain regions. Gustav Fritsch and Eduard Hitzig observed in 1870 that electrical stimulation of certain regions of the cerebral cortex in dogs produced motor responses in the periphery in a discernible pattern (Fritsch and Hitzig 2009). Influenced by Jackson and wanting to extend upon the work of Fritsch and Hitzig, David Ferrier used low intensity faradic stimulation of the cortex in primates to produce a motor map and confirm some earlier thinking of Jackson (Ferrier 1874). Charles Scott Sherrington who was introduced to this field as an undergraduate medical student, later used electrical stimulation to demonstrate the fractional character elicited by stimulation, suggesting that a combination of simple movements could be used together to create a variety of movements (Leyton and Sherrington 1917). The first somatotopic maps of the human cortex were done with the aid of stimulation experiments on patients undergoing neurosurgery and were conducted by Wilder Penfield and Edwin Boldrey (Penfield and Boldrey 1937). It was a colleague of Penfield, Herbert Jasper, who in 1958 pioneered the techniques used to record from single neurons in awake animals, which were later used by Edward Evarts to investigate the properties of neurons in awake monkeys during voluntary movement (Evarts 1964). The

limitations of these studies are summed up by Penfield, "It is a far cry from the gross movement produced by cortical stimulation to the skilled voluntary performance of the hand of man or monkey. Our problem is to discover, if we can, how this cortical mechanism is utilized in the composition of such performance (Penfield and Rasmussen 1950)."

In 1967, Hiroshi Asanuma and colleagues first used intracortical microstimulation (ICMS) as a tool for evaluating the output properties of a population of neural cells in the cortex (Asanuma and Sakata 1967). ICMS became a useful tool for making detailed maps of cortical motor output. Considerable evidence supports the view that ICMS exerts its principal action through indirect, trans-synaptic excitation of corticospinal outputs and once activated these output neurons are able to influence other neurons dispersed through the cortex and accessed via long intracortical axon collaterals (Asanuma et al. 1974; Jones 1984; DeFelipe et al. 1986; Huntley and Jones 1991). Fetz and Cheney developed a new electrophysiological method for evaluating single neurons and their synaptic connections to motoneurons, referred to as spike triggered averaging (SpTA) of EMG activity (Fetz and Cheney 1980). Fetz and Cheney recorded the action potentials of individual cortical neurons and used them as triggers for computing averages of EMG activity from a number of forelimb muscles during voluntary movement. This revealed synaptic effects from single cortical neurons to forelimb motoneurons were generally not confined to a single muscle. Rather the effects from a single cortical neuron were distributed to a large number of muscles acting at a joint. Shortly afterwards, Cheney and Fetz introduced the technique of stimulus triggered averaging(StTA) (Cheney and Fetz 1985). This method consists of using microstimuli delivered at a low rate (20 Hz or less) as triggers for computing averages of EMG activity. StTA or single pulse ICMS has a number of advantages over high frequency trains of stimulation typically used with ICMS. Using single pulses allows

for activation of smaller populations of cells and thus more detailed motor maps. In addition, computing averages of EMG activity produced a more reliable and quantitative end-point measure.

Project 1: To evaluate the organization and characteristics of output from primary motor cortex (M1) to hindlimb muscles using spike triggered averaging (SpTA) of electromyography (EMG) recordings.

The function of a particular cortical area is influenced more by its extrinsic connections than the intrinsic structure (Mountcastle 1978), thus it is important to study the output properties from the motor cortex to understand its basic functions. Spike triggered averaging of EMG activity is well established as an effective method for identifying both excitatory and inhibitory linkages between forelimb motor cortex cells and motoneurons (Fetz and Cheney 1980; Kasser and Cheney 1985; Lemon et al. 1986; Fetz 1990; Davidson et al. 2007). This approach has yielded a rich new knowledge base detailing features of the synaptic organization between individual cortical cells and motoneurons of various forelimb muscles (Buys et al. 1986). It has also enabled investigation of relationships between the task-related activity of neurons and their target muscles (Griffin et al. 2008). Of the projections to spinal motoneurons 30-50 per cent originate in the primary motor cortex (Dum and Strick 1991). In addition, collaterals of single corticomotoneuronal cells appear to make connections with all or nearly all the motoneurons innervating a particular target muscles (Lawrence et al. 1985). Monosynaptic linkages are thought to be most effective in producing postspike facilitation of EMG activity, although less direct synaptic linkages can also be detected (Jankowska et al. 1976; Cheney and Fetz 1985).

These monosynaptic linkages arise from large pyramidal tract neurons, identified first by Ramon y Cajal (Ramon y Cajal 1911). The majority of pyramidal neurons are located in laminae III and V, which is a characteristic feature of the cytoarchitecture of motor cortex (Campbell 1905), (Porter and Lemon 1993). The principal spinal target of neurons in M1 is the dorsolateral part of the intermediate zone and regions of the lateral motoneuronal cell groups innervating the most distal, hand and foot muscles (Kuypers and Brinkman 1970; Coulter and Jones 1977). Jankowska investigated the action of stimulating the hindlimb area of M1 in macaques and found monosynaptic EPSPs in all motoneuronal groups investigated (Jankowska et al. 1975). Jankowska also demonstrated that corticospinal fibers make connections with Ia inhibitory interneurons producing IPSPs in motoneurons of antagonist muscles (Jankowska et al. 1976). In our laboratory, Hudson et al. showed that, compared to the forelimb, hindlimb poststimulus effects are considerably weaker across all muscle groups, especially for distal muscles (Hudson et al. 2010). Nevertheless, there is extensive evidence from intracellular recording experiments of significant monosynaptic input from primary motor cortex to hindlimb motoneurons (Jankowska et al. 1975) suggesting that spike triggered averaging of EMG activity should also be effective in detecting hindlimb synaptic linkages. If postspike effects in hindlimb muscles can be detected, it would provide a powerful and informative means of investigating the synaptic organization of single hindlimb cortical cells with motoneuron pools in comparison to the forelimb. Moreover, it would provide a means of investigating functional relationships between the activity of cells under different task conditions in relation to the activity of the cell's target muscles.

Specific Aim 1: To determine whether postspike effects can be detected in averages of EMG activity of distal and proximal hindlimb muscles.

Specific Aim 2: To compare the properties of hindlimb postspike effects to forelimb postspike effects obtained in previous studies.

Specific Aim 3: To determine the extent to which poststimulus effects in distal and proximal muscles match the postspike effects from a single cell at the same cortical site.

Project 2: To evaluate the organization and characteristics of output from the ipsilateral primary motor cortex (M1) to hindlimb muscles using stimulus triggered averaging (StTA) of electromyography (EMG) recordings.

Electrical stimulation can be used to study the outputs and linkages from the motor cortex that are available for use during natural function (Phillips and Porter 1977). Stimulus triggered averaging (StTA) of EMG activity is well established as an effective method for identifying both excitatory and inhibitory linkages between motor cortex cells and motoneurons (Kasser and Cheney 1985). Divergence to different muscles can also be detected in the averages of EMG (Cheney and Fetz 1985). Using this approach, work from our laboratory has yielded new knowledge of the synaptic organization between cortical cells and motoneurons of forelimb and hindlimb muscles (Park et al. 2001; Boudrias et al. 2006; Griffin et al. 2009; Hudson et al. 2010). Although output effects on muscle activity from contralateral primary motor cortex (M1) have been extensively documented using a variety of methods, studies of output effects from ipsilateral cortex have been much more limited.

Leyton and Sherrington were among the first to observe ipsilateral degeneration in the spinal cord following a unilateral lesion in the arm area of the motor cortex (Leyton and Sherrington

1917). Approximately 10% of the corticospinal axons have been shown anatomically to descend ipsilaterally in the spinal cord (Hutchins et al. 1988; Dum and Strick 1996; Lacroix et al. 2004). Unit recording studies have demonstrated that about 10% of neurons are modulated exclusively with ipsilateral limb movements (Matsunami and Hamada 1978; Tanji et al. 1988; Aizawa et al. 1990) and functional magnetic resonance imaging (fMRI) studies consistently show bilateral activation of motor cortex with unilateral limb movements (Cramer et al. 1999). A small proportion of cortical cells discharge with a wrist extension movement of only the ipsilateral limb (Evarts 1966; Goldring and Ratcheson 1972), and a small portion of cells discharge with movement of either the contralateral or ipsilateral hand (Lemon et al. 1976; Matsunami and Hamada 1978). In these cases pre-movement lead time of ipsilateral cells was similar to that for cells with exclusively contralateral associations (Lemon et al. 1976). Ipsilateral deficits associated with hemiparetic stroke demonstrate the potential functional importance of the ipsilateral motor cortex (Lewis and Brindley 1965; Colebatch and Gandevia 1989; Yarosh et al. 2004). Further evidence of the importance of the ipsilateral cortex in recovery from stroke is evident from bilateral pyramidotomy, which produces more dramatic deficits than a unilateral lesion alone (Porter and Lemon 1993). Also recovery of a patient from a unilateral section of the pyramidal track was partially attributed to intact ipsilateral connections (Bucy et al. 1964). There is also growing evidence for reorganization of the ipsilateral pathways following damage to the motor cortex (Chollet et al. 1991; Fisher 1992). Repetitive transcranial magnetic stimulation (rTMS) experiments have demonstrated that ipsilateral M1 is involved in fine motor tasks (Chen et al. 1997). Moreover, fMRI and TMS studies in patients with hemiparetic stroke show a compensatory recruitment of the ipsilateral corticospinal tract (Caramia et al. 2000; Feydy et al. 2002). Despite the potential functional and clinical importance of the ipsilateral

corticospinal projection (Brus-Ramer et al. 2007; Rosenzweig et al. 2009), relatively little is known about the functional properties of this projection.

Specific Aim 4: To document the properties of poststimulus effects in hindlimb muscles from ipsilateral cortex compared to those from the contralateral cortex.

Specific Aim 5: To evaluate the effect of selectively and reversibly inhibiting portions of the M1 hindlimb representation using injections of the GABA-A agonist muscimol.

Significance

The organization and mechanisms underlying the normal and dysfunctional cortical control of movement is a topic of scientific and clinical importance. Development of new and effective treatments for movement disorders, like stroke, rely on a better understanding of the mechanisms that underlie normal cortical control of movement and recovery of function following injury (Ward 2005). Although the cortical control of the arm and hand in primates has been the focus of a number of electrophysiological studies for many years, comparatively little is known about the cortical control of the leg and foot. The results of these studies will build upon our understanding of the normal control and function of the contralateral and ipsilateral hindlimb representation in primary motor cortex. This knowledge will provide a foundation for better understanding loss of function as well as plasticity and recovery of function after injury. As Porter and Lemon suggest, the qualitative study of associations between the discharges of single, identified neurons and measured aspects of movement performance would be the most fruitful approach to the study of function in the motor cortex (Porter and Lemon 1993).

Evolution of the motor cortex from monkeys to the great apes, including man, has led to far more corticomotoneuronal projections which correlate with increased dexterity and fractionated movements. Maturation of these projections occurs postnatally and coincides with relatively independent finger movements (Kuypers 1962; Heffner and Masterton 1983; Bortoff 1990; Eyre et al. 1991). Getting a clear and more complete understanding of the corticospinal tract is important because "its structure and organization serve as a guide to understanding what the output from the cortex means for the motor apparatus of the limb (Porter and Lemon 1993)."

CHAPTER 2

OUTPUT EFFECTS ON HINDLIMB MUSCLES ASSESED WITH SPIKE TRIGGERED AVERAGING OF EMG ACTIVITY FROM INDIVIDUAL CORTICAL CELLS

INTRODUCTION

Stimulus-triggered averaging of EMG activity has a number of advantages compared to macrostimulation techniques in that it is normally done with awake animals performing a specific behavioral task, thus eliminating the confounding effects of anesthetics. A limitation of intracortical microstimulation, however, is that despite the low rate and magnitude of stimulation a population of cells is inevitably activated, for instance, as many as 4 large pyramidal tract neurons (PTNs) and 800 small PTNs for a 20μA stimulus intensity (Cheney and Fetz 1985; Tehovnik et al. 2006). Spike triggered averaging of EMG activity is done with recording only and eliminates the need for electrical stimulation. Because the trigger events are the spikes of single neurons, SpTA has the potential to reveal the synaptic linkages between single cells whose spikes are being used as triggers and motoneurons of the recorded muscles. Spike triggered averaging of EMG activity is well established as an effective method for identifying both excitatory and inhibitory linkages between forelimb motor cortex cells and motoneurons (Fetz and Cheney 1980; Kasser and Cheney 1985; Schieber and Rivlis 2005). We predict that spike triggered averaging of EMG activity will also be capable of detecting synaptic linkages between motor cortex cells and motoneurons of hindlimb muscles.

The magnitude of PStF in averages of EMG from hindlimb muscles is much weaker than forelimb PStF at the same intensity (Hudson et al. 2010). Forelimb movements, especially the movements of the hand and digits are highly skilled and involve individuated movements. Evidence suggests that these individuated movements require monosynaptic connections between neurons in the motor cortex and motoneurons (Lemon and Griffiths 2005). However movements of the hindlimb and foot are less diverse and more stereotyped, and normally appear

to lack the more complex individuated movements. Previous work from our laboratory has shown that cortical poststimulus effects are much weaker in hindlimb muscles compared to forelimb muscles. The average magnitude of EPSPs in hindlimb muscles from cortical stimulation is also smaller than EPSPs in forelimb muscles (Clough et al. 1968; Jankowska et al. 1975). Accordingly, we predict that postspike effects in hindlimb muscles, although detectable, will be weaker than in forelimb muscles.

MATERIALS AND METHODS

Our methods conformed to the procedures outlined in the Guide for the Care and Use of Laboratory Animals published by the U.S. Department of Health and Human Services and the National Institutes of Health.

Behavioral Task

Three male rhesus macaques (Macaca mulatta) were trained to perform a hindlimb push-pull task as described previously (Hudson et al. 2010). Inside a sound-attenuated chamber, the monkey was seated in a custom-built primate chair facing a computer monitor providing visual feedback. Both of the monkey's forelimbs were comfortably restrained, as well as the monkey's left hindlimb, while the task was performed with the right hindlimb. The task consisted of the monkey grasping a manipulandum with its right hindlimb and pushing the manipulandum to a desired length against the elastic force of a spring. The manipulandum was then held there for a preprogrammed length of time (750ms) before triggering a food reward delivered to a lick plate at the monkey's mouth. The monkey then pulled the manipulandum back against the elastic force of a spring to a different length for a preprogrammed length of time (750ms) before receiving an additional reward and the sequence was repeated (Figure 1). The task was designed to produce broad activation of both proximal and distal hindlimb muscles making it an ideal model for testing the output properties of cortical cells and target muscles using spike triggered averaging of EMG activity. Figure 2 shows representative EMG records for all implanted muscles for two cycles of the push and pull task.

Surgical Procedures

For all surgeries, as a prophylactic measure against infection, the monkey was treated with injectable liquid penicillin (6000 U/kg) on the day before surgery, the day after surgery and at three days after surgery. The monkeys were tranquilized with ketamine (10 mg/kg) for transport and anesthetized with isoflurane gas. Atropine (0.04 mg/kg) was given to reduce secretions and prevent bradycardia. The monkey's forelimb, neck, back, hip, hindlimb and foot were shaved and scrubbed (Betadine: 10% povidone-iodine). Temperature, blood pressure, EKG, and blood oxygenation were monitored.

Cortical Chamber Implant

An MRI was done on each monkey to determine the optimal placement for the cortical chamber based on the monkey's cortical anatomy. Using the intersection of the central sulcus and superior sagittal sinus as a general anatomical landmark, the chambers were centered over the midline and positioned stereotaxically at 14.5mm anterior (10 mm anterior to the landmark). This location provides access to the hindlimb representation of M1 in both hemispheres (Figure 3). A 30mm diameter craniotomy was performed and a titanium cortical chamber was attached to the skull using dental acrylic held in place by 12 titanium screws. A restraining head bar was also attached at this time with dental acrylic and an additional 12 titanium screws. The head bar provided a flexible restraint to limit head movements during cortical recordings.

EMG Modular Subcutaneous Implant

Two small incisions (5 mm) were made approximately half way between the shoulder and the elbow on the lateral surface of the proximal forelimb. This incision was the entry point for the wires running subcutaneously to the hindlimb. A vertical incision (~4 cm) was made on the back near the midpoint between the shoulder blades. This incision functioned first as a turning point for the subcutaneous tunneling of wires from the forelimb to the hindlimb, and second, as a final anchoring point of the wires. Pairs of wires were tunneled subcutaneously through these incisions on the forelimb to the individual target muscles.

The modular implant uses single layer connector modules (ITT, Cannon) that can be affixed to the skin with medical adhesive tape as described by Park et al. (Park et al. 2000). Forty-four multi-stranded stainless steel wires were cut to lengths appropriate for the 22 pairs of EMG wires to be implanted. Twenty-two muscles were selected for implantation. These muscles spanned three joints and were a mix of abductors, adductors, flexors, and extensors (Figure 4). The wires were divided into four modules based on the muscles to be implanted: proximal-lateral (GMAX, SEM, GRA, BFL, SET), proximal-medial (ADB, VM, SAR, RF, TFL, VL), distal-lateral (EDB, EDL, PERL, SOLd, SOLp, LG) and distal-medial (MG, FDL, TA, FHB, AH). Connectors were constructed as described by Park et al. (Park et al. 2000) and the wires were color coded to make identification and implantation more efficient.

Pairs of wires were tunneled subcutaneously through the previously described incisions on the forelimb to the individual target muscles. Custom designed needles, fabricated from stainless steel rods were used to tunnel the EMG wires. Each needle had a sharpened tip with a non-cutting edge. The opposite end was flattened with 3 to 5 eyes. The wires were threaded through the eyes and folded back for tunneling under the skin. Wires were tunneled to their target muscles following a detailed routing plan (Figures 5 and 6).

After tunneling, each wire was cut to length, leaving 6-7 cm exteriorized at the target muscle site. For each wire, 2-3 mm of insulation was removed from the tip. Each wire was then back fed into a 22-gauge hypodermic needle and folded back along the shaft of the needle. The wire was then inserted into the muscle in a proximal direction through the same puncture incision in the skin used for tunneling. The wire was then held at its entry point into the skin and the needle was removed leaving the EMG wire embedded in the muscle belly. Two wires were inserted in each muscle with a separation of approximately 5 mm. Electrical stimulation through the electrode pair was used to confirm proper placement as described previously (Hudson et al. 2010). A loop of wire remained exteriorized until confirmation of proper placement in the target muscle. The wires were then pulled centrally from the opening on the back until the loop disappeared under the skin.

Surgical Follow-up

Following surgery, the monkey was closely monitored until it was fully awake and able to sit and stand without assistance. Post-operative analgesics (buprenorphine, 0.01 mg/kg) were given for 3 days. Wound edges around the cortical chamber were inspected daily and treated with topical antibiotic. Surgeries were performed in a facility accredited by the Association for Assessment and Accreditation of Laboratory Animal Care using full sterile procedures.

Recording

EMG activity, cortical neural activity, and task-related signals were all monitored using Cambridge Electronic Design Spike2 software running custom scripts developed for our laboratory (Spike2 Neural Averager). EMGs and task-related activity were digitized at a rate of 8kHz; cortical neural activity and the stimulus current monitor signal were digitized at a rate of

16kHz. A manual hydraulic microdrive attached to the cortical chamber was used to lower glass insulated platinum-iridium electrodes into layer V of M1 in the hindlimb representation area. The unit signal was processed through an Alpha-Omega Multi-spike Detector for isolation of individual units. A TTL pulse output from the spike detector was used to the trigger the Spike2 software. The Spike2 data provided a continuous recording across all channels of each day's recording session. This data could be used to monitor signals on-line to confirm the quality of the EMG recordings and also offline for computation of spike triggered averages. Spike triggered averages of EMG activity were computed on-line using custom Windows Averager software (Larry Shupe, Seattle, WA). Averages were obtained for all 22 implanted muscles over a 320ms epoch, including 160ms before the trigger to 160ms after the trigger and a minimum of 4000 trigger events. Evaluation of postspike facilitation and postspike suppression was done using both the Windows Averager Software and Spike2 Neural Averager software. For stimulus triggered averages, microstimuli (30, 60, and 120 μA at 5 Hz) were applied through the recording microelectrode. Stimulus triggered averages were obtained for all 22 implanted muscles over a 200ms epoch, including 40ms before the trigger to 160ms after the trigger and a minimum of 2000 trigger events.

RESULTS

Detecting postspike effects in averages of EMG

Table 1 provides a summary of the spike triggered averaging data collected from two adult male rhesus macaque monkeys. 371 individual cells were isolated from M1 hindlimb cortex and recorded along with EMG data from monkeys awake and performing the hindlimb push-pull task. An example of an isolated cell that was modulated with the task and corresponding EMG activity is shown in Figure 9. Cells that were well modulated during the task were preferentially targeted for isolation and recording. Two-hundred-thirteen of these cells produced at least one effect in spike triggered averages. The majority of these (101) produced effects in both proximal and distal muscles. In addition, there was a fairly even distribution of cells that produced only proximal or only distal effects (67 proximal; 45 distal). Postspike effects where classified as one of five different effect types, shown in Figure 7. There were 101 pure postspike facilitation effects (PSpF), revealed by a transient increase in the firing probability of the recorded motoneurons, and 19 pure postspike suppression effects (PSpS), revealed by a transient decrease in the firing probability of recorded motoneurons. Seven-hundred-forty effects were classified as complex. These included 333 synchronous facilitation effects (transient increase in firing probability but the onset was too short to be consistent with a direct linkage), 65 synchronous suppression effects (transient decrease in firing probability but the onset was too short to be consistent with a direct linkage), and 342 synchronous oscillation effects (cyclical effects resembling a dampening sine wave). The distribution of effects in spike triggered averages organized by joint and muscle is shown in Figure 8.

Comparison of hindlimb postspike effects to forelimb postspike effects

Table 2 compares our data set to forelimb M1spike triggered averaging data obtained previously in our laboratory (McKiernan et al. 1998). The forelimb data shows a greater number of postspike effects per cell in cells showing at least one effect (3.08 effects/cell for forelimb M1; 1.45 effects/cell for hindlimb) (Figure 12). Unlike the hindlimb, the forelimb data produced more cells showing effects exclusively in distal muscles (46% of cells for forelimb; 21% of cells for hindlimb). The hindlimb data shows a much higher incidence of complex effects compared to forelimb data (86% of effects for hindlimb; 27% of effects for forelimb), including synchronous oscillation effects that were exclusively found in spike triggered averages from the hindlimb M1.

Characterization of output effects

The magnitudes, onset latencies, and peak latencies of the pure postspike effects are given in Tables 3 and 4. All but 10 of the 101 PSpF effects detected were relatively small magnitude effects (<10 percent peak increase over baseline). Histograms showing the magnitude of pure PSpF by muscle group are shown in Figure 10 along with the mean, standard deviation, median, mode, and range of magnitudes. Unlike the forelimb the average magnitude of PSpF for each hindlimb muscle group does not show an increase in magnitude when moving from proximal to distal muscles. The onset latencies of the majority of hindlimb effects were particularly long, 8ms or longer than latencies reported for the early facilitation peaks in stimulus triggered averages from hindlimb M1, which ranged from 10ms in proximal muscles to 16ms in distal muscles (Hudson et al. 2011). However, there were 25 PSpF effects that had onset latencies that were comparable to the early peak in stimulus triggered averages for corresponding muscles. Histograms showing the different onset latencies of pure PSpF for each muscle group are shown in Figure 11 along with the mean, standard deviation, median, mode, and range of

onset latencies. The distribution and characteristics of these effects for each muscle group are given in Table 5.

Table 5 is a comparison of the pure PStF effects about three joints in the forelimb and the hindlimb, as well as, the PStS effects from the distal hand and foot muscles. The magnitudes of PSpF effects in the forelimb are 30-50% greater than the magnitudes of PSpF effects in the hindlimb. The mean onset latencies of the forelimb PSpF effects are close to the minimum conduction time through the pathway, whereas the mean onset latencies for the hindlimb PSpF effects are 8ms or more than the minimum conduction time through the pathway with a much broader standard deviation.

Figure 13 shows postspike effects that have relatively short latencies and poststimulus effects obtained at the same site. Sixty microamp stimulus triggered averages computed at the sites where these cells were recorded show effects that are similar to those in the spike triggered averages. 73% of these pure PSpF effects have onset latencies and spike characteristics (sign, peak latency, and spike duration) that are similar to those in the stimulus triggered averages. Postspike effects with longer latencies are not as consistently matched to poststimulus effects at the same site.

DISCUSSION

Spike triggered averaging of EMG activity from cells in the hindlimb representation of primary motor cortex (M1) revealed detectable postspike effects. These effects were less frequent than effects reported for spike triggered averaging from cells in the forelimb representation of M1. The mean magnitude of effects in hindlimb were relatively uniform across all three joints, unlike the forelimb where a consistent increase in magnitude occurs in going from proximal to more distal muscles. The more stereotyped movements of the hindlimb and less diverse repertoire of movements may require a less prominent role of monosynaptic connections than what is required for forelimb where fractionation of digits movements is critical for effective use of the hand. PSpF in hindlimb M1 was weaker and less diverse than effects in forelimb M1. This difference is especially prominent when comparing intrinsic foot and intrinsic hand muscles. In addition, synchrony effects were much more common for hindlimb M1. Our results correlated with the fact that hindlimb EPSP size is also smaller than that of forelimb EPSP size (Jankowska et al. 1975). This difference in EPSP magnitude is likely to contribute to the weaker hindlimb postspike effects compared to forelimb M1. Similarly, poststimulus effects in hindlimb muscles are also weaker than effects in forelimb muscles (Hudson et al. 2011). The muscle field size for cells isolated in hindlimb M1 was considerable smaller than the muscle field size for cells isolated in forelimb M1. This may be due in part to weaker hindlimb PSpF.

Although some effects had latencies similar to short latency PStF, most had latencies that were significantly longer. Effects that show latencies longer than poststimulus facilitation are likely to be mediated by oligosynaptic linkages and/or slow conducting cortical cells. Another striking difference between hindlimb and forelimb effects is the increased number of synchrony effects observed in spike triggered averages from cells in hindlimb M1. These synchrony effects

suggest that synchronous firing of hindlimb corticospinal cells during movement tasks in awake freely behaving monkeys is much more prominent than in the forelimb. This may be associated with the more stereotyped movements in the hindlimb, and less reliance on fractionation of movements. Comparable patterns of muscle facilitation in StTAs and SpTAs computed at the same cortical site has been reported for forelimb M1 (Cheney and Fetz 1985). In the hindlimb, seventy-three percent of pure PSpF effects with onset latencies in monosynaptic ranges (10-16ms) showed matching PStF from a cell recorded at the same site. However, this represents only 25% of the total pure PSpF effects. Moreover, PSpF effects with longer latencies did not show matching PStF at the same site. This suggests an organization in which neighboring corticospinal neurons are less likely to have similar target muscles than in forelimb M1 cortex.

Table 1. Summary of Spike Triggered Averaging Data Collected

	Monkey E	Monkey M	Total
Cells tested during push - pull task	221	150	371
Cells with one or more effects in spike triggered averages	137 (62%)	76 (51%)	213 (57%)
Cells with effects on proximal muscles only	35 (26%)	32 (42%)	67 (31%)
Cells with effects on distal muscles only	24 (18%)	21 (28%)	45 (21%)
Cells with effects on proximal and distal muscles	78 (57%)	23 (30%)	101 (47%)
Total postspike effects	66 (10%)	54 (30%)	120 (14%)
PSpF	57 (86%)	44 (81%)	101 (84%)
PSpS	9 (14%)	10 (19%)	19 (16%)
Total complex effects	616 (90%)	124 (70%)	740 (86%)
Synchrony PSpF	249 (40%)	84 (68%)	333 (45%)
Synchrony PSpS	40 (6%)	25 (20%)	65 (9%)
Synchrony Oscillation	327 (54%)	15 (12%)	342 (46%)

Table 2. Comparison of effects in spike triggered averages of EMG activity from cells in hindlimb versus forelimb M1

	Hindlimb M1	Forelimb M1*
Cells tested during push-pull task/reach-to-grasp task	371	174
Cells with one or more effects in spike triggered averages	213 (57%)	112 (64%)
Cells with effects in proximal muscles only	67 (31%)	11 (10%)
Cells with effects in distal muscles only	45 (21%)	51 (46%)
Cells with effects in proximal and distal muscles	101 (47%)	50 (45%)
Total pure postspike effects	120 (14%)	345 (73%)
PSpF	101 (84%)	244 (71%)
PSpS	19 (16%)	101 (29%)
Total complex effects	740 (86%)	128 (27%)
Synchrony PSpF	333 (45%)	56 (44%)
Synchrony PSpS	65 (9%)	72 (56%)
Synchrony Oscillation	342 (46%)	N/A

*Data from (McKiernan et al., 1998)

Table 3. Characteristics of Monkey E postspike effects

Monkey E

PStF

	Magnitude, %				Onset Latency, ms				Peak Latency, ms			
Joint	n	Mean		SD	n	Mean		SD	n	Mean		SD
Hip	7	12.5	±	13.4	7	28.4	±	14.7	7	32.3	±	16.6
Knee	16	4.7	±	1.5	16	19.7	±	8.1	16	22.7	±	8.5
Ankle	15	5.9	±	3.7	15	26.1	±	11.6	15	29.2	±	11.9
Digit	10	3.9	±	1.9	10	22.4	±	9.6	10	25.1	±	9.7
Intrinsic	9	4.6	±	3.5	9	31.9	±	14.6	9	33.7	±	14.8
Total	57	5.8	±	6.0	57	24.9	±	12.2	57	27.8	±	12.6

PStS

	Magnitude, %				Onset Latency, ms				Trough Latency, ms			
Joint	n	Mean		SD	n	Mean		SD	n	Mean		SD
Hip	0				0				0			
Knee	5	-3.1	±	1.2	5	17.4	±	3.4	5	20.7	±	4.0
Ankle	3	-10.0	±	5.9	3	27.0	±	11.4	3	31.3	±	10.2
Digit	1	-1.7			1	20.0			1	22.0		
Intrinsic	0				0				0			
Total	9	-5.2	±	4.9	9	20.9	±	8.3	9	24.4	±	8.2

Table 4. Characteristics of Monkey M postspike effects

Monkey M

PStF

	Magnitude, %				Onset Latency, ms				Peak Latency, ms			
Joint	n	Mean		SD	n	Mean		SD	n	Mean		SD
Hip	9	4.0	±	2.0	9	14.9	±	6.0	9	16.8	±	5.8
Knee	21	6.8	±	3.2	21	20.6	±	7.9	21	23.3	±	8.2
Ankle	9	5.8	±	4.1	9	21.0	±	5.5	9	23.0	±	5.7
Digit	1	3.8			1	34.8			1	36.1		
Intrinsic	4	4.5	±	1.5	4	26.8	±	19.4	4	28.4	±	19.7
Total	44	5.7	±	3.3	44	20.4	±	9.6	44	22.7	±	9.8

PStS

	Magnitude, %				Onset Latency, ms				Trough Latency, ms			
Joint	n	Mean		SD	n	Mean		SD	n	Mean		SD
Hip	1	-4.1			1	8.8			1	9.2		
Knee	4	-5.0	±	2.9	4	23.1	±	7.1	4	24.9	±	7.4
Ankle	1	-6.3			1	43.6			1	45.9		
Digit	2	-2.8	±	0.8	2	16.7	±	3.8	2	20.0	±	4.9
Intrinsic	2	-6.6	±	3.4	2	30.4	±	5.4	2	32.3	±	6.1
Total	10	-4.9	±	2.7	10	23.9	±	10.5	10	25.9	±	10.8

Table 5. Characteristics of all postspike effects

Total

PStF

Joint	Magnitude, % n	Mean		SD	Onset Latency, ms n	Mean		SD	Peak Latency, ms n	Mean		SD
Hip	16	7.7	±	9.9	16	20.8	±	12.7	16	23.6	±	14.1
Knee	37	5.9	±	2.8	37	20.2	±	8.0	37	23.1	±	8.3
Ankle	24	5.8	±	3.8	24	24.2	±	10.1	24	26.9	±	10.5
Digit	11	3.9	±	1.8	11	23.5	±	9.8	11	26.1	±	9.7
Intrinsic	13	4.6	±	3.0	13	30.3	±	16.4	13	32.1	±	16.6
Total	101	5.8	±	5.0	101	22.9	±	11.4	101	25.5	±	11.8

PStS

Joint	Magnitude, % n	Mean		SD	Onset Latency, ms n	Mean		SD	Trough Latency, ms n	Mean		SD
Hip	1	-4.1			1	8.8			1	9.2		
Knee	9	-3.9	±	2.3	9	19.9	±	6.1	9	22.6	±	6.1
Ankle	4	-9.1	±	5.3	4	31.2	±	12.2	4	34.9	±	10.9
Digit	3	-2.4	±	0.8	3	17.8	±	3.5	3	20.6	±	4.1
Intrinsic	2	-6.6	±	3.4	2	30.4	±	5.4	2	32.3	±	6.1
Total	19	-5.1	±	3.9	19	22.5	±	9.7	19	25.2	±	9.7

Table 6. Comparison of the magnitude of effects in spike triggered averages of EMG activity from cells in hindlimb versus forelimb M1

PSpF

	Magnitude, %						
	Hindlimb				Forelimb*		
Joint	n	Mean		SD	n	Mean		SD
Knee/Elbow	37	5.9	±	2.8	24	7.8	±	4.0
Ankle and Digits/Wrist and Digits	35	5.2	±	3.5	74	8.0	±	3.4
Intrinsic Foot/Intrinsic Hand	13	4.6	±	3.0	20	9.2	±	4.3

PSpS

	Magnitude, %						
	Hindlimb				Forelimb*		
Joint	n	Mean		SD	n	Mean		SD
Foot Muscles/Hand Muscles	9	-6.3	±	4.9	28	-7.8	±	4.0

*Data from (McKiernan et al., 1998)

Table 7. Comparison of the onset latency of effects in spike triggered averages of EMG activity from cells in hindlimb versus forelimb M1

PSpF

	Onset Latency, ms							
	Hindlimb				Forelimb*			
Joint	n	Mean		SD	n	Mean		SD
Knee/Elbow	37	20.2	±	8.0	24	7.7	±	2.6
Ankle and Digits/Wrist and Digits	35	24.0	±	10.0	74	8.6	±	2.8
Intrinsic Foot/Intrinsic Hand	13	30.3	±	16.4	20	9.5	±	2.8

PSpS

	Onset Latency, ms							
	Hindlimb				Forelimb*			
Joint	n	Mean		SD	n	Mean		SD
Foot Muscles/Hand Muscles	9	26.5	±	10.7	28	11.1	±	2.8

*Data from (McKiernan et al., 1998)

Table 8. Comparison of the peak/trough latency of effects in spike triggered averages of EMG activity from cells in hindlimb versus forelimb M1

PSpF

	Peak Latency, ms							
	Hindlimb				Forelimb*			
Joint	n	Mean	±	SD	n	Mean	±	SD
Knee/Elbow	37	23.1	±	8.3	24	9.8	±	2.9
Ankle and Digits/Wrist and Digits	35	26.6	±	10.3	74	11.1	±	3.0
Intrinsic Foot/Intrinsic Hand	13	32.1	±	16.6	20	12.9	±	2.9

PSpS

	Trough Latency, ms							
	Hindlimb				Forelimb*			
Joint	n	Mean	±	SD	n	Mean	±	SD
Foot Muscles/Hand Muscles	9	29.6	±	10.4	28	13.3	±	2.6

*Data from (McKiernan et al., 1998)

Figure 1. Hindlimb push-pull task (adapted from Hudson, 2010). The task consisted of the monkey grasping a manipulandum with their right hindlimb and pushing the manipulandum to a desired length against the elastic force of a spring. The manipulandum was then held there for a preprogrammed length of time (750ms) before triggering a food reward delivered to a lick plate at the monkey's mouth. The monkey then pulled the manipulandum back against the elastic force of a spring to a different length for a preprogrammed length of time (750ms) before receiving an additional reward and the sequence was repeated.

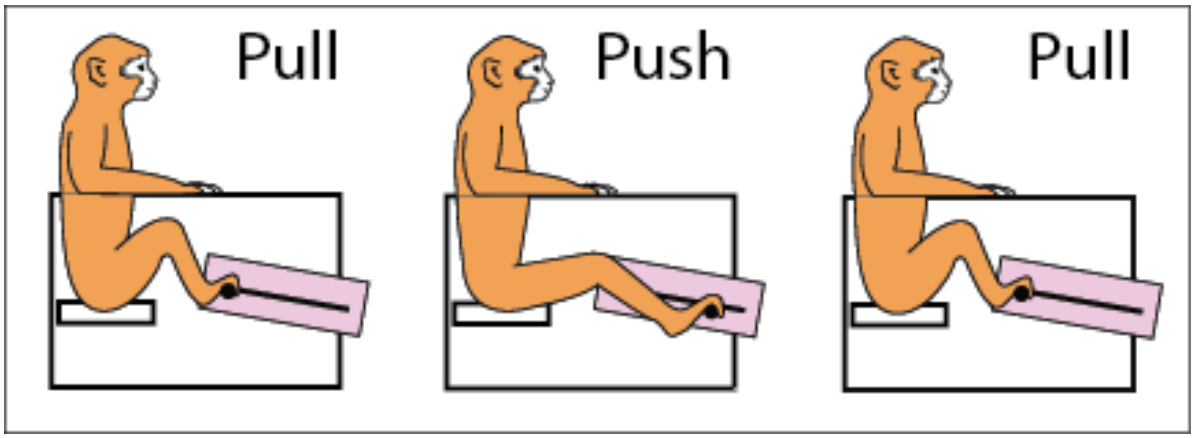
Pull
Push
Pull

Figure 2. Muscle activity during task performance. The left panel shows raw, unprocessed EMG recordings during two cycles of the push-pull task. The task provides a solid baseline EMG in all muscles for doing spike and stimulus triggered averages. The right panel shows the same EMG, but full wave rectified and low pass filtered.

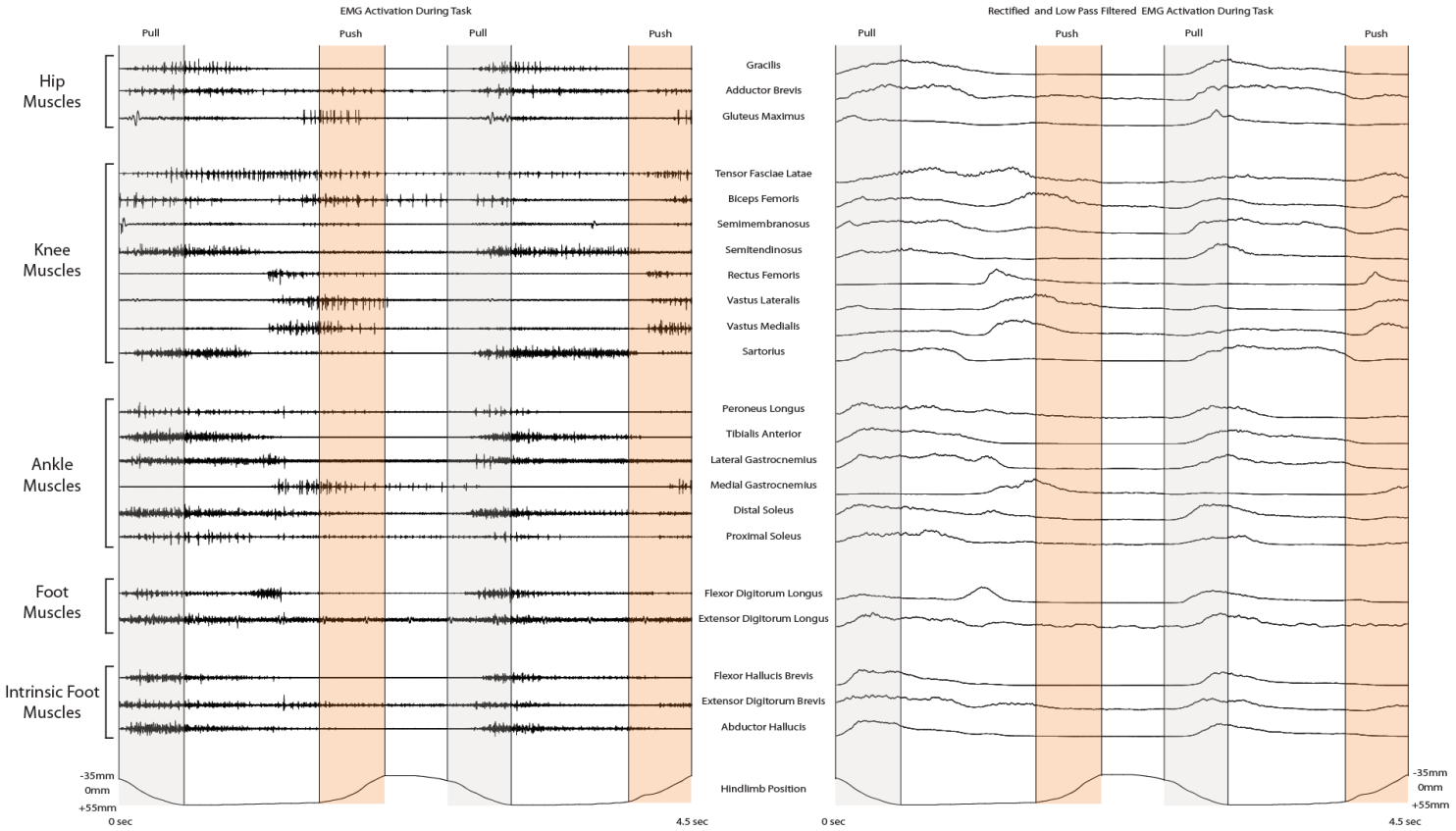
EMG Activation During Task
Rectified and Low Pass Filtered EMG Activation During Task
Pull
Push
Pull
Push
Hip Muscles
Knee Muscles
Ankle Muscles
Foot Muscles
Intrinsic Foot Muscles
Gracilis
Adductor Brevis
Gluteus Maximus
Tensor Fasciae Latae
Biceps Femoris
Semimembranosus
Semitendinosus
Rectus Femoris
Vastus Lateralis
Vastus Medialis
Sartorius
Peroneus Longus
Tibialis Anterior
Lateral Gastrocnemius
Medial Gastrocnemius
Distal Soleus
Proximal Soleus
Flexor Digitorum Longus
Extensor Digitorum Longus
Flexor Hallucis Brevis
Extensor Digitorum Brevis
Abductor Hallucis
Hindlimb Position
-35mm
0mm
+55mm
0 sec
4.5 sec

Figure 3. Cortical chamber implant for Monkey L. Placement of the cortical chamber along the midline allows easy access to the hindlimb M1 representation of both hemispheres. The solid line runs posterior (P) to anterior (A) along the superior sagittal sinus. The dashed lines trace the central sulcus for both the contralateral (upper) and ipsilateral (lower) hemispheres. Inside diameter of the chamber is 30 mm.

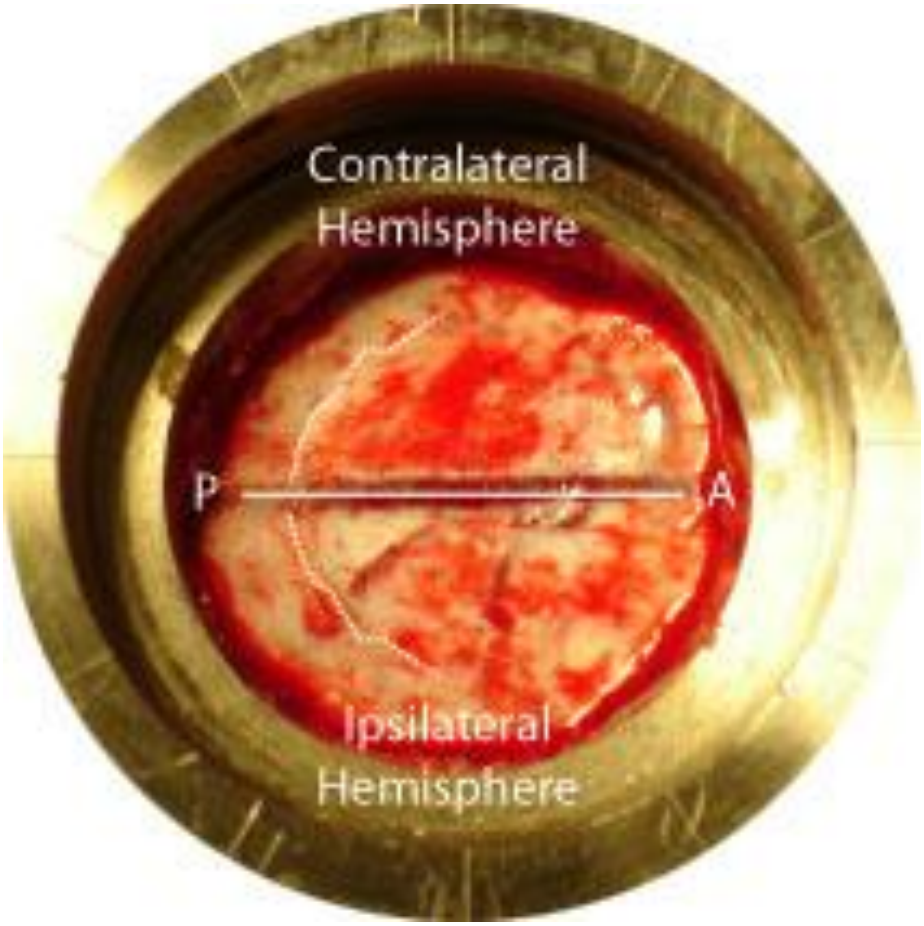
Contralateral
Hemisphere
P
A
Ipsilateral
Hemisphere

Figure 4. Muscles selected for EMG implantation. The wires were divided into four modules based on the muscles to be implanted: proximal-lateral (GMAX, SEM, GRA, BFL, SET), proximal-medial (ADB, VM, SAR, RF, TFL, VL), distal-lateral (EDB, EDL, PERL, SOLd, SOLp, LG) and distal-medial (MG, FDL, TA, FHB, AH).

Muscle Selection

Hip Muscles	Knee Muscles	Ankle Muscles
Gracilis (GRA)	Tensor Fasciae Latae (TFL)	Peroneus Longus (PERL)
Adductor Brevis (ADB)	Biceps Femoris (BFL)	Tibialis Anterior (TA)
Gluteus Maximus (GMAX)	Semimembranosus (SEM)	Lateral Gastrocnemius (LG)
	Semitendinosus (SET)	Medial Gastrocnemius (MG)
	Rectus Femoris (RF)	Distal Soleus (SOLd)
	Vastus Lateralis (VL)	Proximal Soleus (SOLp)
	Vastus Medialis (VM)	
	Sartorius (SAR)	

Digit Muscles	Intrinsic Foot Muscles
Flexor Digitalis Longus (FDL)	Flexor Hallucis Brevis (FHB)
Extensor Digitalis Longus (EDL)	Extensor Digitorum Brevis (EDB)
	Abductor Hallucis (AH)

Figure 5. Lateral leg tunneling layout. Wires were color coded and tunneled to their target muscles along the pre-planned route. The wires were divided into four modules based on the muscles to be implanted. The two lateral modules were proximal-lateral (GMAX, SEM, GRA, BFL, SET) and distal-lateral (EDB, EDL, PERL, SOLd, SOLp, LG). Color coding the EMG wires allowed for fast identification of wires to be implanted from individual groups. The diagram is overlaid onto a digitally processed photo of a rhesus macaque hindlimb dissection.

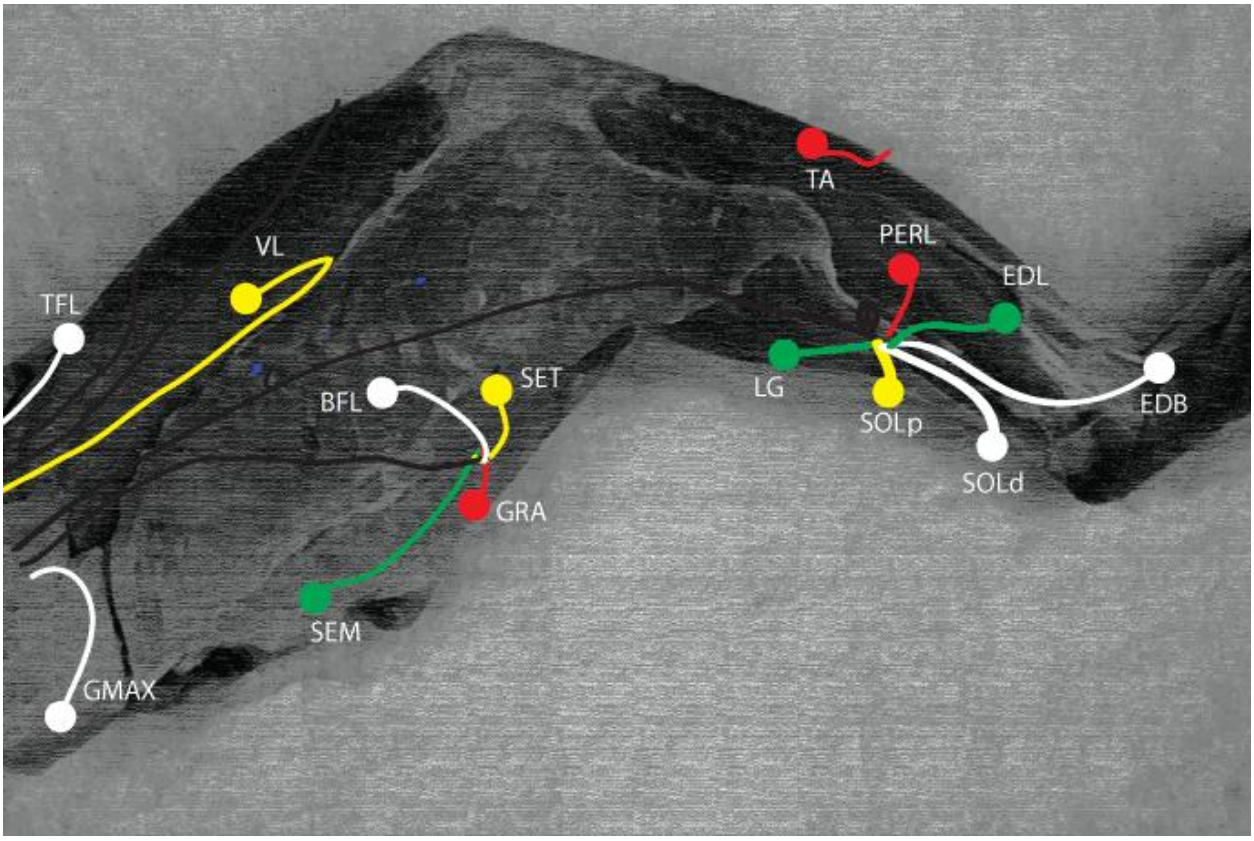
TA
PERL
EDL
VL
TFL
LG
SET
BFL
SOLp
EDB
SOLd
GRA
SEM
GMAX

Figure 6. Medial leg tunneling layout. Wires were color coded and tunneled to their target muscles along a pre-planned route. The wires were divided into four modules based on the muscles to be implanted. The two medial modules were proximal-medial (ADB, VM, SAR, RF, TFL, VL) and distal-medial (MG, FDL, TA, FHB, AH). Color coding the EMG wires allowed for fast identification of wires to be implanted from individual groups. The diagram is overlaid onto a digitally processed photo of a rhesus macaque hindlimb dissection.

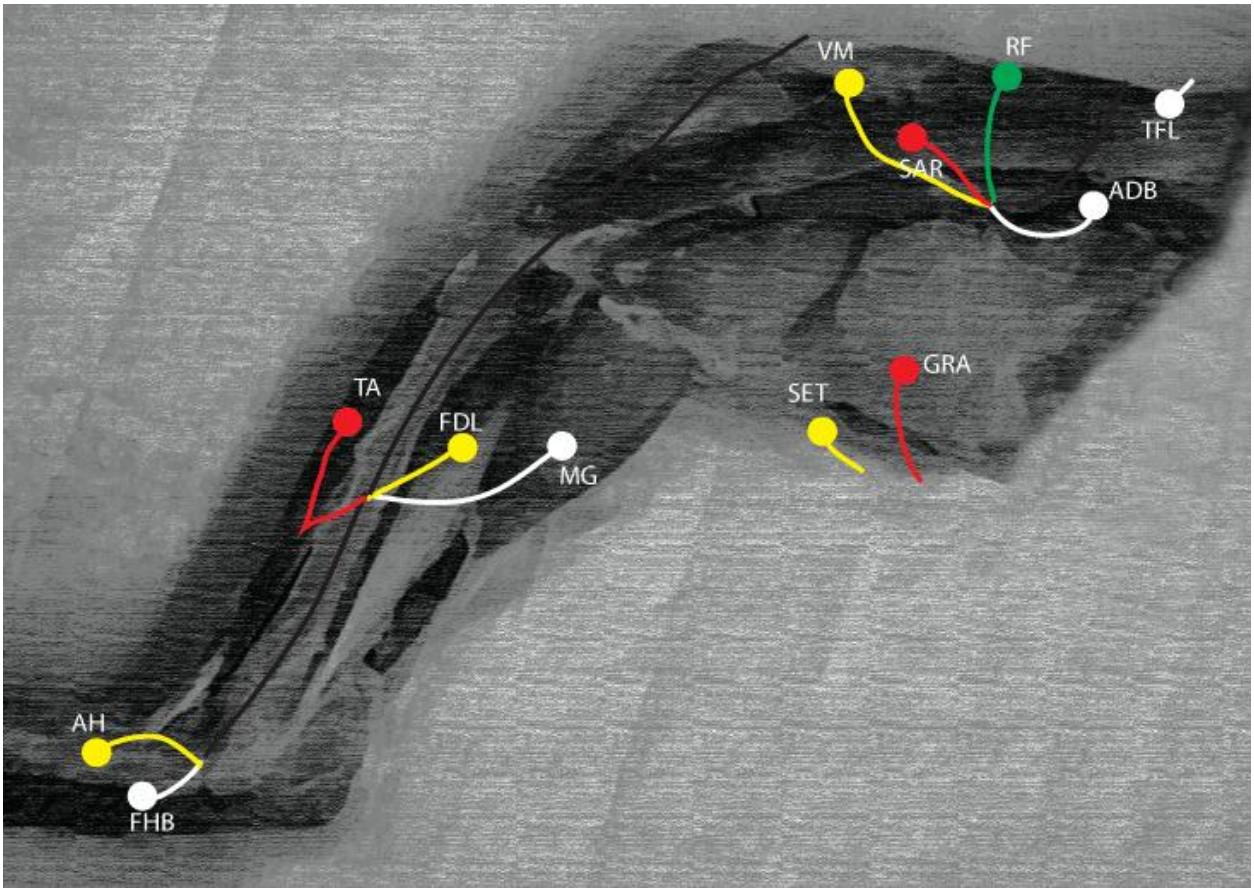
VM
RF
TFL
SAR
ADB
GRA
SET
TA
FDL
MG
AH
FHB

Figure 7. Types of postspike effects. There are two types of pure postspike effects, A) postspike facilitation (PSpF) which is a transient increase in firing probability, suggesting a facilitatory linkage; B) postspike suppression (PSpS) which is a transient decrease in firing probability, suggesting an inhibitory linkage. We also classified three types of complex effects detected in spike triggered averages: C) synchronous facilitation effects are transient increases in firing probability but with latencies that are too short to be compatible with direct monosynaptic connections and are likely caused by synchronous firing of cells; D) synchronous suppression effects are transient decreases in firing probability but with latencies that are too short to be consistent with direct anatomical connections and are likely caused by synchronous firing of cells; E) synchrony oscillation.

Types of Postspike Effects

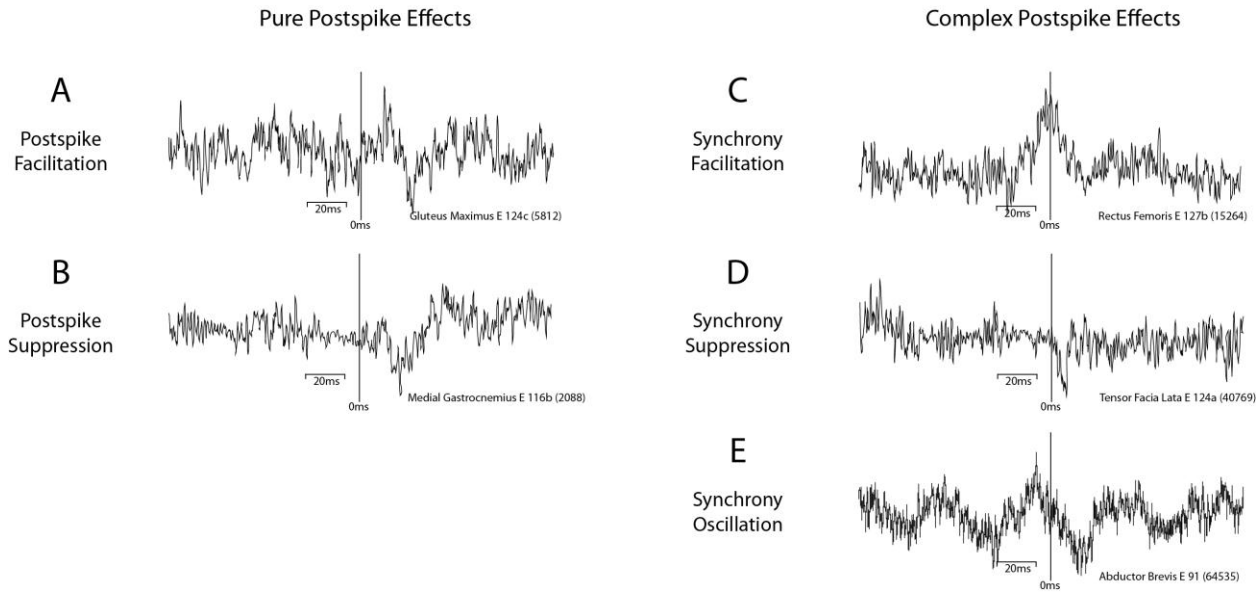

Figure 8. Distribution of effects in spike triggered averages separated by muscle and joint. The number of effects for each muscle are shown with the type of effect broken into their respective groups (PSpF, PSpS, synchrony facilitation, synchrony suppression, synchrony oscillation).

Distribution of Spike Triggered Effects by Joint and Muscle

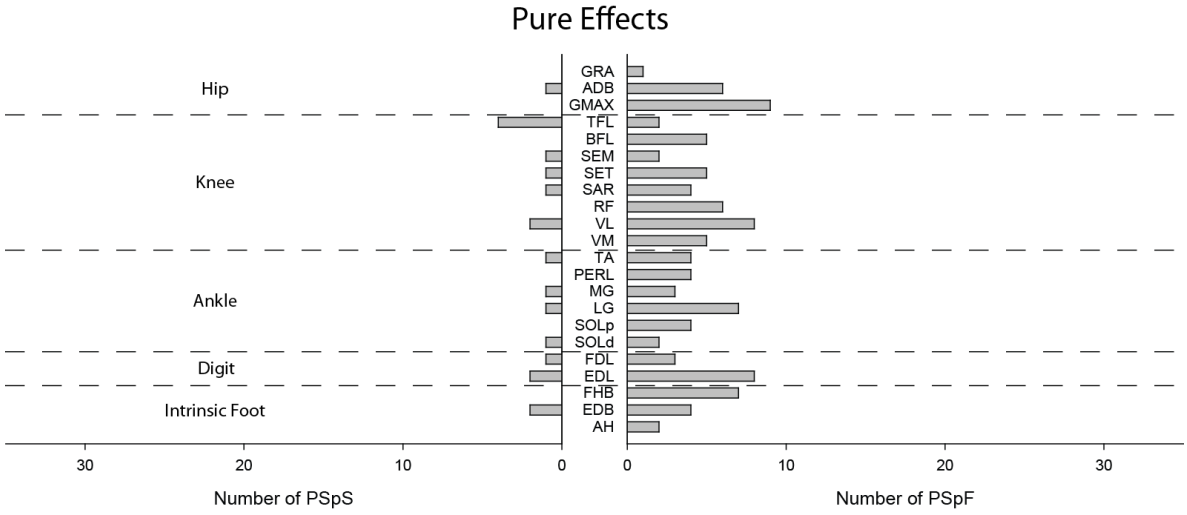

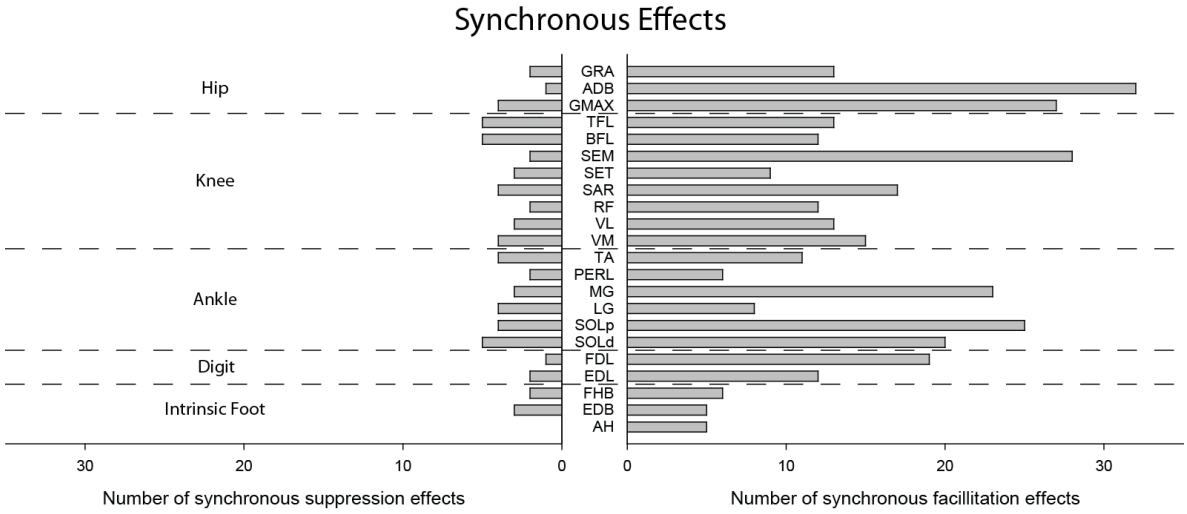

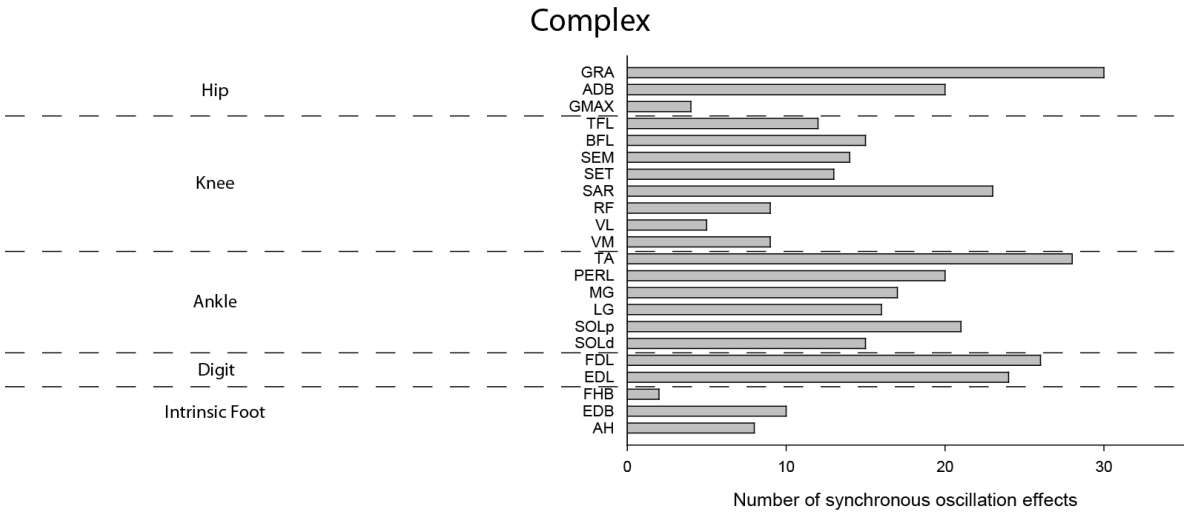

Figure 9. Isolated neuron showing modulated activity associated with the pull phase of the task. An isolated neuron (Unit shown in light blue) recorded with the relative task position (HindPos shown in black) and 6 of the respective EMG channels (LG, TA, AH, SEM, RF, and SAR). A wavemark channel contains the filtered unit signal (only cell spikes used in spike triggered averages) shown in brown. The isolated cell increases its firing rate during the ramp and hold of the pull phase of the task (shown as a downward deflection and leveling out of the HindPos channel). This increase in firing rate also corresponds to increases in EMG firing in four EMG channels (LG, TA, SEM, and SAR shown in orange). The cell is not modulated with respect to the other two EMG channels (AH, and RF shown in pink).

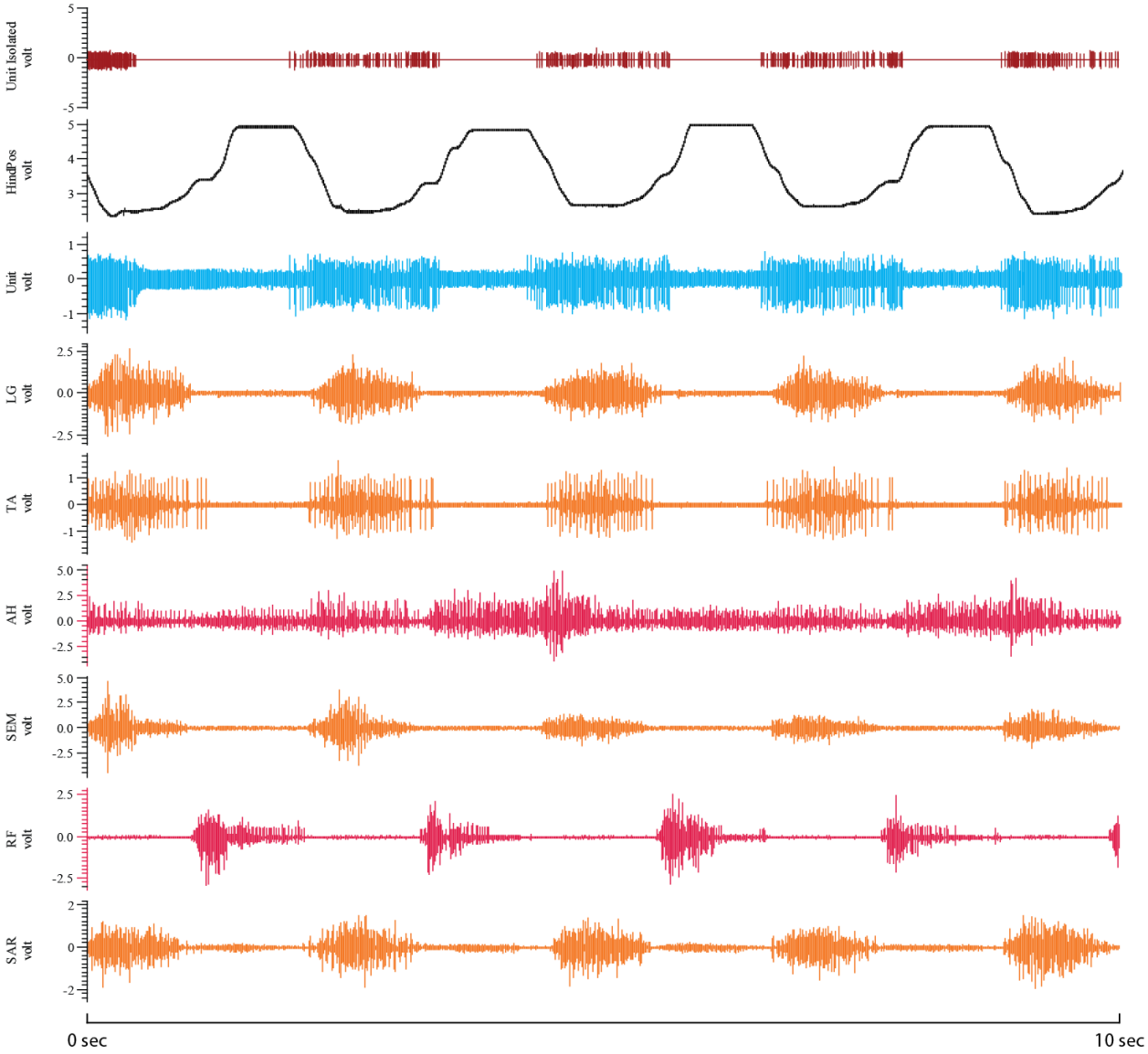
Unit Isolated
volt
5
0
-5
HindPos
volt
5
4
3
Unit
volt
1
0
-1
LG
volt
2.5
0.0
-2.5
TA
volt
1
0
-1
AH
volt
5.0
2.5
0.0
-2.5
SEM
volt
5.0
2.5
0.0
-2.5
RF
volt
2.5
0.0
-2.5
SAR
volt
2
0
-2
0 sec
10 sec

Figure 10. Distribution of the magnitude of pure PSpF effects for hip, knee, ankle, digit, and intrinsic foot muscles, and a composite plot of all muscles. With the exception of two hip muscle PSpF effects that had magnitudes greater than 30 percent peak increase over baseline, all PSpFs detected were of relatively small magnitude (<15 percent peak increase (PPI) over baseline). The mean, median, mode, % of effects above 20PPI, and range for each muscle group is also shown.

Magnitude of PSpF

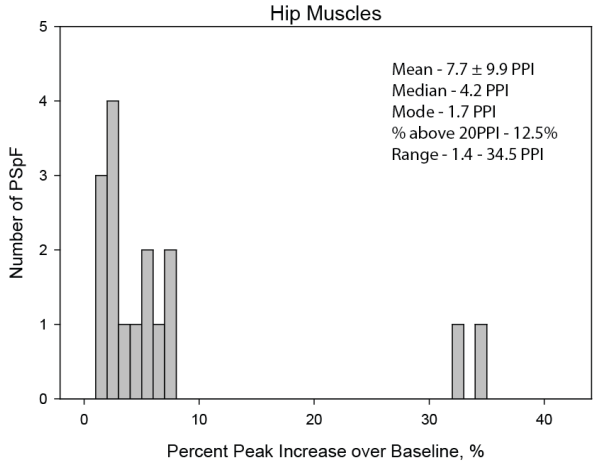

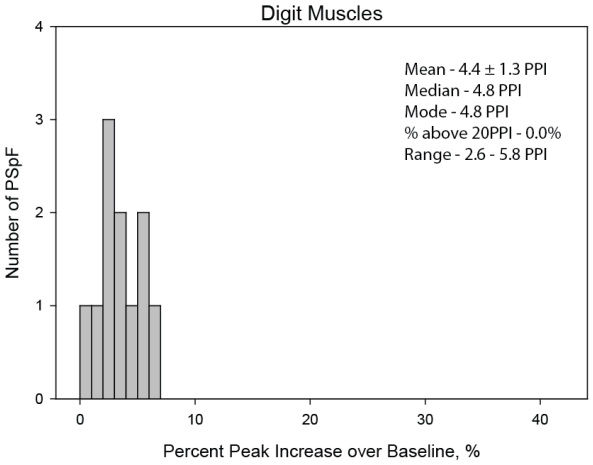

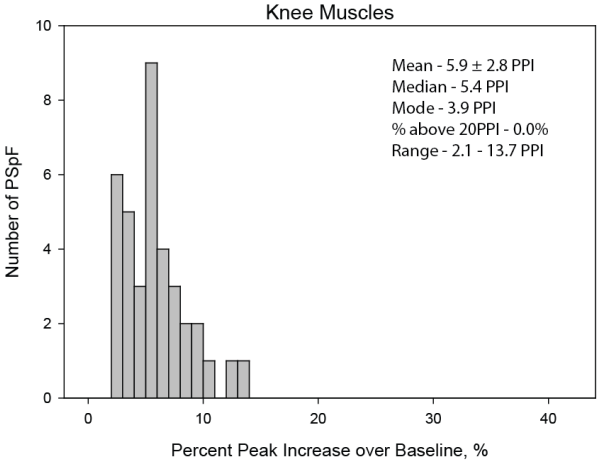

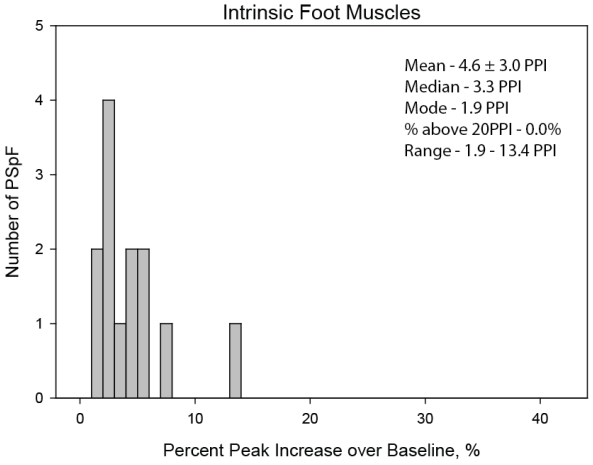

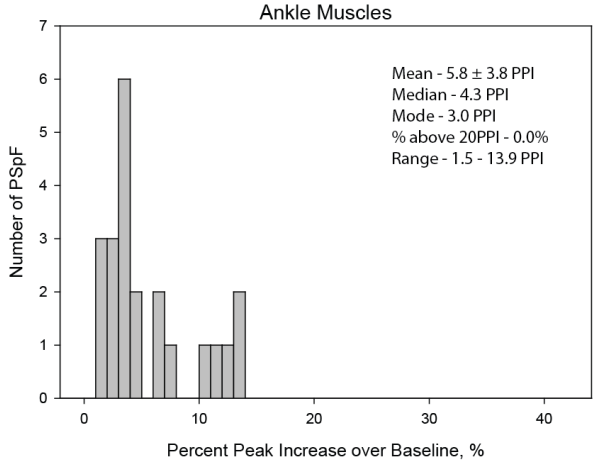

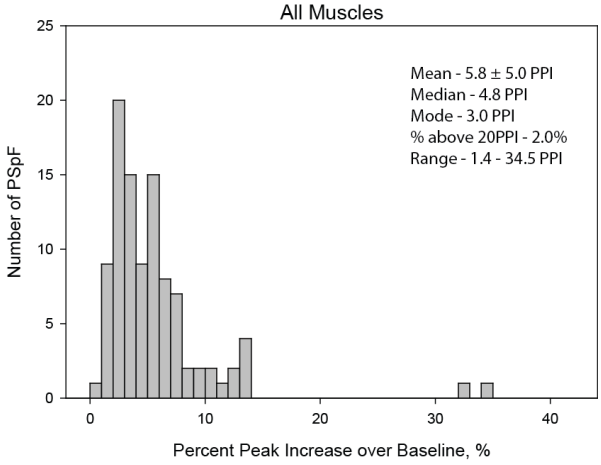

Figure 11. Distribution of onset latencies of PSpF effects for hip, knee, ankle, digit, and intrinsic foot joints, and a composite plot of all muscles. There is a large range of latencies with no dominant peak, although there is a tendency for more effects around 10ms. This is very different from forelimb effects. The mean, median, mode, % of latencies over 20ms, and range for each muscle group is also shown.

Onset Latency of PSpF

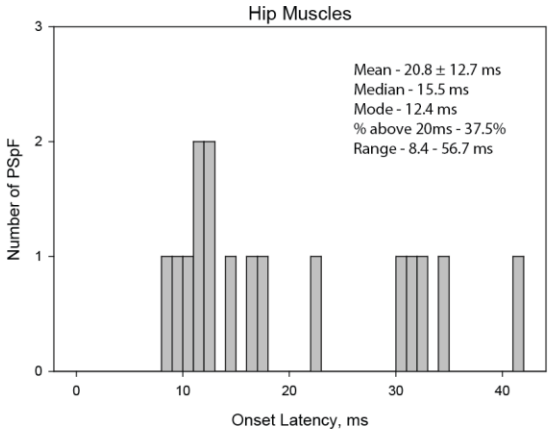

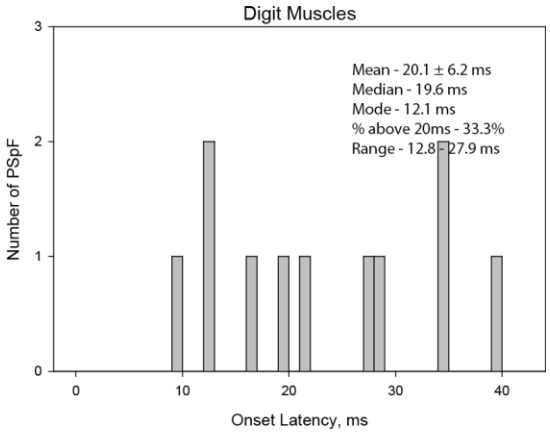

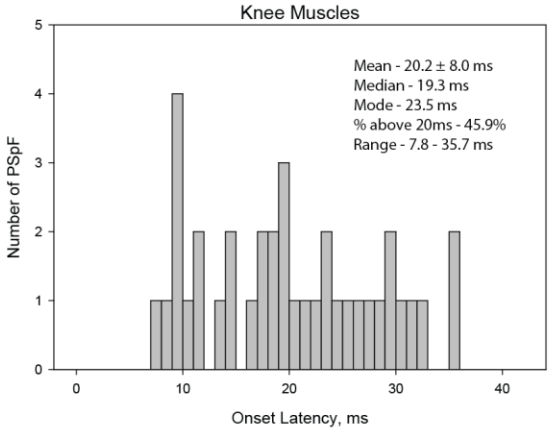

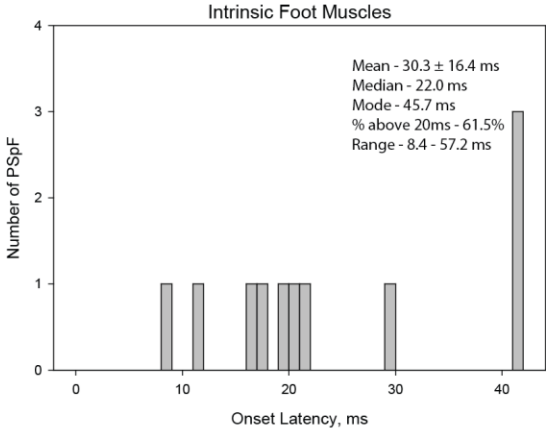

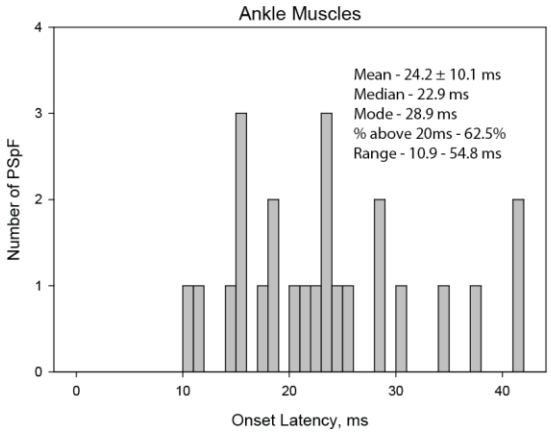

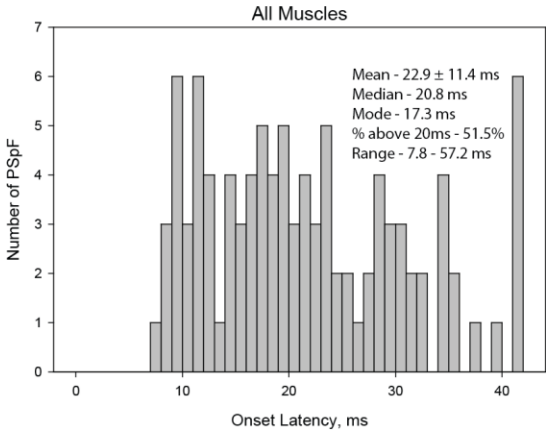

Figure 12. Histograms showing the number of cells with a given muscle field size. A: average muscle field for PSpF was 1.34 ± 0.71. B: average muscle field for all effects was 1.46 ± 0.81. Only one cell showed suppression in the absence of any facilitations effects.

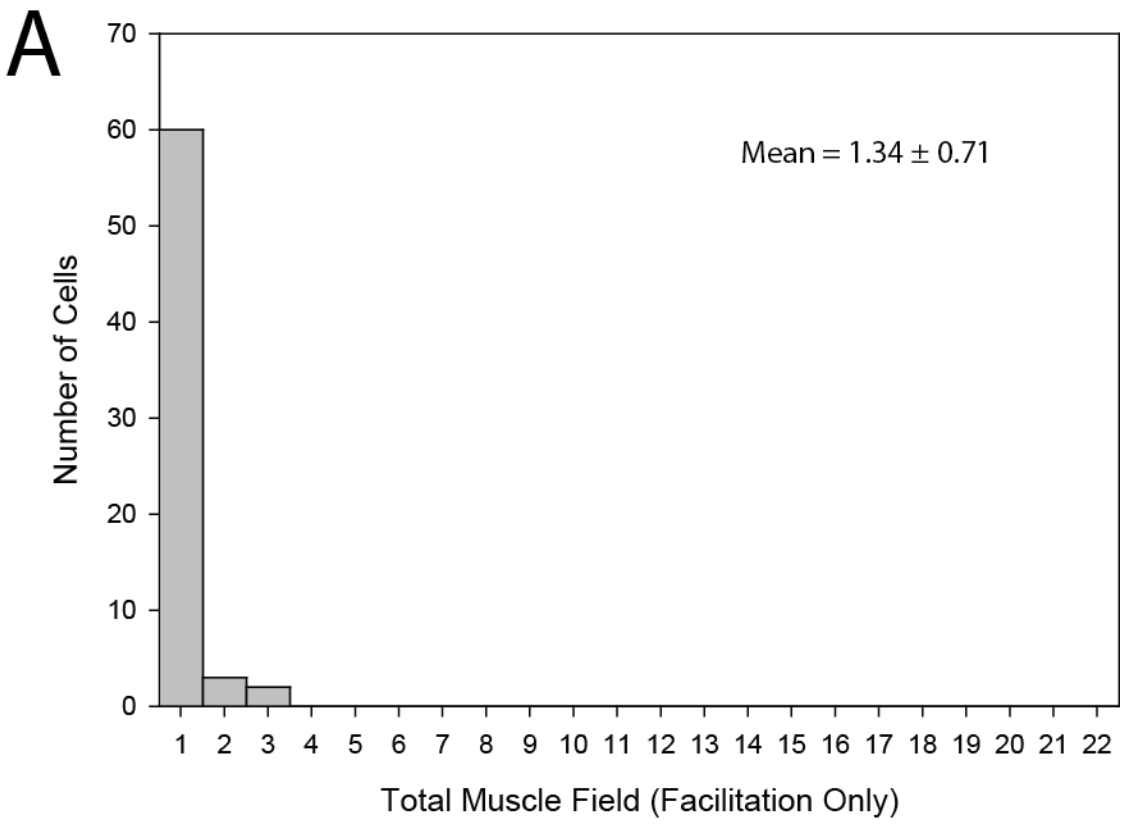
A
Mean = 1.34 ± 0.71
Number of Cells
Total Muscle Field (Facilitation Only)

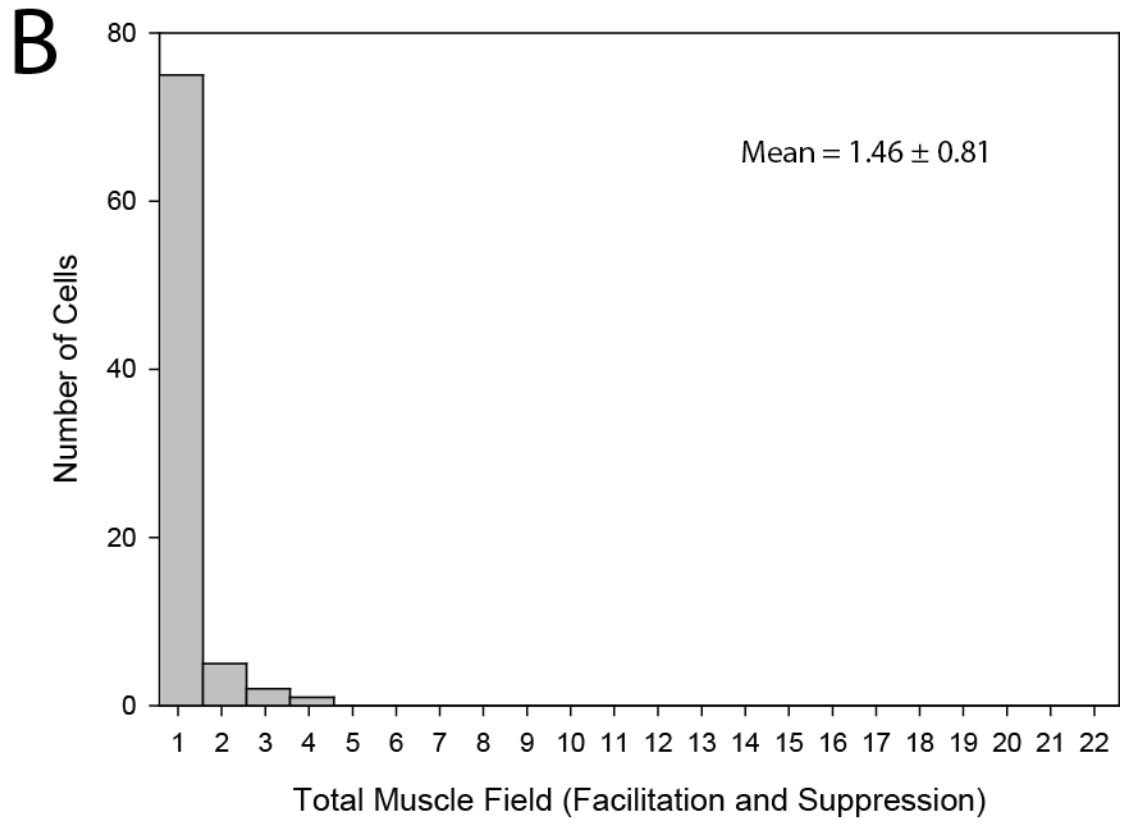
B
Mean = 1.46 ± 0.81
Number of Cells
Total Muscle Field (Facilitation and Suppression)

Figure 13. Comparison of postspike effects and poststimulus effects computed at the same site. The postspike facilitation effects evident in the spike triggered averages of panels A-C are matched by poststimulus facilitation in stimulus triggered averages at 60 μA done at the same site. In panel D the suppression following the facilitation effect in the spike triggered average is also evident in the stimulus triggered average at 60 μA done at the same site. In panel E the postspike facilitation in the spike triggered average is matched by poststimulus facilitation in the stimulus triggered average at 60 μA done at the same site.

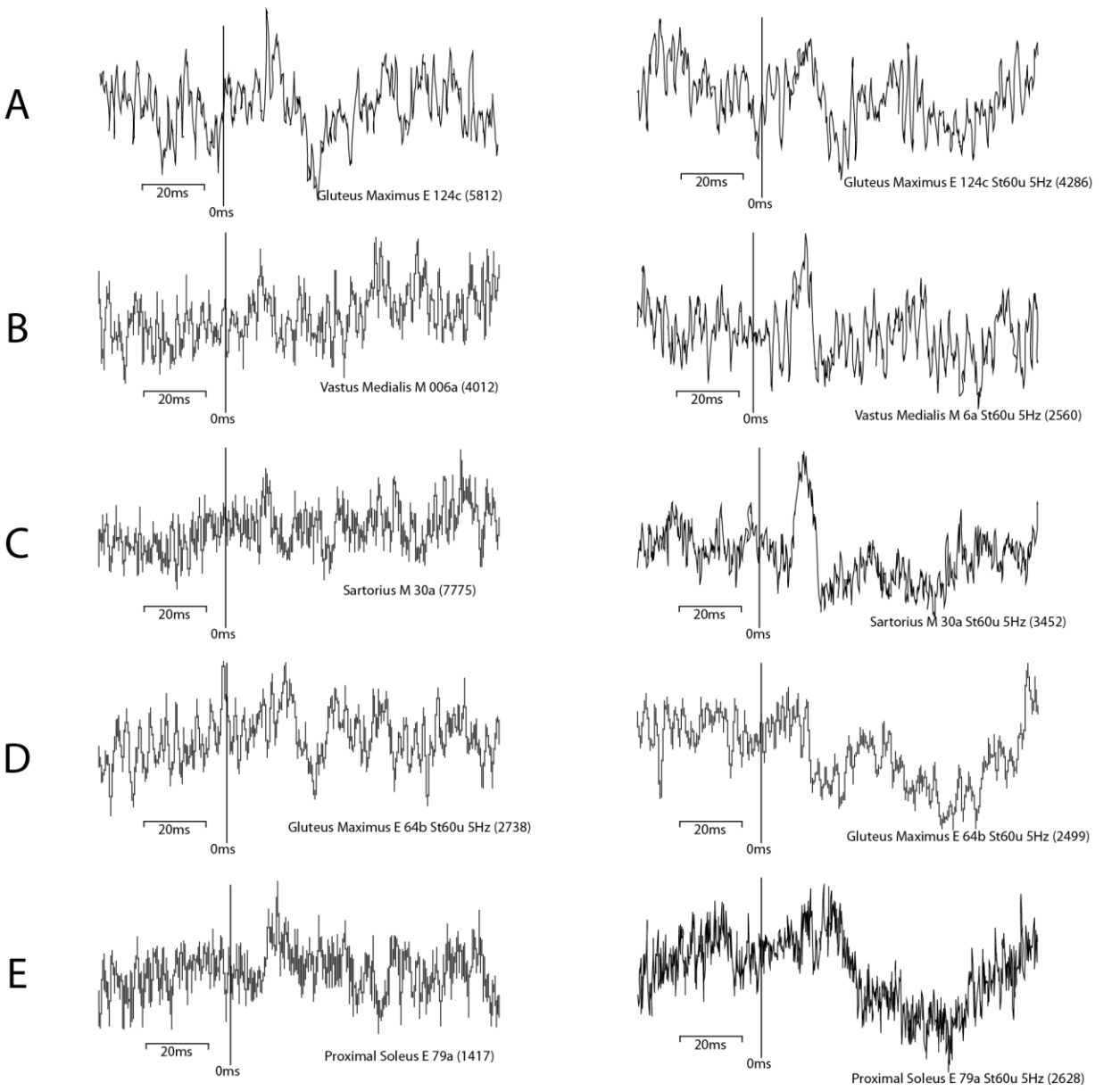
Postspike Effects
Poststimulus Effects at 60µA
A
B
C
D
E
20ms
0ms
Gluteus Maximus E 124c (5812)
Gluteus Maximus E 124c St60u 5Hz (4286)
Vastus Medialis M 006a (4012)
Vastus Medialis M 6a St60u 5Hz (2560)
Sartorius M 30a (7775)
Sartorius M 30a St60u 5Hz (3452)
Gluteus Maximus E 64b St60u 5Hz (2738)
Gluteus Maximus E 64b St60u 5Hz (2499)
Proximal Soleus E 79a (1417)
Proximal Soleus E 79a St60u 5Hz (2628)

CHAPTER 3

CORTICAL EFFECTS ON IPSILATERAL HINDLIMB MUSCLES REVEALED WITH STIMULUS TRIGGERED AVERAGING OF EMG ACTIVITY IN MACAQUE MONKEYS

INTRODUCTION

Approximately 10% of the corticospinal axons have been shown anatomically to descend ipsilaterally in the spinal cord (Hutchins et al. 1988; Dum and Strick 1996; Lacroix et al. 2004). Unit recording studies have demonstrated that about 10% of neurons are modulated exclusively with ipsilateral limb movements (Matsunami and Hamada 1978; Tanji et al. 1988; Aizawa et al. 1990) and functional magnetic resonance imaging (fMRI) studies consistently show bilateral activation of motor cortex with unilateral limb movements (Kuypers and Brinkman 1970; Cramer et al. 1999). A small fraction of cortical cells discharge with a wrist extension movement of only the ipsilateral limb (Evarts 1966; Goldring and Ratcheson 1972), and a small portion of cells discharge with movement of either the contralateral or ipsilateral hand (Lemon et al. 1976; Matsunami and Hamada 1978). In these cases pre-movement lead time of ipsilateral cells was similar to that for cells with exclusively contralateral associations (Lemon et al. 1976). Ipsilateral deficits associated with hemiparetic stroke demonstrate the potential functional importance of the ipsilateral motor cortex (Lewis and Brindley 1965; Colebatch and Gandevia 1989; Yarosh et al. 2004). Further evidence of the importance of the ipsilateral cortex in recovery from stroke is the finding that bilateral pyramidotomy produces more severe deficits than a unilateral lesion alone (Porter and Lemon 1993). Moreover, recovery of a patient from a unilateral section of the pyramidal tract was partially attributed to intact ipsilateral connections (Bucy et al. 1964). Also, there is growing evidence for the reorganization of the ipsilateral pathways following damage to the motor cortex (Chollet et al. 1991; Fisher 1992). Repetitive transcranial magnetic stimulation (rTMS) experiments have demonstrated that ipsilateral M1 is involved in fine motor tasks (Chen et al. 1997). fMRI and TMS studies in patients with hemiparetic stroke show a compensatory recruitment of the ipsilateral motor cortex (Caramia et

al. 2000; Feydy et al. 2002). Despite the potential functional and clinical importance of the ipsilateral corticospinal projection (Brus-Ramer et al. 2007; Rosenzweig et al. 2009), relatively little is known about the functional properties of this projection.

The position of the M1 hindlimb representation in primates on the midline of the hemisphere provides optimal access to both ipsilateral and contralateral M1 through a single recording chamber and presents an ideal opportunity to collect definitive data on the properties (sign, strength, latency and muscle distribution) of the ipsilateral corticospinal projection using stimulus-triggered averaging of EMG activity in awake monkeys. Stimulus triggered averaging (StTA) of EMG activity is well established as an effective method for identifying both excitatory and inhibitory linkages between motor cortex cells and motoneurons (Kasser and Cheney 1985). Divergence to different muscles can also be detected in the averages of EMG (Cheney and Fetz 1985). Using this approach, work from our laboratory has yielded new knowledge of the synaptic organization between cortical cells and motoneurons of forelimb and hindlimb muscles (Park et al. 2001; Boudrias et al. 2006; Griffin et al. 2009; Hudson et al. 2010). Although output effects on muscle activity from contralateral primary motor cortex (M1) have been extensively documented using a variety of methods, studies of output effects from ipsilateral cortex have been much more limited. The goal of this study is to quantify the output properties of ipsilateral M1 cortex relative to contralateral M1 in terms of magnitude, latency and distribution of effects. Also, maps of cortical output to muscles of the hindlimb will provide a basis for comparing the spatial representation within hindlimb M1 to forelimb M1.

MATERIALS AND METHODS

Materials and Methods for this work are identical to those described in Chapter 2

RESULTS

Detecting poststimulus effects in averages of EMG activity from microstimuli applied to ipsilateral M1 cortex

Using microstimuli of intensities ranging from 30-120 μA we were able to detect both excitatory and inhibitory effects on hindlimb muscle EMG activity as illustrated in Figure 1. Poststimulus facilitation (PStF) is a transient increase in EMG activity and suggests an excitatory synaptic linkage between the population of stimulated cells and the target motoneurons. Poststimulus suppression (PStS) is a transient decrease in EMG activity and suggests an underlying inhibitory synaptic linkage between the population of stimulated cells and the target motoneurons. Averages that show no poststimulus change in average EMG activity are interpreted as lacking a synaptic linkage with motoneurons.

To produce poststimulus effects in EMG activity from the ipsilateral cortex we used various stimulus intensities (30 μA, 60 μA, 120 μA, two pulses at 120 μA) (Figure 2). Poststimulus effects were generally clear at 60 μA; however, to facilitate comparison of effects to those from contralateral cortex we also used 120 μA.

Table 1 summarizes the data collected from the contralateral and ipsilateral M1 of two male rhesus macaques. Data was obtained from a total of 679 electrode tracks (monkey M, 337 shown in Figure 3; monkey L, 342 shown in Figure 4). Stimulus triggered averages were collected from 22 muscles of the hip, knee, ankle, digit, and intrinsic foot for a total of 20,416 averages. At 57 sites ICMS (13 pulse train at 333Hz, 120 μA) was used to test for motor output effects outside the hindlimb representation including trunk, shoulder, and tail movements. An additional 67 sites tested positive for sensory responses aiding in the detection of the border of

primary somatosensory cortex. Of the 20,416 averages 9,833 showed some poststimulus effect, 7,871 of which were PStFs and 1,962 of which were PStSs. Only StTAs where the earliest effect was suppression were counted as PStS effects. Many PStF effects were biphasic with suppression following facilitation. The number of PStF effects sorted by joint and muscle at each stimulus intensity is shown in Figure 5.

Comparison of contralateral effects to ipsilateral effects

Tables 2-10 summarize the average magnitude (percent peak increase over baseline (PPI)), onset latency (ms), and peak latency (ms) of poststimulus effects for both monkeys and the overall totals. The data for each individual joint (hip, knee, ankle, digit, and intrinsic foot) are presented as well as the overall means.

At the same stimulus intensity (120 μA), the average magnitude of contralateral effects is 2-6 times greater (monkey M, 23.2 to 9.4 PPI; monkey L, 57.8 to 10.2 PPI) than ipsilateral effects. The standard deviation of the onset latency for ipsilateral effects is greater than for the contralateral effects (monkey M, 4.8ms versus 3.2ms; monkey L, 6.7ms to 3.2ms). However, there is significant overlap of the mean onset latency and standard deviations between contralateral and ipsilateral effects. The trend holds true for peak latency of PStF between contralateral and ipsilateral effects.

Figures 6-8 are histograms of the magnitude of PStF effects in hip muscles produced at the same stimulus intensity (120 μA) from contralateral and ipsilateral cortex. There are a larger number of stronger (greater than 20 PPI) effects in the contralateral data (31.7% of effects > 20 PPI), while the ipsilateral effects are generally much smaller in magnitude (only 1.2% of effects

>20 PPI). This was especially true for Monkey L. The onset latency distributions for PStF effects in hip muscles are shown in Figures 21-23. Although longer latency PStF effects are more common from ipsilateral cortex (18.1% of effects over 20ms ipsilaterally, compared to 2.5% contralaterally), the shortest onset latencies for effects from the contralateral and ipsilateral cortices are very similar for all muscles with effects.

Figures 9-11 are histograms of the magnitude of PStF effects in knee muscles produced at the same stimulus intensity (120 μA) from contralateral and ipsilateral cortex. There are a number of larger (greater than 20 PPI) effects in the contralateral muscles (43.8% of effects > 20 PPI), while the ipsilateral effects are generally much smaller in magnitude (3.5% of effects >20 PPI). The onset latency distributions for PStF effects in knee muscles are shown in Figure 24-26. Although longer latency PStF effects are more common from ipsilateral cortex (15.3% of effects over 20ms ipsilaterally, compared to 3.5% contralaterally), the shortest onset latencies for effects from the contralateral and ipsilateral cortices are very similar for all muscles showing effects.

Figures 12-14 are histograms of the magnitude of PStF effects in ankle muscles produced at the same stimulus intensity (120 μA) from contralateral and ipsilateral cortex. There are a number of larger (greater than 20 PPI) effects in the contralateral data (59.6% of effects > 20 PPI), while the ipsilateral effects are generally much smaller in magnitude (1.4% of effects >20 PPI). The onset latency distributions for PStF effects in ankle muscles are shown in Figure 27-29. Although longer latency PStF effects are more common from ipsilateral cortex (18.2% of effects over 20ms ipsilaterally, compared to 0.6% contralaterally), the shortest onset latencies for effects from the contralateral and ipsilateral cortices are very similar for all muscles showing effects.

Figures 15-17 are histograms of the magnitudes of PStF effects in digit and intrinsic foot muscles produced at the same stimulus intensity (120 μA) from contralateral and ipsilateral cortex. There are a number of larger (greater than 20 PPI) effects in the contralateral data (46.2% of effects > 20 PPI), while the ipsilateral effects are generally much smaller in magnitude (2.3% of effects >20 PPI). The onset latency distributions for PStF effects in digit and intrinsic foot muscles are shown in Figure 30-32. Although longer latency PStF effects are more common from ipsilateral cortex (42.9% of effects over 20ms ipsilaterally, compared to 1.8% contralaterally), the shortest onset latencies for effects from the contralateral and ipsilateral cortices are very similar for all muscles showing effects. Also of note is the bimodal appearance of the latency effects in some digit and intrinsic foot muscles. The most striking example of which is, flexor hallucis brevis (FHB) which both contralaterally and ipsilaterally shows latency peaks on the histogram at 8-11ms and 15-20ms. There is also an increase in the number of very large magnitude (>200 PPI) effects contralaterally as we move from proximal to more distal muscles.

Comparison of map organization

The 2D heat maps in Figure 36 show the spatial representation of PStF for each hip muscle based on single 120 μA stimulus pulses in contralateral M1 and twin pulses at 120 μA (3 ms interpulse interval) in ipsilateral M1. Two pulses were used in the ipsilateral cortex to illicit stronger PStF effects for greater map resolution (the general somatotopic organization is the same as for single pulses in the ipsilateral cortex). The ipsilateral representation of gracilis (GRA), adductor brevis (ADB), and gluteus maximus (GMAX) are shifted anteriorly and laterally in both monkeys when compared to the contralateral representation. In all cases, the

representation in the contralateral cortex was largely non-overlapping with the mirror image location in the ipsilateral cortex.

The 2D heat maps in Figure 37 show the spatial representation of PStF for each knee muscle based on single 120 μA stimulus pulses in contralateral M1 and twin pulses at 120 μA (3 ms interpulse interval) in ipsilateral M1. The ipsilateral representation of tensor fascia latae (TFL), semimembranosus (SEM), semitendinosus (SET), of sartorius (SAR), rectus femoris (RF), vastus lateralis (VL), vastus medialis (VM) were shifted anteriorly and either laterally or medially in both monkeys when compared to the contralateral representation (due to an artifact maps are not available for TFL in Monkey M and SET for Monkey L). In all cases, the representation in the contralateral cortex was largely non-overlapping with the mirror image location in the ipsilateral cortex.

The 2D heat maps in Figure 38 show the spatial representation of PStF for each ankle muscle based on single 120 μA stimulus pulses in contralateral M1 and twin pulses at 120 μA (3 ms interpulse interval) in ipsilateral M1. The ipsilateral representation of tibialis anterior (TA), peroneus longus (PERL), and distal portion of soleus (SOLd) were shifted anteriorly and laterally in both monkeys when compared to the contralateral representation. In all cases, the representation in the contralateral cortex was largely non-overlapping with the mirror image location in the ipsilateral cortex.

The 2D heat maps in Figure 39 show the spatial representation of PStF for each digit and intrinsic foot muscle based on single 120 μA stimulus pulses in contralateral M1 and twin pulses at 120 μA (3 ms interpulse interval) in ipsilateral M1. The ipsilateral representation of flexor digitorum longus (FDL), flexor hallucis brevis (FHB), extensor digitorum brevis (EDB), and

abductor hallucis (AH) were shifted anteriorly and either laterally or medially in both monkeys when compared to the contralateral representation. In all cases, the representation in the contralateral cortex was largely non-overlapping with the mirror image location in the ipsilateral cortex.

DISCUSSION

Detecting poststimulus effects in EMG from microstimuli in the ipsilateral cortex

Our approach to finding the optimal stimulus parameters for detecting poststimulus effects (PStEs) in muscles from microstimuli applied to the ipsilateral cortex parallels the work done in a previous study of the contralateral hindlimb which determined the optimal stimulus parameters for comparison with forelimb poststimulus effects (Hudson et al. 2010). Hindlimb ipsilateral effects were almost completely absent at 30 μA and there were relatively few at 60 μA – intensities that yield strong effects in the contralateral M1. This was expected since we are activating a small population of corticospinal cells and only 10% of them have been shown to descend ipsilaterally (Dum and Strick 1996). To generate an adequate number of ipsilateral effects for comparison with contralateral effects we increased the stimulus intensity to 120 μA and also tried using two pulses at 120 μA separated by 3ms (twin pulse stimulation). These parameters produced reliable effects that we could effectively compare with those from contralateral cortex in terms of sign, latency, magnitude and incidence. To investigate the spatial organization of cells in the cortex, we used twin pulses at 120 μA, which yielded stronger effects, allowing us to construct more detailed maps of the cortical localization for each muscle. Our data set contains 1,852 PStEs ipsilaterally for comparison with 4,439 PStEs contralaterally. In conclusion, these stimulus parameters provided reliable motor output effects from ipsilateral cortex that could be quantified and compared to those from contralateral cortex obtained under the same conditions.

Comparison of ipsilateral and contralateral PStEs

Ipsilateral effects from M1 had the same general ratio of PStF to PStS effects as contralateral M1. A similar number of agonist muscles were facilitated and antagonist muscles were suppressed. This suggests that the two cortices exhibit a generally similar pattern of control over hindlimb muscles, specifically with reference to muscle synergies. The finding that contralateral effects are 2-6 times stronger than ipsilateral effects can again be explained by the relatively small number of corticospinal cells that have been shown to descend ipsilaterally.

We next examined how these effects are mediated. If they are mediated through polysynaptic pathways (cortico-cortical, rubriospinal, propriospinal, etc.) we would expect to see longer onset latencies for ipsilateral effects compared to contralateral effects. Looking at just the mean onset latency (contralateral total 12.7 ± 3.2 ms; ipsilateral total 14.0 ± 6.1 ms) it seems that the ipsilateral effects have a slightly greater mean onset latency. The mean onset latency for ipsilateral effects, however, has double the standard deviation due to some longer latency effects. Another way to evaluate onset latency is to look at a histogram of the onset latencies for all effects across all muscles (Figure 35). Although the onset latencies for effects from both cortices have a similar range of effects for each muscle group, as do peak latencies, the mean ipsilateral latencies are generally 1-4 ms longer than contralateral latencies. However, most noteworthy is the fact that the shortest onset latencies for ipsilateral effects as short as the shortest latencies for contralateral effects. This strongly suggests that at least some corticospinal cells in the ipsilateral M1 affect motoneurons through a pathway that is as direct as corticospinal cells in contralateral M1.

Comparison of map organization

We also wanted to characterize the location of cells producing ipsilateral effects. Previous work in humans performing a finger tapping task showed bilateral activation on fMRI (Cramer et al. 1999). In that study the ipsilateral representation they observed on fMRI was anterior and lateral to the representation in the contralateral hemisphere. Also Asanuma and colleagues found a region outside the typical forelimb representation that had a higher proportion of cells that responded to ipsilateral movements (Asanuma et al. 1974). When we explored the boundaries of the hindlimb representation ipsilaterally we found that the greatest magnitude effects from all muscles taken together formed a circularly shaped representation surrounding the mirror image location of the contralateral representation. This area of ipsilateral cortex would presumably contain the representation of the contralateral muscles for the hemisphere we are calling ipsilateral cortex. This organization is evident when comparing all muscles together in a 2D contour map (Figure 40). Our results suggest that on the boundaries of the hindlimb contralateral representation there exists a population of cells that are synaptically linked to motoneurons of ipsilateral muscles. These cells may be exploited and possibly expand their representation following a lesion to the contralateral cortex to aid in recovery of lost function.

Our results demonstrate clear effects from hindlimb M1 cortex on motoneurons of ipsilateral muscles. Although these effects were much weaker than those from contralateral cortex, the shortest onset latencies for all muscles tested were as short as those from contralateral cortex suggesting an equally direct synaptic linkage. (Soteropoulos et al. 2011) focused on effects from ipsilateral forelimb M1 cortex on motoneurons. Using spike triggered averaging of EMG activity from ipsilateral and contralateral muscles recorded simultaneously; they reported that effects on ipsilateral muscles were essentially non-existent. However, they used stimulus currents that were relatively weak (30μA) compared to our study. Moreover, they did not

systematically explore ipsilateral cortex but rather focused on the area of ipsilateral cortex producing the strongest effects in contralateral muscles. Our results show that this is not the region of cortex that contains the representation of ipsilateral muscles. The combination of these factors probably contributed to the fact that they were unable to identify clear ipsilateral effects. It is also possible that there is a real difference between forelimb and hindlimb M1 cortex with respect to the representation of ipsilateral muscles.

Table 1. Summary of Data Collected

	Monkey M			Monkey L			Total
Electrode tracks	337			342			679
ICMS sites*	31			26			57
Sensory test	38			29			67
	Contralateral 120 μA	Ipsilateral 120 μA	Ipsilateral 2 pulse 120 μA	Contralateral 120 μA	Ipsilateral 120 μA	Ipsilateral 2 pulse 120 μA	
Sites stimulated	143	156	156	157	158	158	928
StTA records (all)	3146	3432	3432	3454	3476	3476	20416
Sites yielding PStEs	143	152	156	155	158	158	922
Sites yielding PStF	143	151	156	155	158	158	921
Sites yielding PStS	125	91	106	110	106	132	670
PStEs obtained	1940	776	1404	2499	1076	2138	9833
PStF effects	1506	622	1107	2175	827	1634	7871
PStS effects	434	154	297	324	249	504	1962

* 13 pulse train at 333Hz, 120 μA done for testing sites outside the hindlimb representation

Table 2. Comparison of Magnitudes from Contralateral and Ipsilateral Cortices in Monkey M

Monkey M

PStF

	Magnitude, %											
	Contralateral 120 μA				Ipsilateral 120 μA				Ipsi 2 pulse 120 μA			
Joint	n	Mean		SD	n	Mean		SD	n	Mean		SD
Hip	228	13.6	±	12.1	81	7.5	±	2.4	138	11.2	±	8.4
Knee	539	21.8	±	17.7	312	10.0	±	4.4	466	15.8	±	9.0
Ankle	414	28.6	±	28.0	94	8.7	±	2.6	279	11.5	±	4.4
Digit	96	19.3	±	14.5	25	8.5	±	2.5	56	9.2	±	3.1
Intrinsic	229	28.6	±	38.5	110	10.8	±	4.6	168	14.4	±	9.1
Total	1506	23.3	±	24.8	622	9.6	±	4.1	1107	13.6	±	8.1

PStS

	Magnitude, %											
	Contralateral 120 μA				Ipsilateral 120 μA				Ipsi 2 pulse 120 μA			
Joint	n	Mean		SD	n	Mean		SD	n	Mean		SD
Hip	108	-12.3	±	5.5	38	-7.2	±	2.2	80	-8.3	±	3.7
Knee	177	-14.6	±	6.3	68	-8.7	±	2.6	101	-11.2	±	4.2
Ankle	85	-16.7	±	7.6	34	-8.4	±	2.1	95	-10.6	±	4.1
Digit	12	-11.1	±	4.9	4	-8.2	±	1.6	5	-8.5	±	2.0
Intrinsic	52	-18.2	±	8.2	10	-7.3	±	1.6	16	-9.3	±	3.1
Total	434	-14.8	±	6.9	154	-8.2	±	2.4	297	-10.1	±	4.1

Table 3. Comparison of Onset Latencies from Contralateral and Ipsilateral Cortices in Monkey M

Monkey M

PStF

	Onset Latency, ms											
	Contralateral 120 μA				Ipsilateral 120 μA				Ipsi 2 pulse 120 μA			
Joint	n	Mean		SD	n	Mean		SD	n	Mean		SD
Hip	228	12.0	±	3.5	81	15.7	±	6.2	138	16.9	±	9.1
Knee	539	11.7	±	3.6	312	12.1	±	4.1	466	13.8	±	4.5
Ankle	414	12.8	±	2.1	94	14.0	±	5.8	279	12.8	±	3.8
Digit	96	13.6	±	1.7	25	15.0	±	4.9	56	14.2	±	4.1
Intrinsic	229	14.3	±	2.8	110	12.8	±	4.7	168	15.0	±	4.7
Total	1506	12.6	±	3.2	622	13.1	±	5.0	1107	14.2	±	5.3

PStS

	Onset Latency, ms											
	Contralateral 120 μA				Ipsilateral 120 μA				Ipsi 2 pulse 120 μA			
Joint	n	Mean		SD	n	Mean		SD	n	Mean		SD
Hip	108	22.2	±	9.2	38	22.3	±	10.1	80	20.4	±	6.3
Knee	177	18.4	±	6.2	68	19.8	±	10.7	101	20.4	±	8.7
Ankle	85	19.7	±	8.0	34	19.3	±	4.0	95	23.1	±	7.0
Digit	12	19.7	±	8.0	4	14.5	±	4.2	5	18.2	±	1.4
Intrinsic	52	23.7	±	6.5	10	21.3	±	5.5	16	29.2	±	7.9
Total	434	20.6	±	7.5	154	20.3	±	9.2	297	21.7	±	7.8

Table 4. Comparison of Peak and Trough Latencies from Contralateral and Ipsilateral Cortices in Monkey M

Monkey M

PStF

Peak Latency, ms

	Contralateral 120 μA				Ipsilateral 120 μA				Ipsi 2 pulse 120 μA			
Joint	n	Mean	±	SD	n	Mean	±	SD	n	Mean	±	SD
Hip	228	14.9	±	3.9	81	19.0	±	7.9	138	21.8	±	11.2
Knee	539	14.9	±	4.4	312	14.6	±	4.4	466	17.4	±	5.6
Ankle	414	16.1	±	2.4	94	16.6	±	6.4	279	15.9	±	4.4
Digit	96	16.3	±	2.0	25	17.1	±	5.2	56	16.9	±	4.9
Intrinsic	229	17.5	±	3.2	110	15.3	±	4.9	168	18.6	±	5.9
Total	1506	12.6	±	3.2	622	15.7	±	5.6	1107	17.7	±	6.6

PStS

Trough Latency, ms

	Contralateral 120 μA				Ipsilateral 120 μA				Ipsi 2 pulse 120 μA			
Joint	n	Mean	±	SD	n	Mean	±	SD	n	Mean	±	SD
Hip	108	33.0	±	15.7	38	29.4	±	13.8	80	27.3	±	8.9
Knee	177	26.7	±	13.1	68	24.5	±	12.9	101	26.6	±	10.8
Ankle	85	38.1	±	14.9	34	23.1	±	4.9	95	29.7	±	8.9
Digit	12	28.2	±	16.4	4	17.7	±	6.2	5	21.5	±	2.0
Intrinsic	52	37.5	±	14.3	10	27.8	±	10.9	16	35.2	±	10.3
Total	434	31.8	±	15.2	154	25.4	±	11.9	297	28.2	±	9.9

Table 5. Comparison of Magnitudes from Contralateral and Ipsilateral Cortices in Monkey L

Monkey L

PStF

	Magnitude, %											
	Contralateral 120 μA				Ipsilateral 120 μA				Ipsi 2 pulse 120 μA			
Joint	n	Mean		SD	n	Mean		SD	n	Mean		SD
Hip	299	29.8	±	33.0	162	9.1	±	3.8	218	11.1	±	4.8
Knee	707	33.1	±	35.1	320	10.2	±	5.2	541	16.1	±	13.7
Ankle	656	84.0	±	117.4	115	9.4	±	4.0	450	14.5	±	7.3
Digit	129	81.5	±	121.5	38	7.6	±	2.1	54	9.0	±	3.3
Intrinsic	384	72.6	±	125.2	192	10.5	±	3.7	371	13.3	±	6.9
Total	2175	57.8	±	94.5	827	9.8	±	4.4	1634	14.1	±	9.7

PStS

	Magnitude, %											
	Contralateral 120 μA				Ipsilateral 120 μA				Ipsi 2 pulse 120 μA			
Joint	n	Mean		SD	n	Mean		SD	n	Mean		SD
Hip	116	-19.5	±	9.2	75	-9.3	±	2.0	148	-14.6	±	6.4
Knee	125	-17.8	±	7.9	91	-10.1	±	3.1	202	-14.6	±	6.0
Ankle	39	-14.6	±	7.2	45	-8.4	±	1.9	79	-10.6	±	4.0
Digit	18	-19.1	±	9.5	20	-9.5	±	2.2	62	-11.2	±	3.5
Intrinsic	26	-17.4	±	11.7	18	-8.1	±	2.2	13	-10.0	±	3.4
Total	324	-18.1	±	8.9	249	-9.4	±	2.6	504	-13.4	±	-13.4

Table 6. Comparison of Onset Latencies from Contralateral and Ipsilateral Cortices in Monkey L

Monkey L

PStF

	Onset Latency, ms											
	Contralateral 120 μA				Ipsilateral 120 μA				Ipsi 2 pulse 120 μA			
Joint	n	Mean		SD	n	Mean		SD	n	Mean		SD
Hip	299	11.8	±	2.3	162	14.2	±	7.2	218	13.5	±	4.8
Knee	707	12.1	±	3.6	320	15.5	±	6.8	541	15.8	±	5.0
Ankle	656	13.3	±	2.1	115	17.5	±	6.4	450	16.1	±	5.6
Digit	129	13.7	±	3.3	38	22.3	±	7.7	54	19.5	±	6.6
Intrinsic	384	13.7	±	3.9	192	14.1	±	5.7	371	16.3	±	6.5
Total	2175	12.8	±	3.2	827	15.5	±	6.9	1634	15.8	±	5.7

PStS

	Onset Latency, ms											
	Contralateral 120 μA				Ipsilateral 120 μA				Ipsi 2 pulse 120 μA			
Joint	n	Mean		SD	n	Mean		SD	n	Mean		SD
Hip	116	14.9	±	3.7	75	15.9	±	5.7	148	16.2	±	3.7
Knee	125	16.3	±	3.9	91	17.3	±	5.6	202	17.3	±	3.9
Ankle	39	19.6	±	4.0	45	17.9	±	4.1	79	22.5	±	6.9
Digit	18	18.5	±	4.8	20	19.4	±	6.3	62	20.1	±	5.0
Intrinsic	26	20.8	±	5.6	18	22.2	±	10.3	13	31.3	±	10.6
Total	324	16.7	±	4.5	249	17.5	±	6.1	504	18.5	±	5.7

Table 7. Comparison of Peak and Trough Latencies from Contralateral and Ipsilateral Cortices in Monkey L

Monkey L

PStF

Peak Latency, ms

	Contralateral 120 μA				Ipsilateral 120 μA				Ipsi 2 pulse 120 μA			
Joint	n	Mean	±	SD	n	Mean	±	SD	n	Mean	±	SD
Hip	299	14.3	±	2.7	162	16.6	±	8.2	218	16.1	±	5.4
Knee	707	15.4	±	3.9	320	18.0	±	7.4	541	19.5	±	5.9
Ankle	656	16.6	±	2.6	115	19.7	±	6.7	450	19.4	±	6.0
Digit	129	16.0	±	3.2	38	23.9	±	7.8	54	21.8	±	7.2
Intrinsic	384	17.0	±	4.3	192	16.1	±	5.9	371	19.1	±	6.8
Total	2175	15.9	±	3.6	827	17.8	±	7.4	1634	19.0	±	6.3

PStS

Trough Latency, ms

	Contralateral 120 μA				Ipsilateral 120 μA				Ipsi 2 pulse 120 μA			
Joint	n	Mean	±	SD	n	Mean	±	SD	n	Mean	±	SD
Hip	116	20.1	±	6.4	75	19.1	±	6.2	148	21.4	±	4.5
Knee	125	20.9	±	6.1	91	21.0	±	6.5	202	22.4	±	4.6
Ankle	39	24.4	±	8.2	45	20.6	±	4.1	79	27.4	±	9.2
Digit	18	23.7	±	6.8	20	21.9	±	6.8	62	23.6	±	6.1
Intrinsic	26	25.4	±	8.1	18	25.2	±	11.8	13	37.4	±	13.2
Total	324	21.6	±	7.0	249	20.8	±	6.8	504	23.4	±	6.8

Table 8. Comparison of Magnitudes from Contralateral and Ipsilateral Cortices

Total

PStF

	Magnitude, %											
	Contralateral 120 μA				Ipsilateral 120 μA				Ipsi 2 pulse 120 μA			
Joint	n	Mean		SD	n	Mean		SD	n	Mean		SD
Hip	527	22.8	±	27.3	243	8.5	±	3.5	356	11.2	±	6.4
Knee	1246	28.2	±	29.4	632	10.1	±	4.8	1007	15.9	±	11.7
Ankle	1070	62.6	±	97.4	209	9.1	±	3.5	729	13.4	±	6.5
Digit	225	55.0	±	97.5	63	8.0	±	2.3	110	9.1	±	3.2
Intrinsic	613	56.2	±	104.1	302	10.6	±	4.1	539	13.6	±	7.7
Total	3681	43.7	±	76.3	1449	9.7	±	4.3	2741	13.9	±	9.1

PStS

	Magnitude, %											
	Contralateral 120 μA				Ipsilateral 120 μA				Ipsi 2 pulse 120 μA			
Joint	n	Mean		SD	n	Mean		SD	n	Mean		SD
Hip	224	-16.0	±	8.4	116	-8.0	±	4.3	228	-12.4	±	6.3
Knee	302	-15.9	±	7.2	167	-8.6	±	5.3	303	-13.4	±	5.7
Ankle	124	-16.0	±	7.6	85	-7.4	±	4.4	174	-10.6	±	4.0
Digit	30	-15.9	±	8.9	26	-8.5	±	3.7	67	-11.0	±	3.5
Intrinsic	78	-18.0	±	9.6	31	-6.7	±	3.9	29	-9.6	±	3.3
Total	758	-16.2	±	8.0	425	-8.1	±	4.7	801	-12.2	±	5.5

Table 9. Comparison of Onset Latencies from Contralateral and Ipsilateral Cortices

Total

PStF

	Onset Latency, ms											
	Contralateral 120 μA				Ipsilateral 120 μA				Ipsi 2 pulse 120 μA			
Joint	n	Mean		SD	n	Mean		SD	n	Mean		SD
Hip	527	11.9	±	2.9	243	14.7	±	6.9	356	14.8	±	7.0
Knee	1246	11.9	±	3.6	632	13.8	±	5.9	1007	14.9	±	4.8
Ankle	1070	13.1	±	2.1	209	15.9	±	6.4	729	14.9	±	5.2
Digit	225	13.6	±	2.7	63	19.4	±	7.6	110	16.8	±	6.1
Intrinsic	613	14.0	±	3.6	302	13.7	±	5.4	539	15.9	±	6.0
Total	3681	12.7	±	3.2	1449	14.5	±	6.3	2741	15.2	±	5.6

PStS

	Onset Latency, ms											
	Contralateral 120 μA				Ipsilateral 120 μA				Ipsi 2 pulse 120 μA			
Joint	n	Mean		SD	n	Mean		SD	n	Mean		SD
Hip	224	18.4	±	7.8	116	18.0	±	8.1	228	17.7	±	5.2
Knee	302	17.5	±	5.5	167	18.4	±	8.3	303	18.4	±	6.1
Ankle	124	21.0	±	6.0	85	18.5	±	4.1	174	22.8	±	7.0
Digit	30	19.0	±	6.3	26	18.6	±	6.3	67	20.0	±	4.8
Intrinsic	78	22.7	±	6.4	31	21.9	±	8.9	29	30.1	±	9.3
Total	758	18.9	±	6.7	425	18.6	±	7.6	801	19.7	±	6.7

Table 10. Comparison of Peak and Trough Latencies from Contralateral and Ipsilateral Cortices

Total

PStF

Peak Latency, ms

	Contralateral 120 μA				Ipsilateral 120 μA				Ipsi 2 pulse 120 μA			
Joint	n	Mean	±	SD	n	Mean	±	SD	n	Mean	±	SD
Hip	527	14.6	±	3.3	243	17.4	±	8.2	356	18.3	±	8.6
Knee	1246	15.2	±	4.1	632	16.3	±	6.3	1007	18.5	±	5.8
Ankle	1070	16.4	±	2.6	209	18.3	±	6.7	729	18.1	±	5.7
Digit	225	16.1	±	2.7	63	21.2	±	7.7	110	19.3	±	6.6
Intrinsic	613	17.2	±	3.9	302	15.8	±	5.6	539	18.9	±	6.6
Total	3681	15.8	±	3.6	1449	16.9	±	6.3	2741	18.5	±	6.4

PStS

Trough Latency, ms

	Contralateral 120 μA				Ipsilateral 120 μA				Ipsi 2 pulse 120 μA			
Joint	n	Mean	±	SD	n	Mean	±	SD	n	Mean	±	SD
Hip	224	26.3	±	13.5	116	22.6	±	10.7	228	23.5	±	7.0
Knee	302	24.3	±	11.1	167	22.5	±	9.9	303	23.8	±	7.5
Ankle	124	33.8	±	14.6	85	21.7	±	4.6	174	28.6	±	9.1
Digit	30	25.5	±	11.9	26	21.2	±	6.9	67	23.5	±	6.0
Intrinsic	78	33.5	±	13.8	31	26.1	±	11.5	29	36.2	±	11.7
Total	758	27.4	±	13.3	425	22.5	±	9.4	801	25.2	±	8.4

Figure 1. Types of poststimulus effects observed in stimulus triggered averages of EMG activity. Poststimulus facilitation (PStF) is a transient increase in firing probability suggesting a facilitatory linkage between the population of cells stimulated and target motoneurons. Poststimulus suppression (PStS) is a transient decrease in firing probability suggesting an inhibitory linkage between the population of cells stimulated and target motoneurons.

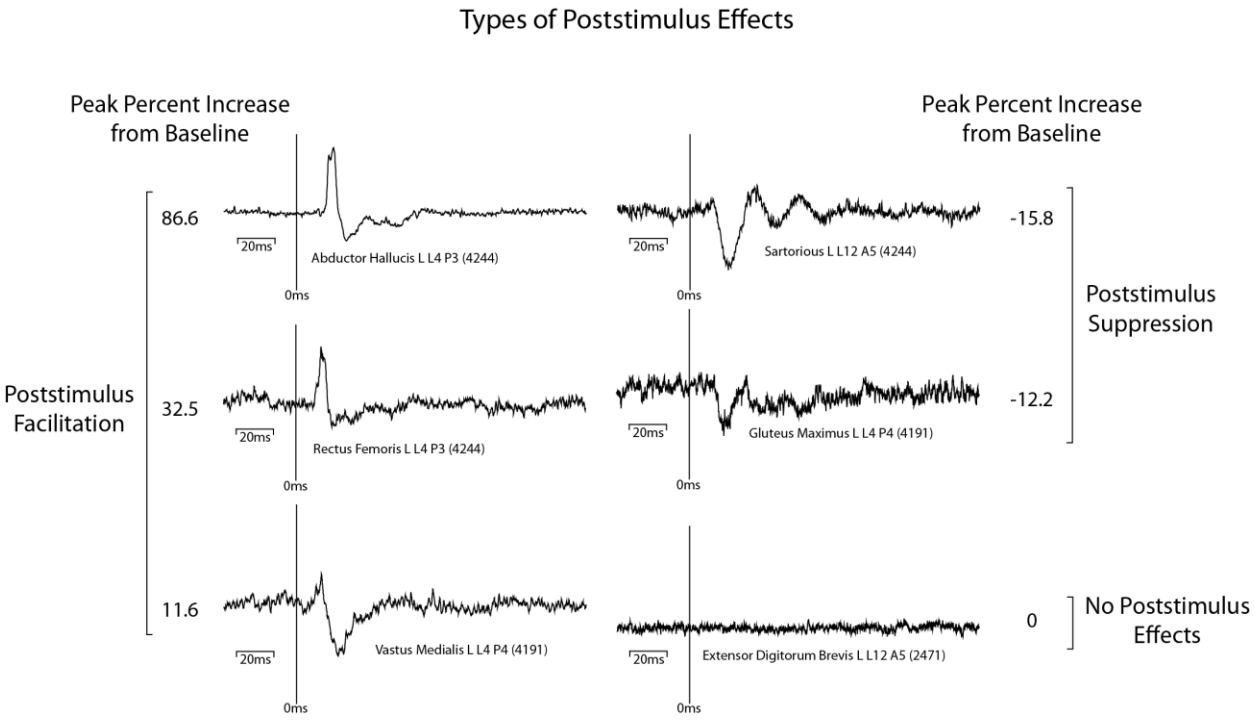
Types of Poststimulus Effects
Peak Percent Increase from Baseline
Peak Percent Increase from Baseline
86.6
20ms
Abductor Hallucis L L4 P3 (4244)
0ms
-15.8
20ms
Sartorious L L12 A5 (4244)
0ms
Poststimulus Suppression
Poststimulus Facilitation
32.5
20ms
Rectus Femoris L L4 P3 (4244)
0ms
-12.2
20ms
Gluteus Maximus L L4 P4 (4191)
0ms
11.6
20ms
Vastus Medialis L L4 P4 (4191)
0ms
0
20ms
Extensor Digitorum Brevis L L12 A5 (2471)
0ms
No Poststimulus Effects

Figure 2. Stimulus triggered averages of EMG activity using various microstimuli (30 μA, 60 μA, 120 μA, 2 pulses of 120 μA) in the ipsilateral and contralateral cortices. Effects from stimulation of the ipsilateral cortex at 30 μA are almost completely absent, and effects at 60 μA are too weak and too few in number for adequate comparison to contralateral effects. Effects from simulation of the ipsilateral cortex at 120 μA yield effects that can be compared to contralateral effects in terms of sign, latency, and magnitude.

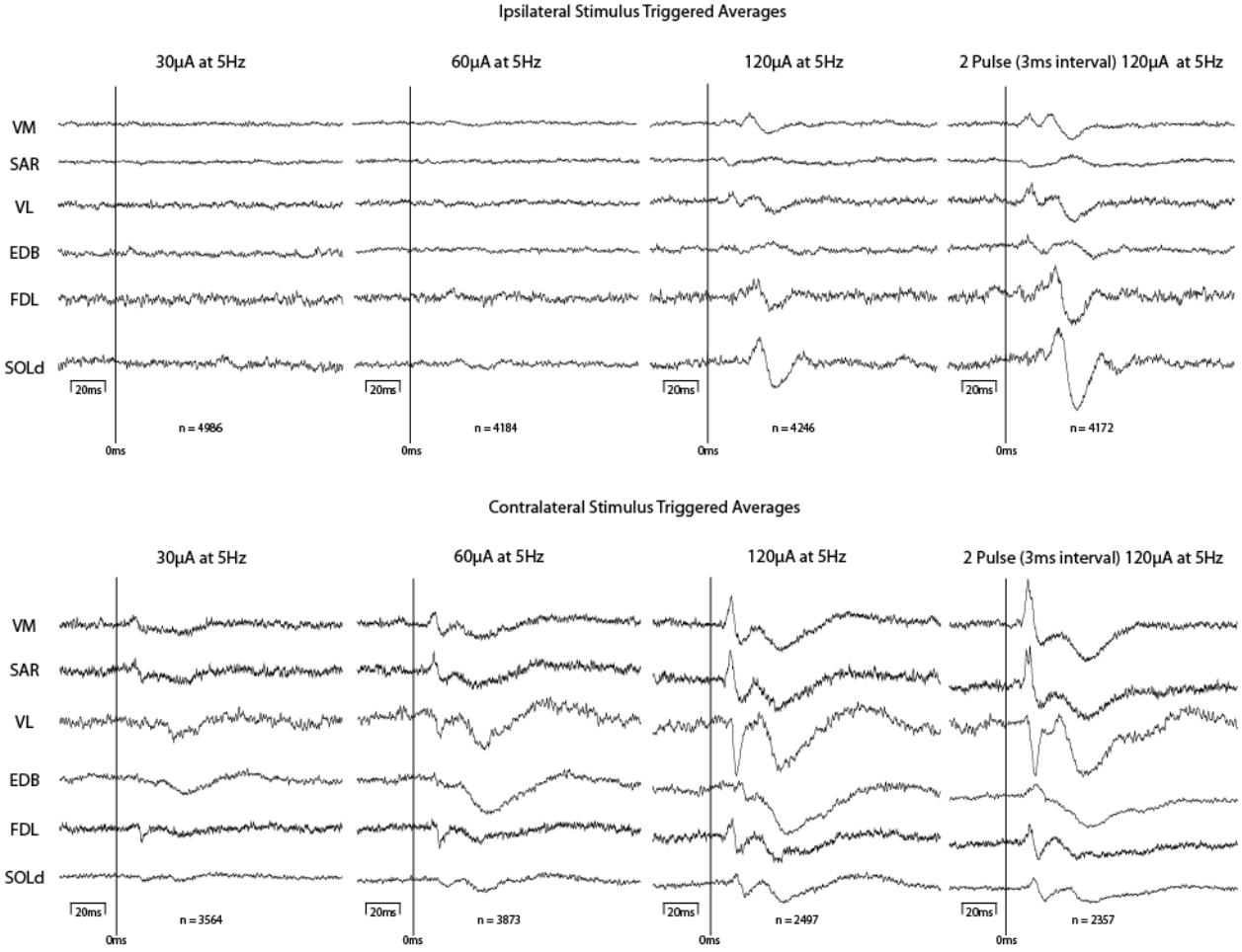
Ipsilateral Stimulus Triggered Averages
30µA at 5Hz
60µA at 5Hz
120µA at 5Hz
2 Pulse (3ms interval) 120µA at 5Hz
VM
SAR
VL
EDB
FDL
SOLd
20ms
0ms
n = 4986
n = 4184
n = 4246
n = 4172
Contralateral Stimulus Triggered Averages
30µA at 5Hz
60µA at 5Hz
120µA at 5Hz
2 Pulse (3ms interval) 120µA at 5Hz
VM
SAR
VL
EDB
FDL
SOLd
20ms
0ms
n = 3564
n = 3873
n = 2497
n = 2357

Figure 3. Contralateral and ipsilateral tracks in Monkey M. A 1mm x 1mm grid superimposed onto a 3D reconstruction of Monkey M's MRI, the dark circle outlines the interior circumference of the implanted cortical chamber. Solid circles represent electrode tracks that produced hindlimb movement with ICMS. Open circles represent electrode tracks that produced non-hindlimb (trunk, tail, etc.) with ICMS. Stars represent electrode tracks that did not produce visible movement on ICMS. Open boxes represent electrode tracks that were positive on a sensory test and helps identify the border of the somatosensory area.

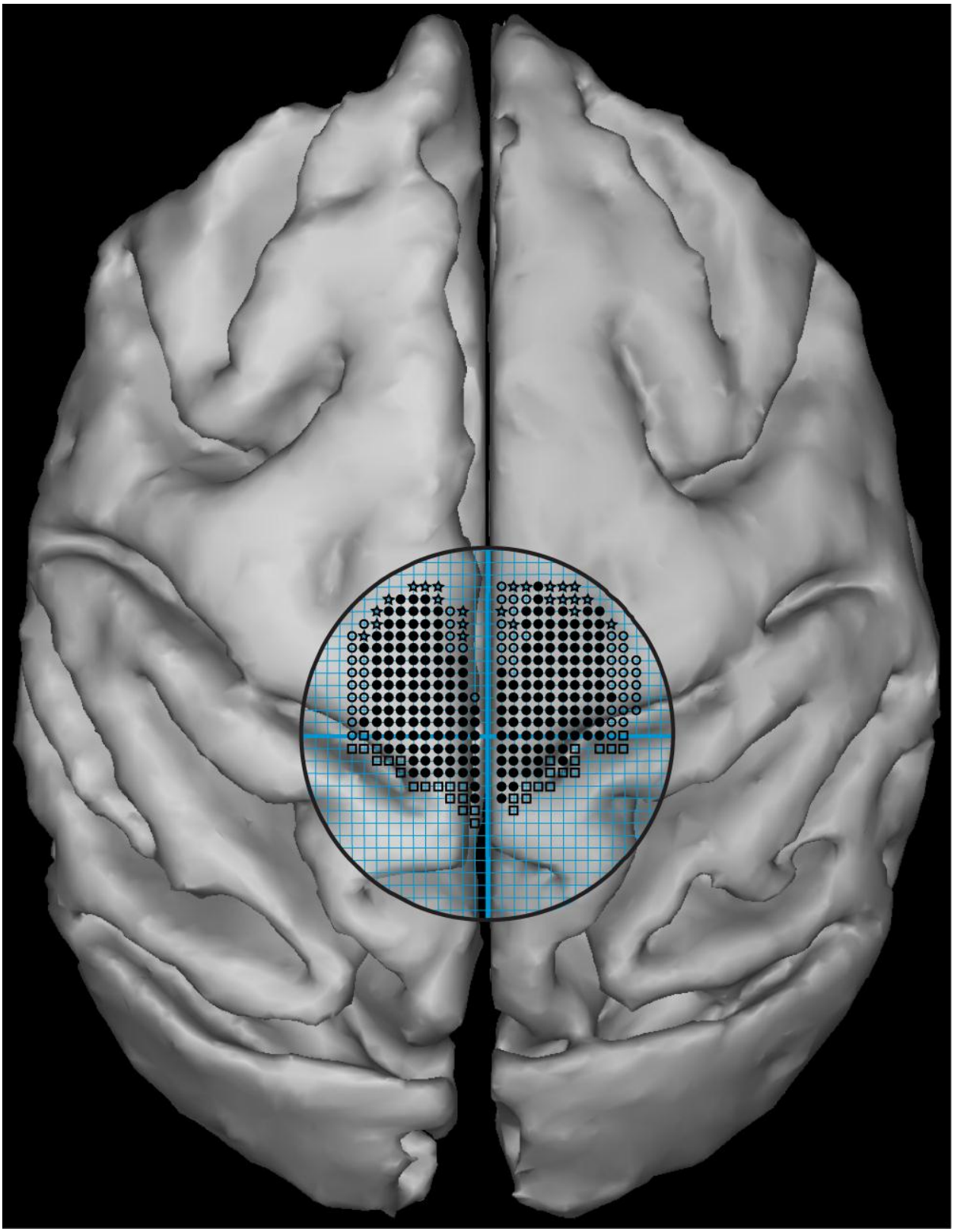

Figure 4. Contralateral and ipsilateral tracks in Monkey L. A 1mm x 1mm grid superimposed onto a 3D reconstruction of Monkey L's MRI, the dark circle outlines the interior circumference of the implanted cortical chamber. Solid circles represent electrode tracks that produced hindlimb movement with ICMS. Open circles represent electrode tracks that produced non-hindlimb (trunk, tail, etc.) with ICMS. Stars represent electrode tracks that did not produce visible movement on ICMS. Open boxes represent electrode tracks that were positive on a sensory test and helps identify the border of the somatosensory area.

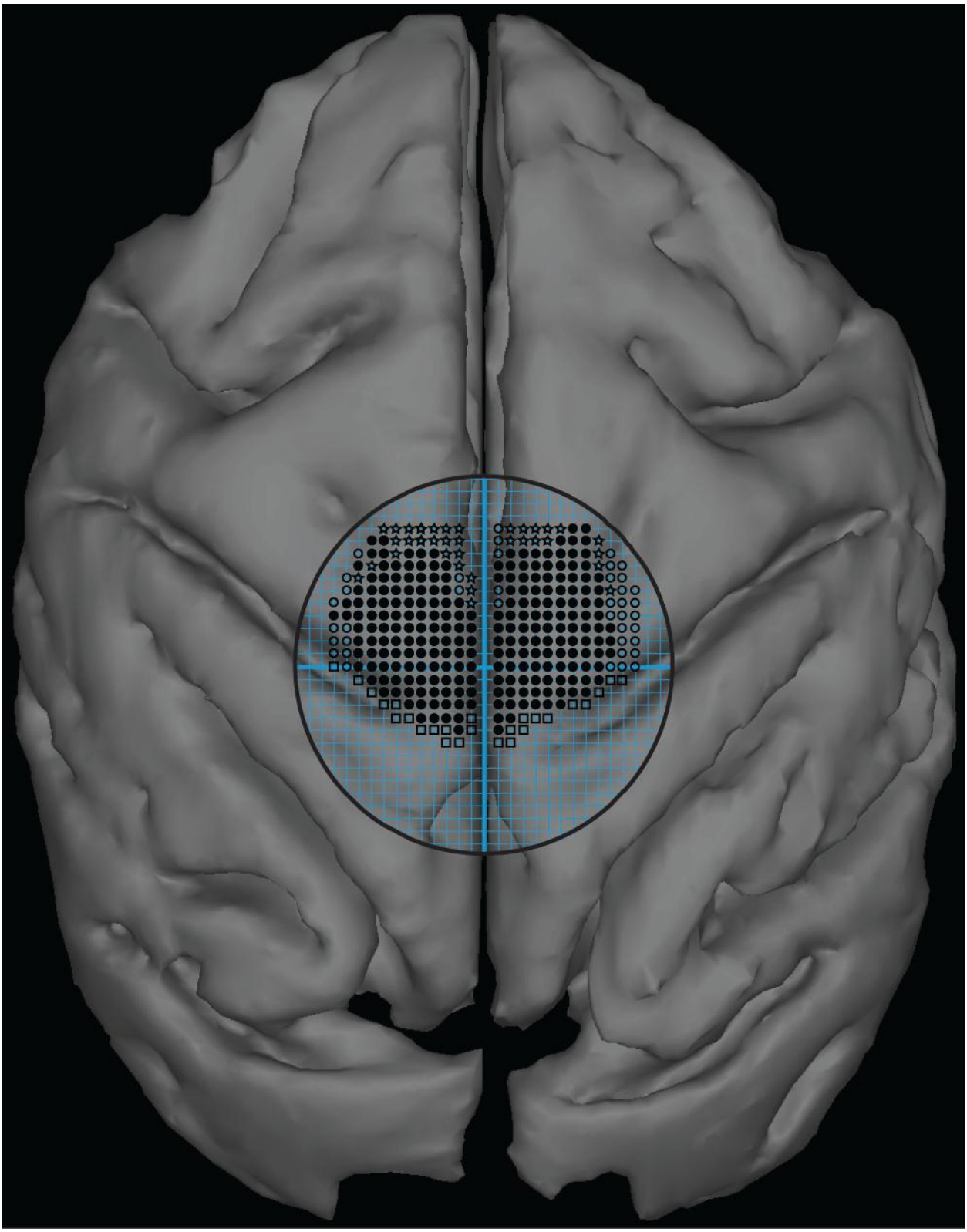

Figure 5. Number of PStF and PStS effects in each muscle separated by joint using 120 μA stimulus in the contralateral and ipsilateral hemisphere, as well as a two pulse, 120 μA stimulus (3 ms interval) in the ipsilateral hemisphere.

Distribution of Post Stimulus Effects by Joint and Muscle

Contralateral 120µA

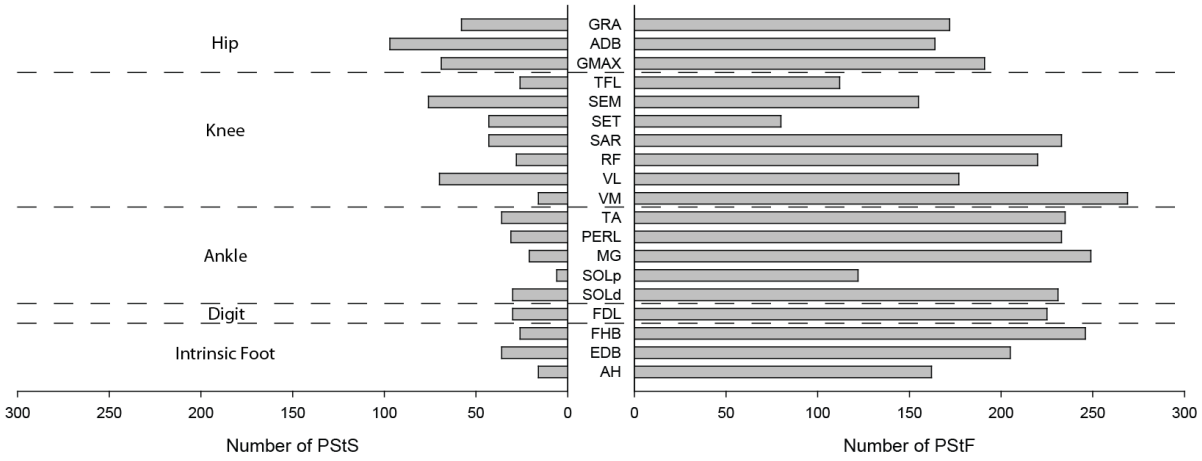

Ipsilateral 120µA

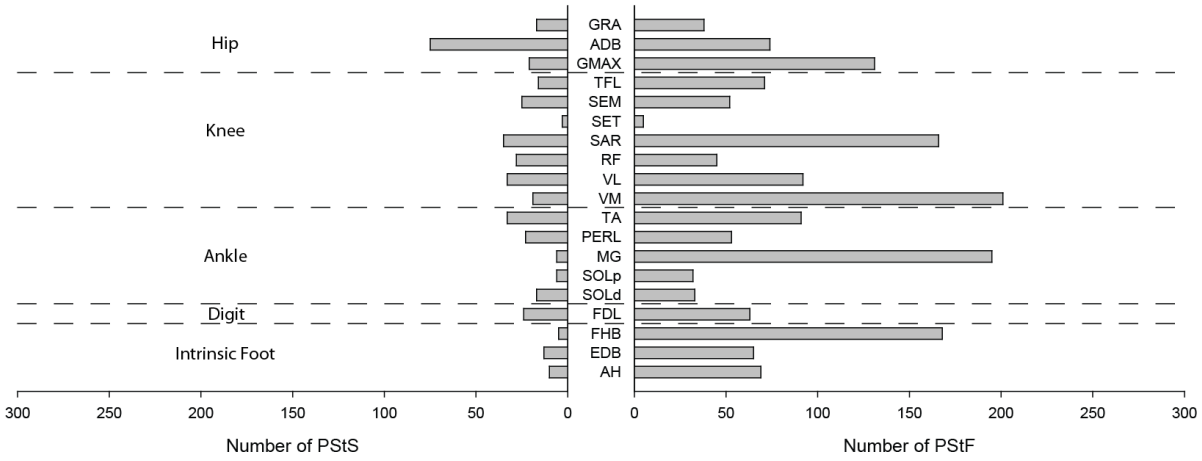

Ipsilateral 2Pulse 120µA

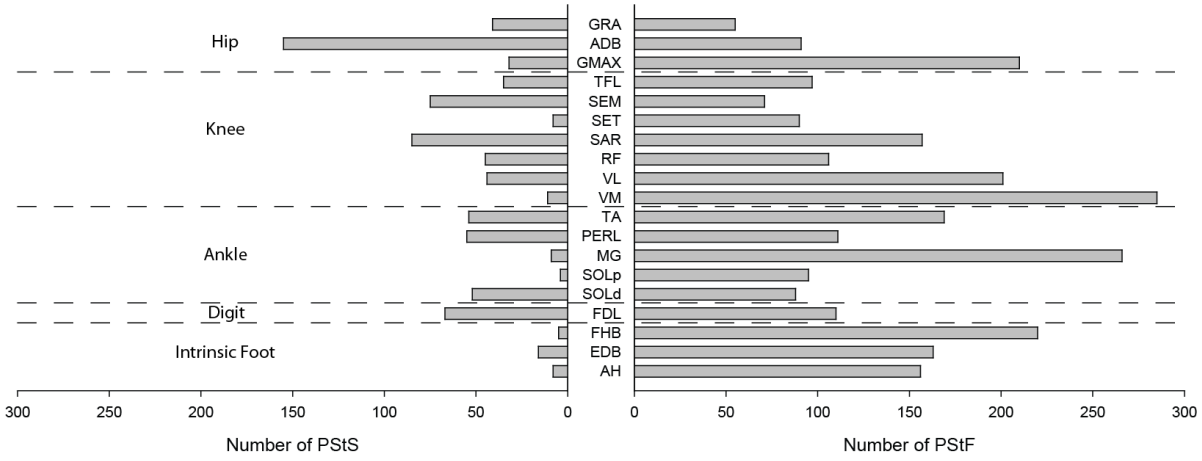

Figure 6. Distribution of PStF magnitudes for hip muscles using 120 μA stimulus in the contralateral and ipsilateral hemisphere for Monkey M. The mean, median, mode, % of effects above 20PPI, and range for each muscle group is also shown.

Hip Muscles

Monkey M

Contralateral 120µA

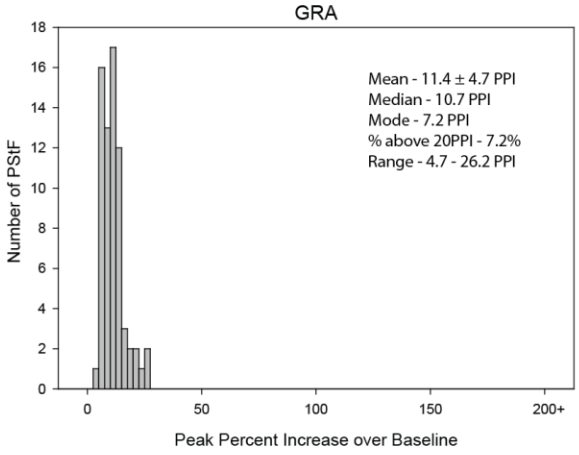

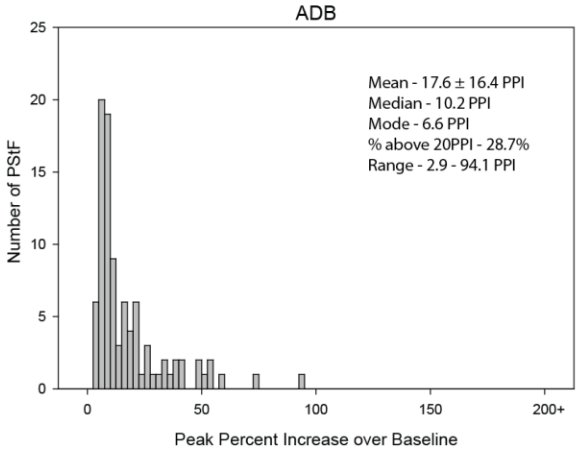

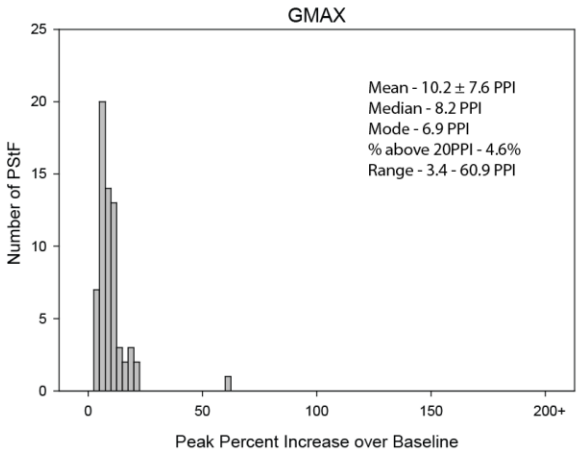

Ipsilateral 120µA

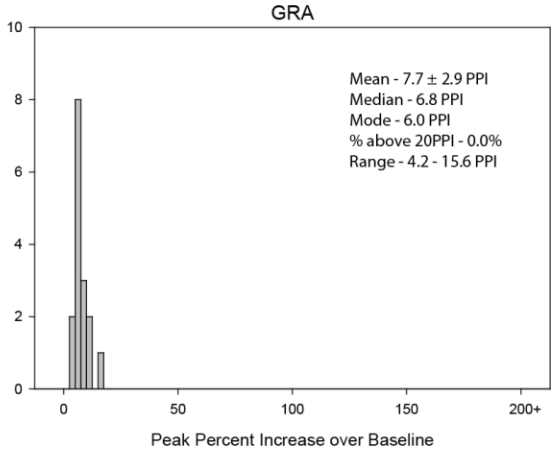

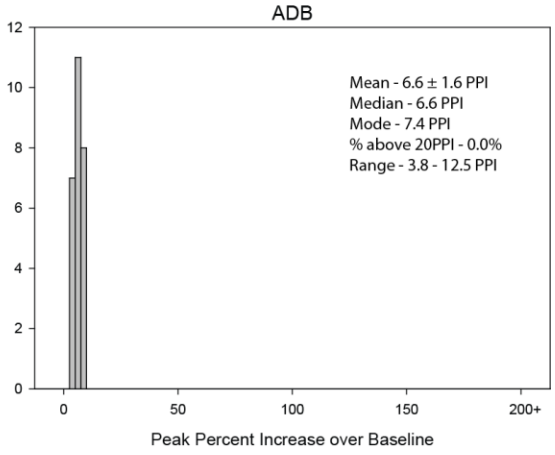

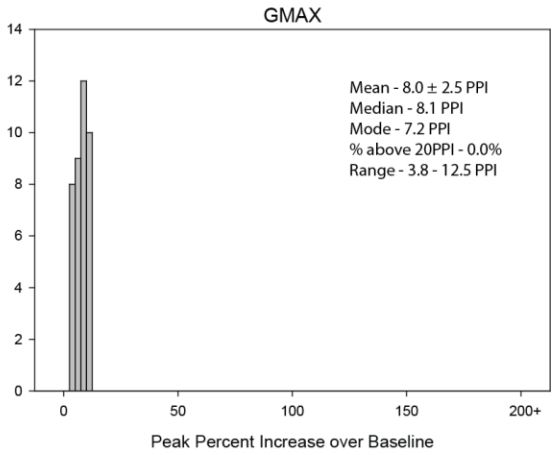

Figure 7. Distribution of PStF magnitudes for hip muscles using 120 μA stimulus in the contralateral and ipsilateral hemisphere for Monkey L. The mean, median, mode, % of effects above 20PPI, and range for each muscle group is also shown.

Hip Muscles

Monkey L

Contralateral 120µA

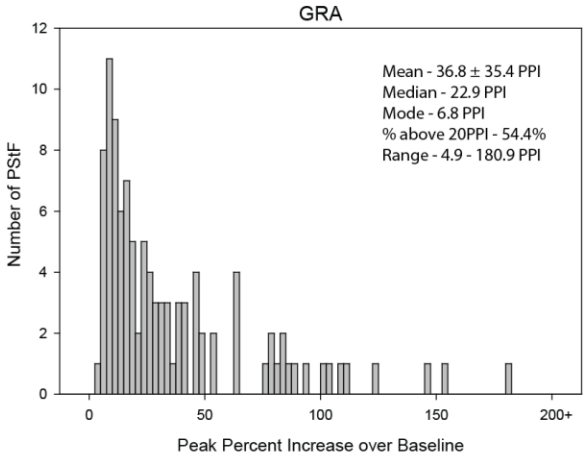

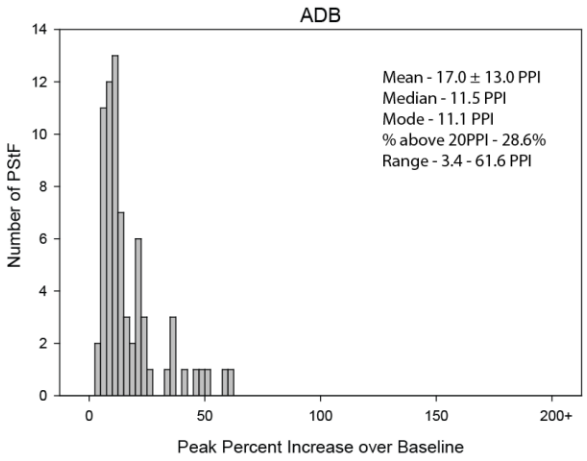

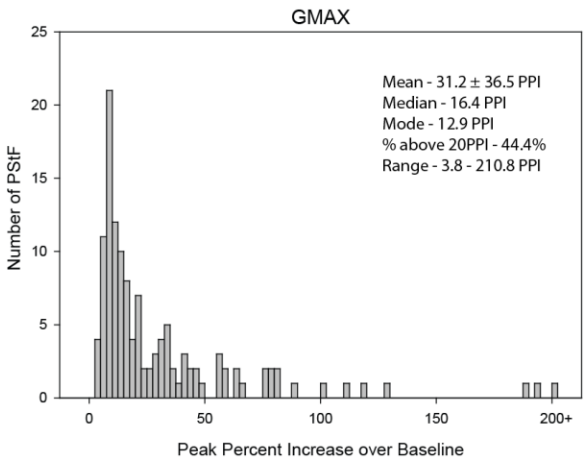

Ipsilateral 120µA

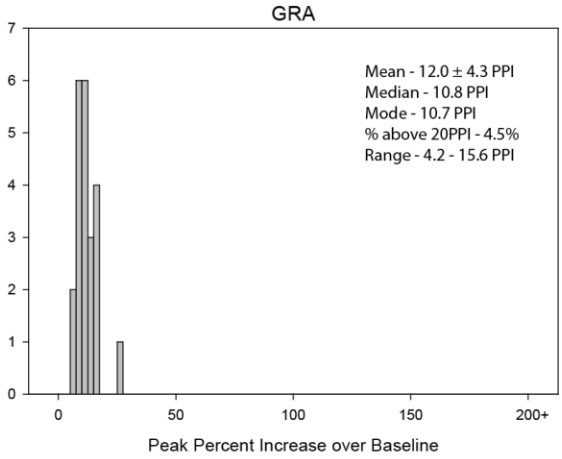

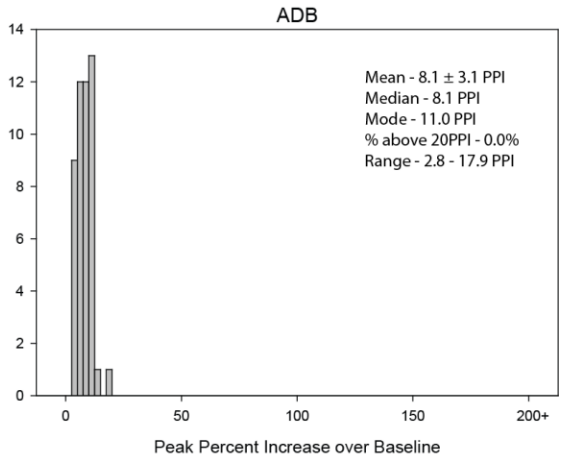

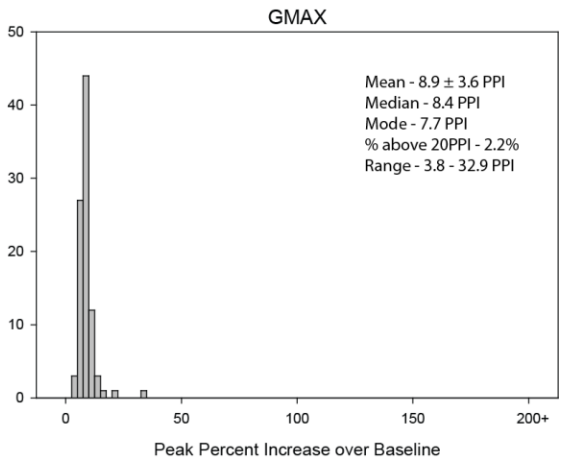

Figure 8. Distribution of PStF magnitudes for hip muscles using 120 μA stimulus in the contralateral and ipsilateral hemisphere for both monkeys. The mean, median, mode, % of effects above 20PPI, and range for each muscle group is also shown.

Hip Muscles

Total

Contralateral 120µA

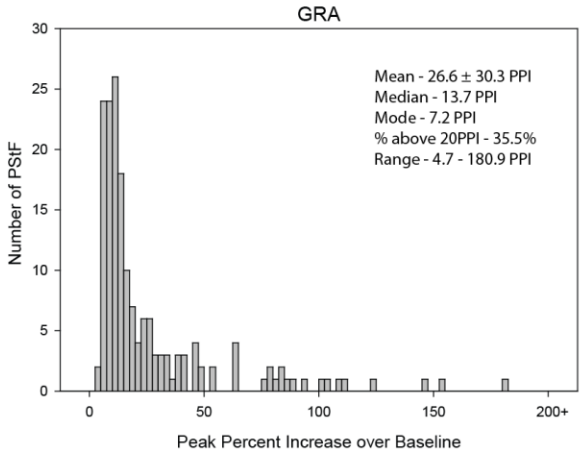

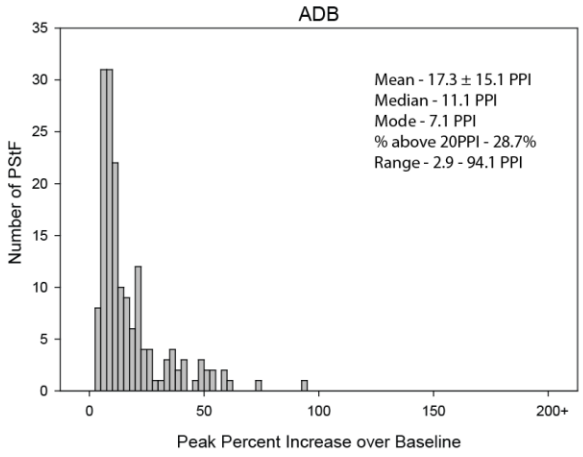

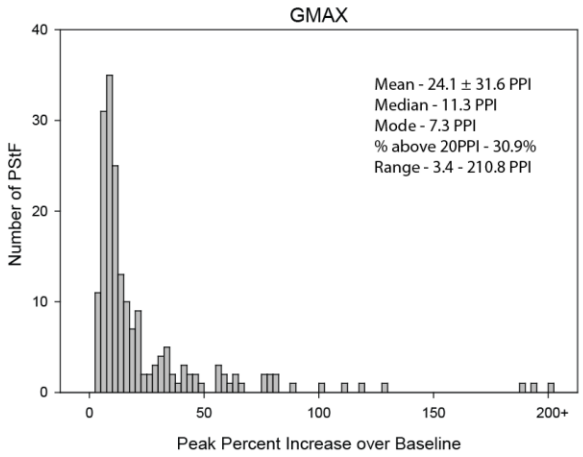

Ipsilateral 120µA

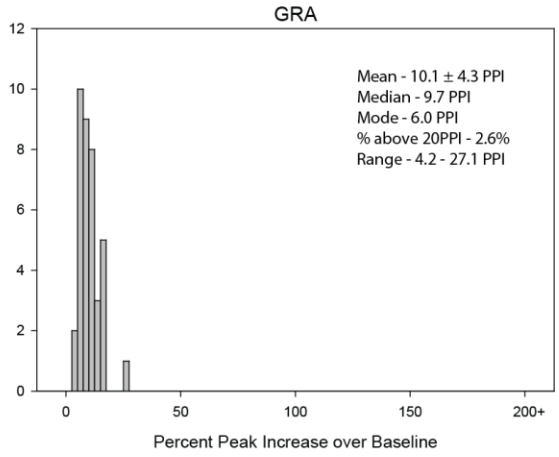

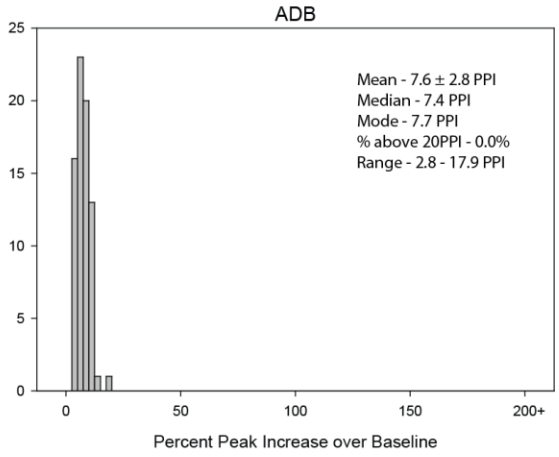

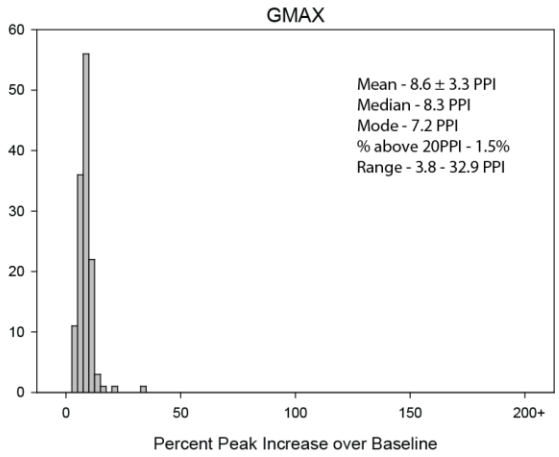

Figure 9. Distribution of PStF magnitudes for knee muscles using 120 μA stimulus in the contralateral and ipsilateral hemisphere for Monkey M. The mean, median, mode, % of effects above 20PPI, and range for each muscle group is also shown.

Knee Muscles

Monkey M

Contralateral 120µA

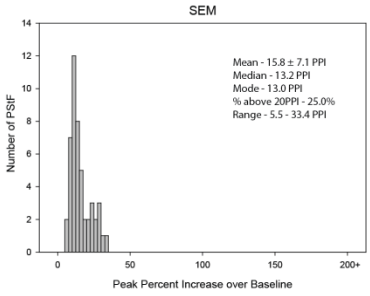

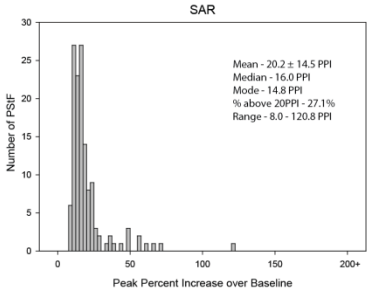

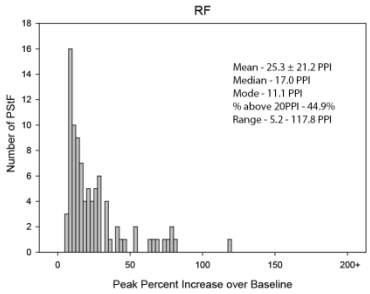

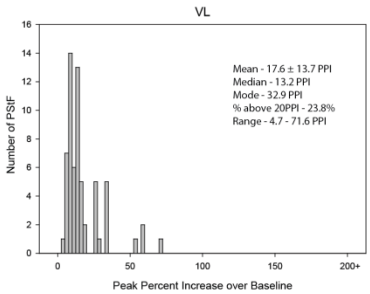

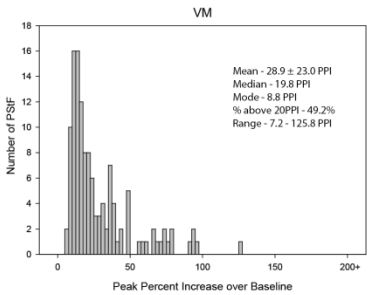

Ipsilateral 120µA

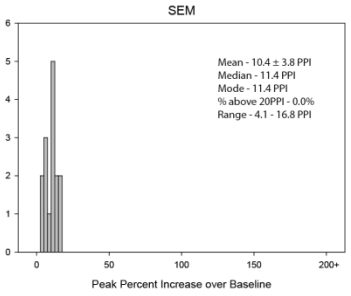

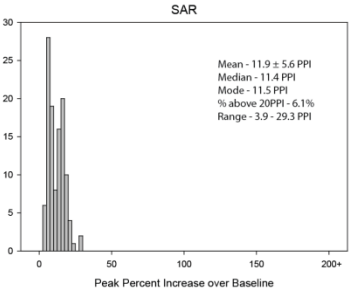

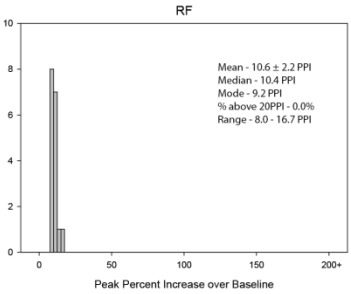

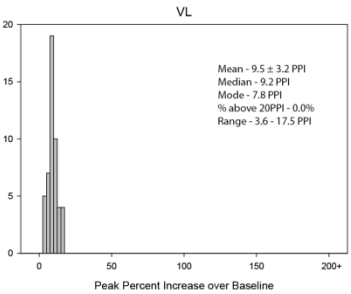

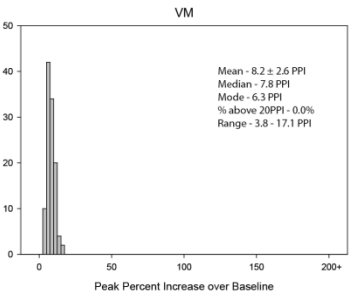

Figure 10. Distribution of PStF magnitudes for knee muscles using 120 μA stimulus in the contralateral and ipsilateral hemisphere for Monkey L. The mean, median, mode, % of effects above 20PPI, and range for each muscle group is also shown.

Knee Muscles

Monkey L

Contralateral 120µA

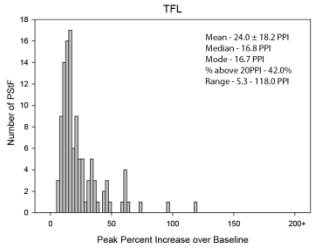

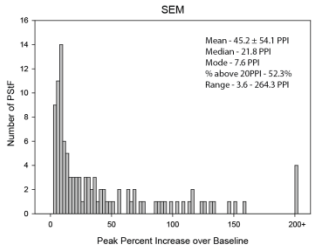

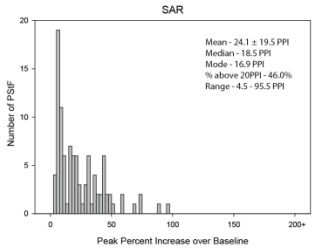

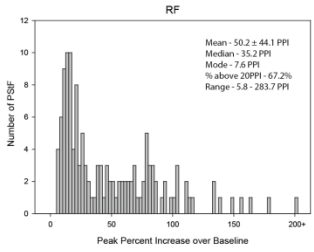

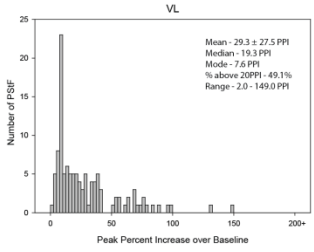

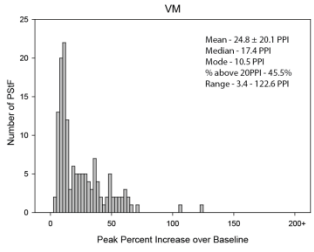

Ipsilateral 120µA

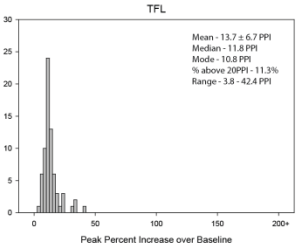

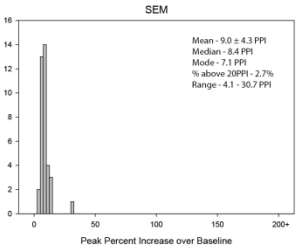

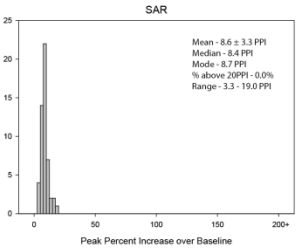

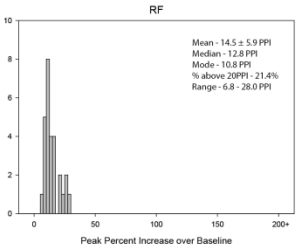

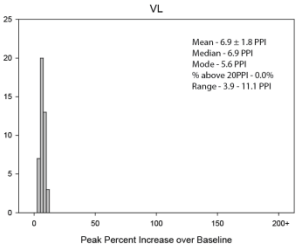

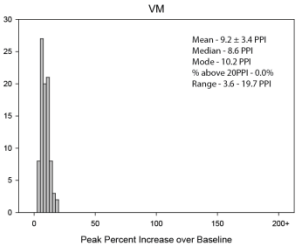

Figure 11. Distribution of PStF magnitudes for knee muscles using 120 μA stimulus in the contralateral and ipsilateral hemisphere for both monkeys. The mean, median, mode, % of effects above 20PPI, and range for each muscle group is also shown.

Knee Muscles

Total

Contralateral 120μA

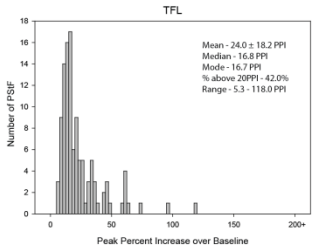

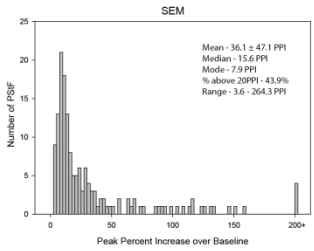

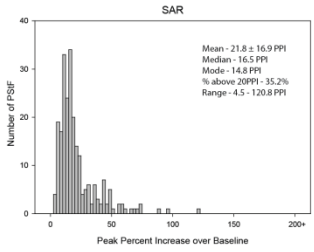

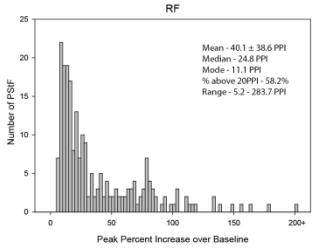

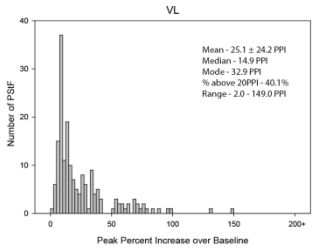

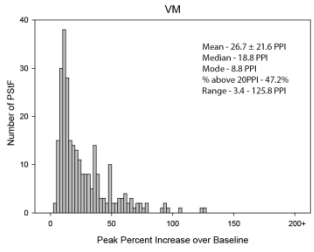

Ipsilateral 120μA

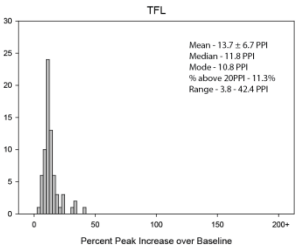

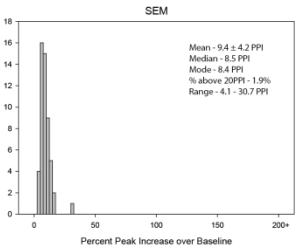

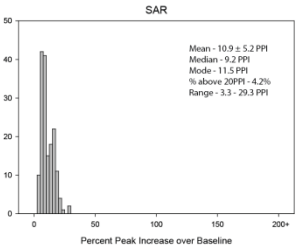

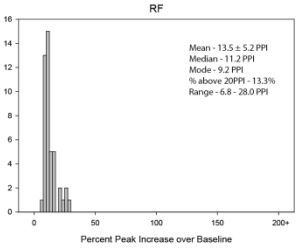

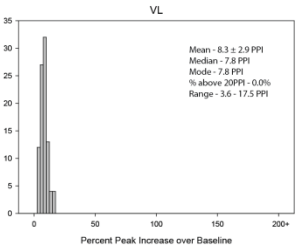

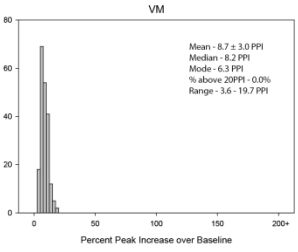

Figure 12. Distribution of PStF magnitudes for ankle muscles using 120 μA stimulus in the contralateral and ipsilateral hemisphere for Monkey M. The mean, median, mode, % of effects above 20PPI, and range for each muscle group is also shown.

Ankle Muscles

Monkey M

Contralateral 120µA

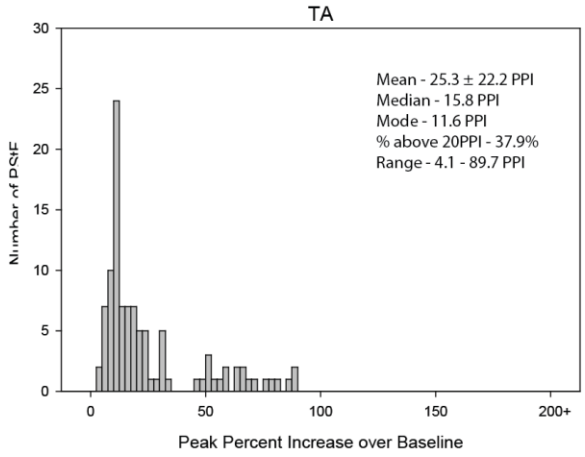

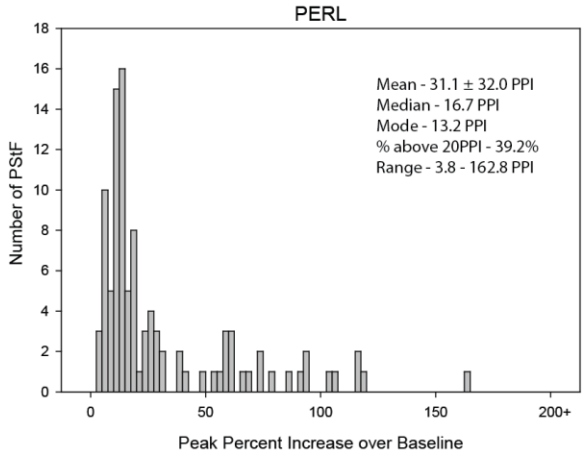

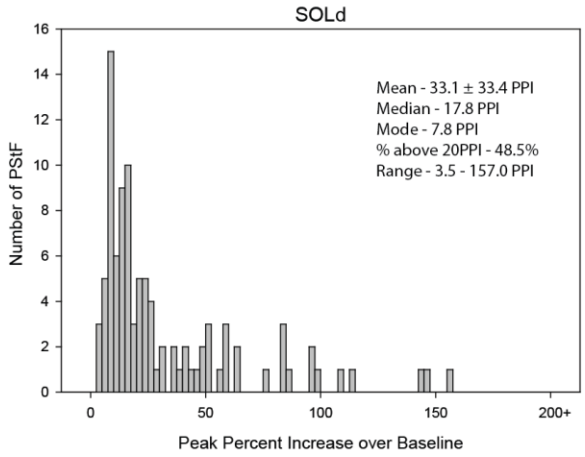

Ipsilateral 120µA

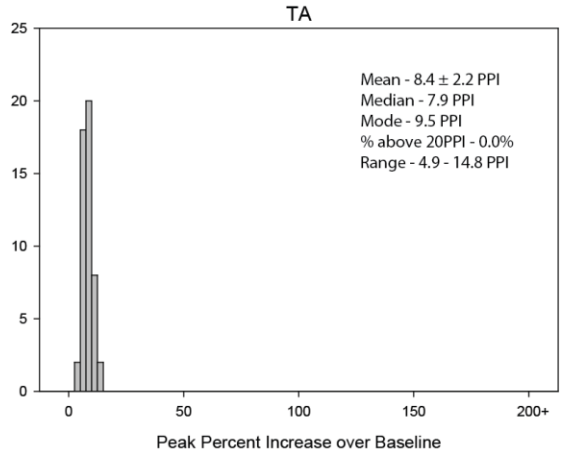

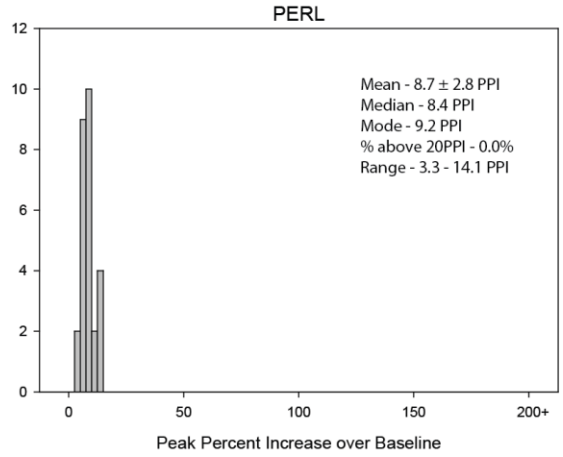

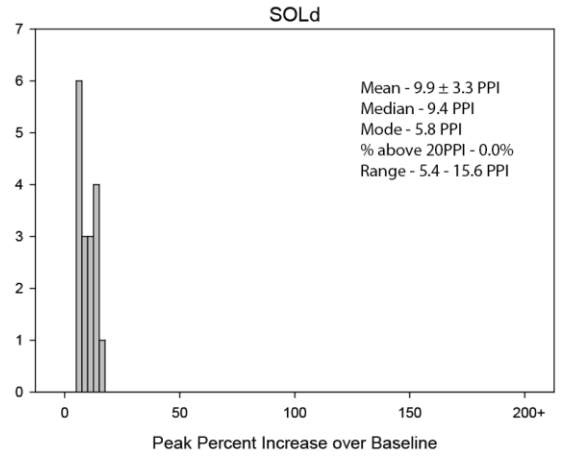

Figure 13. Distribution of PStF magnitudes for ankle muscles using 120 μA stimulus in the contralateral and ipsilateral hemisphere for Monkey L. The mean, median, mode, % of effects above 20PPI, and range for each muscle group is also shown.

Ankle Muscles

Monkey L

Contralateral 120µA

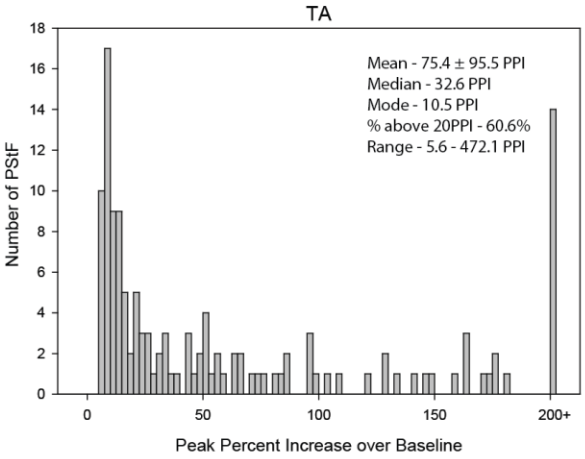

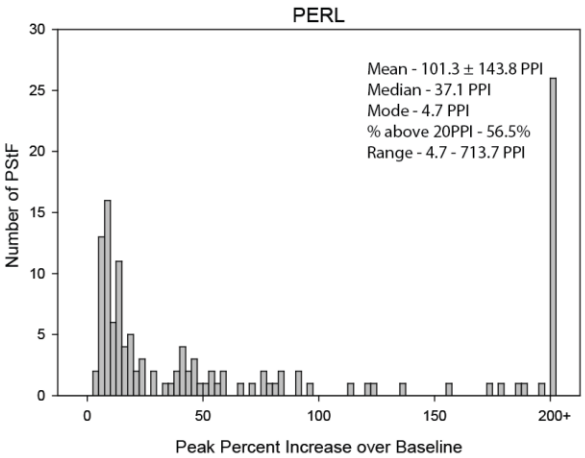

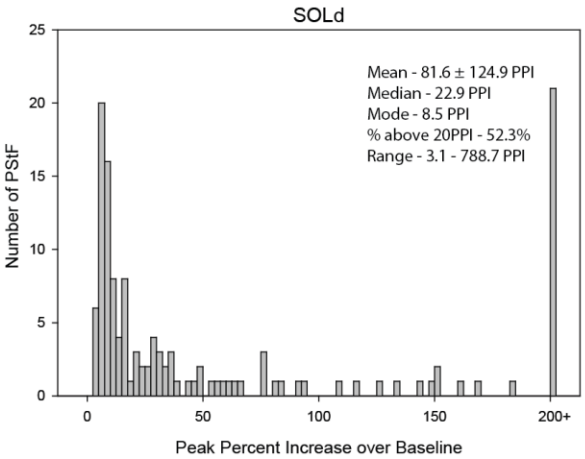

Ipsilateral 120µA

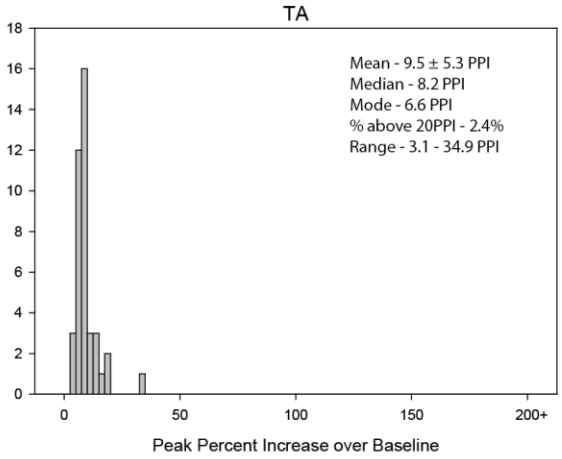

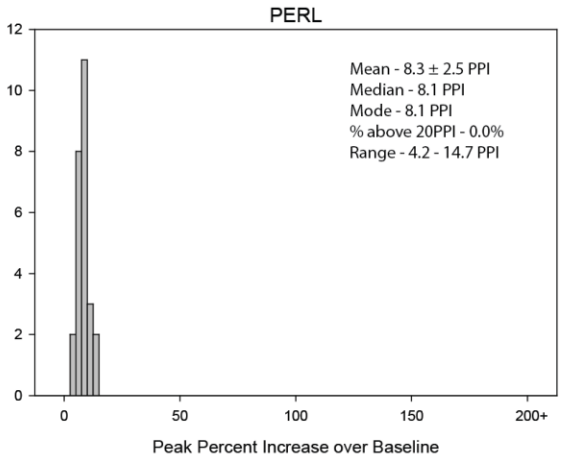

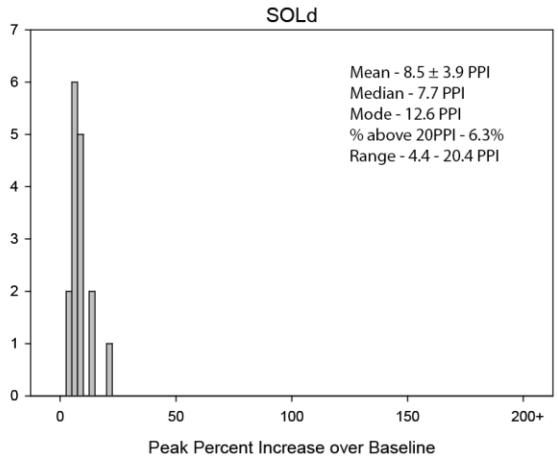

Figure 14. Distribution of PStF magnitudes for ankle muscles using 120 μA stimulus in the contralateral and ipsilateral hemisphere for both monkeys. The mean, median, mode, % of effects above 20PPI, and range for each muscle group is also shown.

Ankle Muscles

Total

Contralateral 120µA

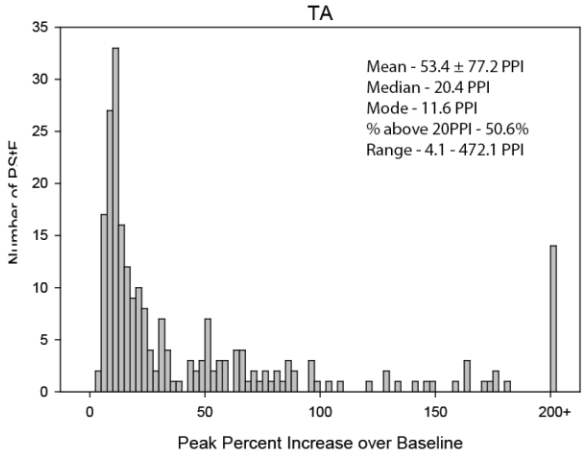

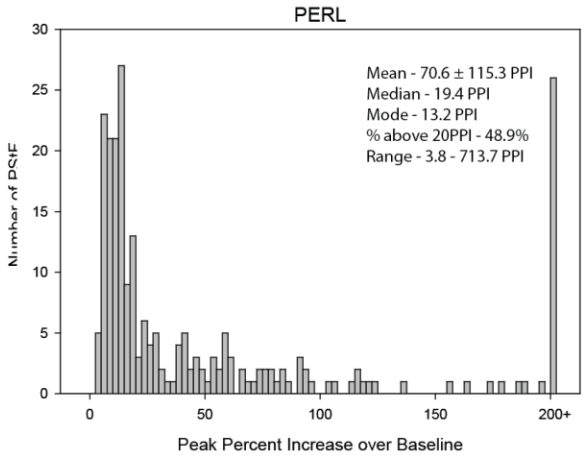

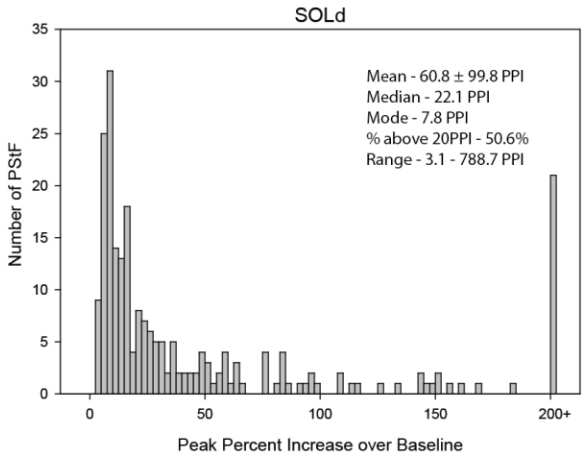

Ipsilateral 120µA

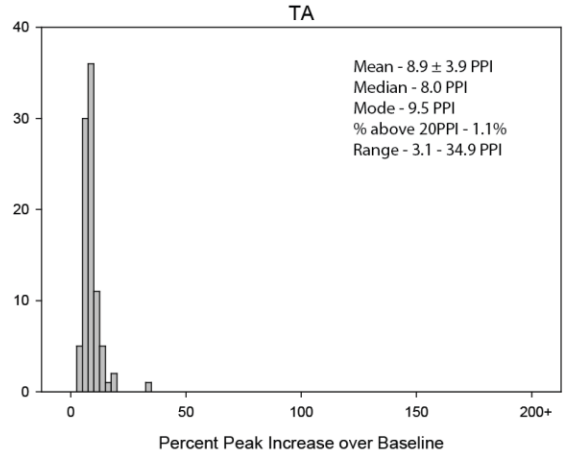

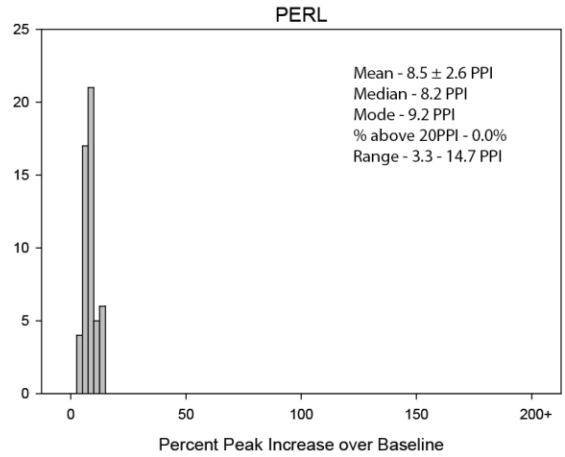

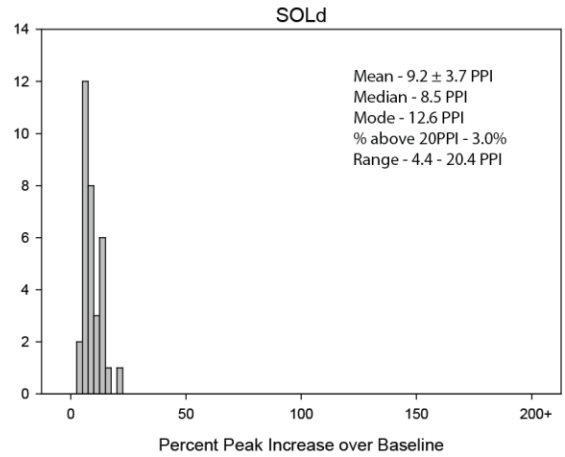

Figure 15. Distribution of PStF magnitudes for digit and intrinsic foot muscles using 120 μA stimulus in the contralateral and ipsilateral hemisphere for Monkey M. The mean, median, mode, % of effects above 20PPI, and range for each muscle group is also shown.

Digit Muscles

Monkey M

Contralateral 120µA

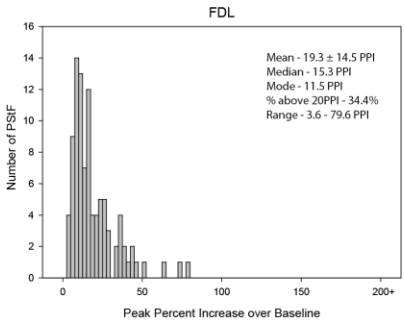

Ipsilateral 120µA

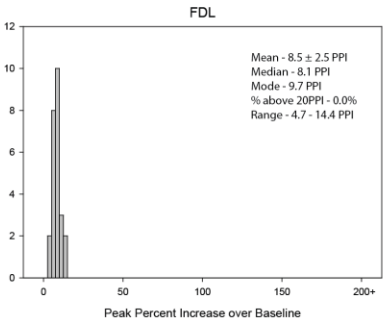

Intrinsic Foot Muscles

Monkey M

Contralateral 120µA

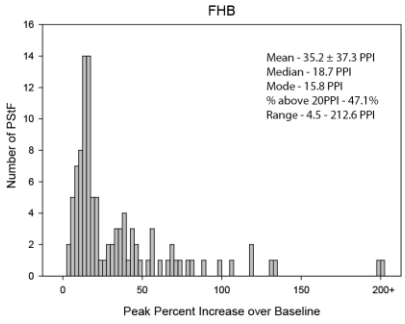

Ipsilateral 120µA

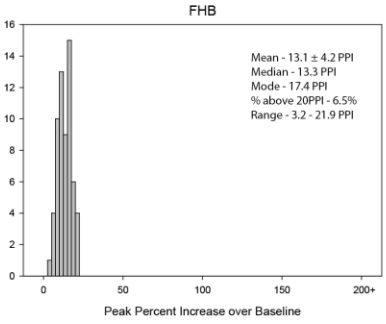

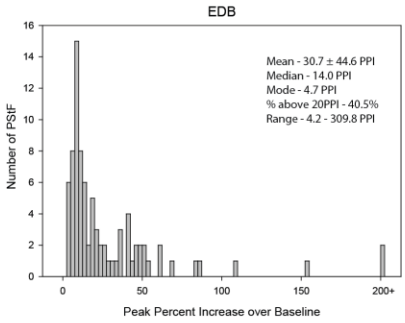

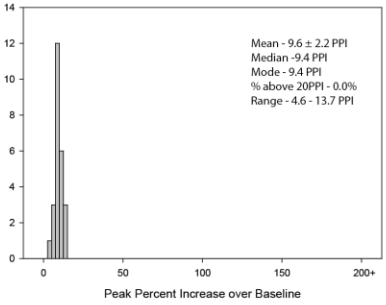

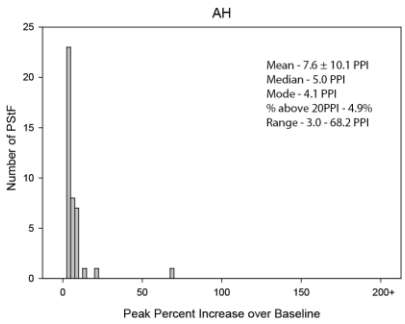

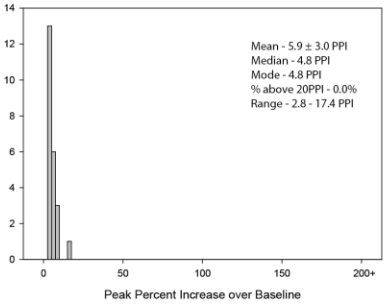

Figure 16. Distribution of PStF magnitudes for digit and intrinsic foot muscles using 120 μA stimulus in the contralateral and ipsilateral hemisphere for Monkey L. The mean, median, mode, % of effects above 20PPI, and range for each muscle group is also shown.

Digit Muscles

Monkey L

Contralateral 120µA

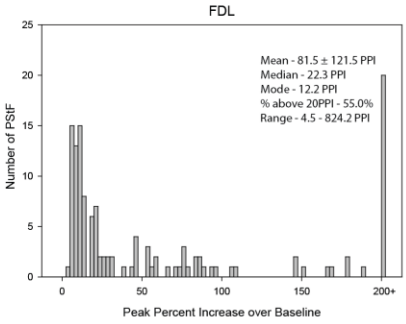

Ipsilateral 120µA

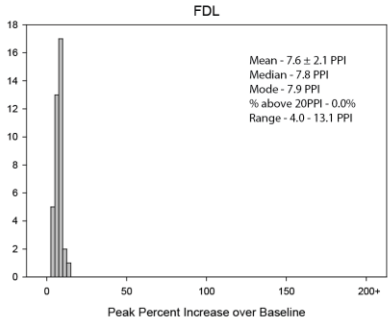

Intrinsic Foot Muscles

Monkey L

Contralateral 120µA

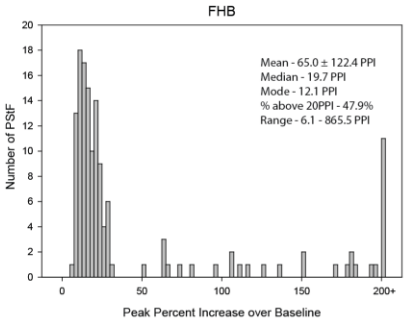

Ipsilateral 120µA

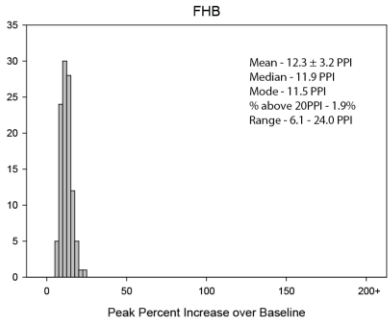

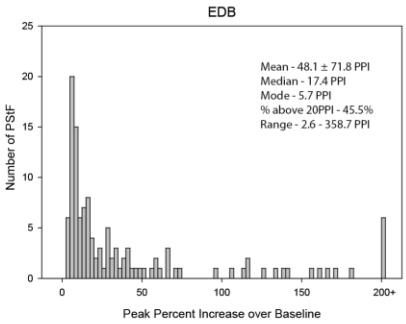

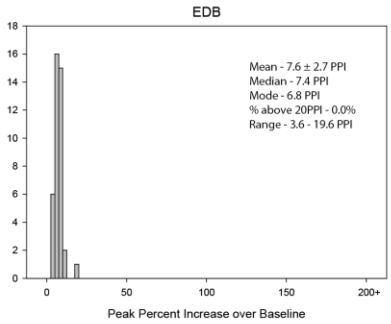

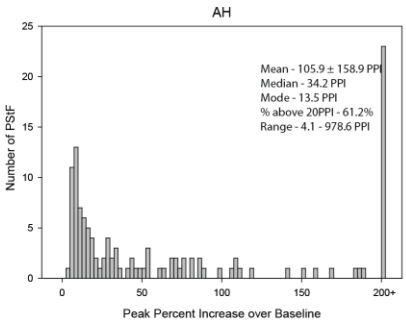

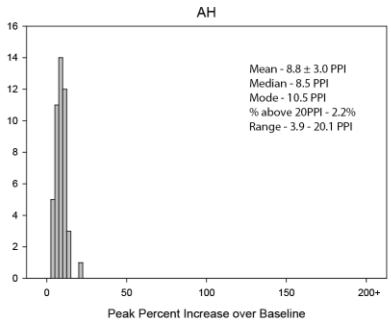

Figure 17. Distribution of PStF magnitudes for digit and intrinsic foot muscles using 120 μA stimulus in the contralateral and ipsilateral hemisphere for both monkeys. The mean, median, mode, % of effects above 20PPI, and range for each muscle group is also shown.

Digit Muscles

Total

Contralateral 120μA

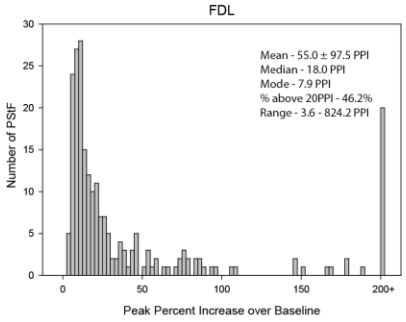

Ipsilateral 120μA

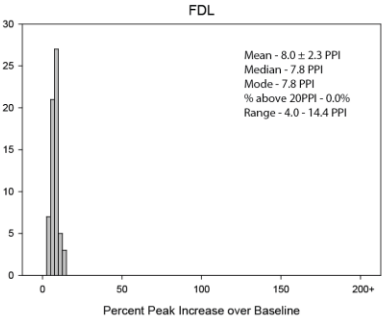

Intrinsic Foot Muscles

Total

Contralateral 120μA

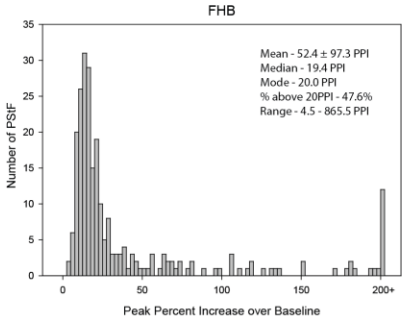

Ipsilateral 120μA

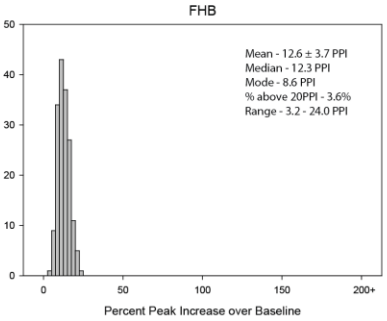

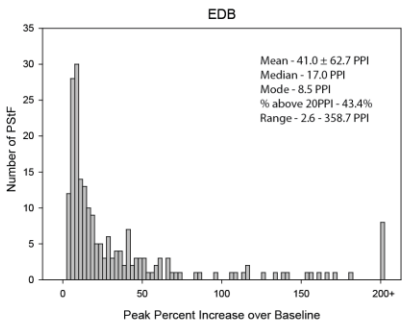

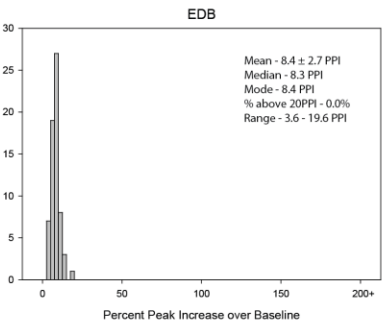

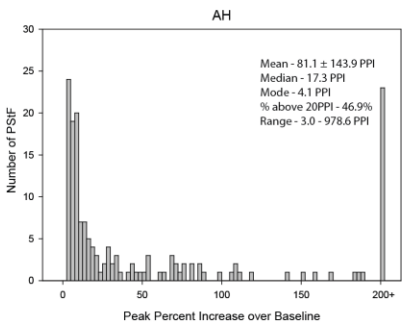

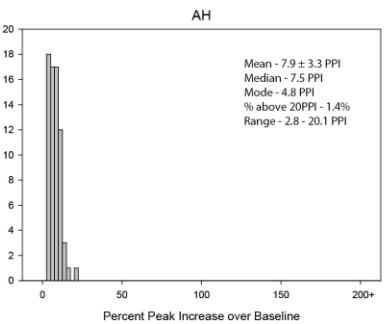

Figure 18. Distribution of PStF magnitudes for all muscles at the hip, knee, ankle, digit, and intrinsic foot joints using 120 μA stimulus in the contralateral and ipsilateral hemisphere for Monkey M. The mean, median, mode, % of effects above 20PPI, and range for each muscle group is also shown.

All Muscles

Monkey M

Contralateral 120µA

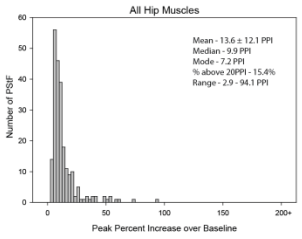

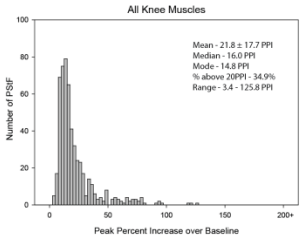

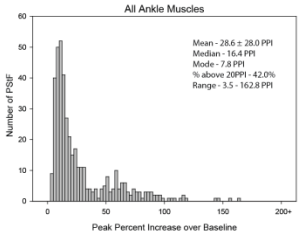

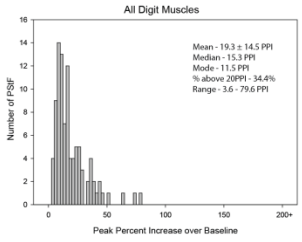

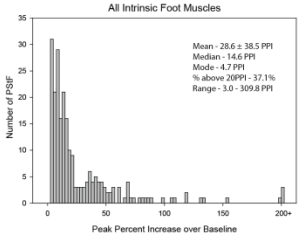

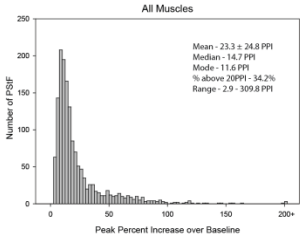

Ipsilateral 120µA

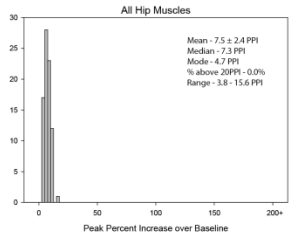

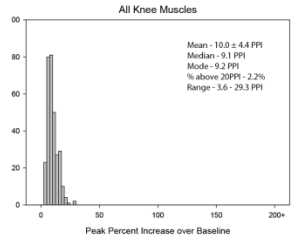

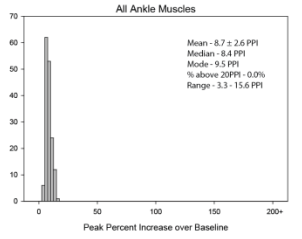

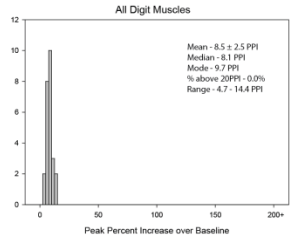

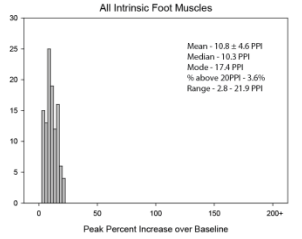

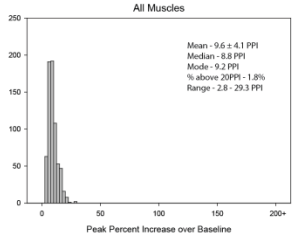

Figure 19. Distribution of PStF magnitudes for all muscles at the hip, knee, ankle, digit, and intrinsic foot joints using 120 μA stimulus in the contralateral and ipsilateral hemisphere for Monkey L. The mean, median, mode, % of effects above 20PPI, and range for each muscle group is also shown.

All Muscles

Monkey L

Contralateral 120µA

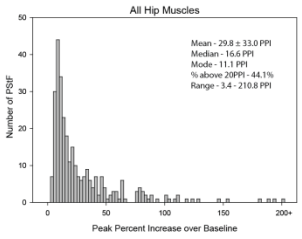

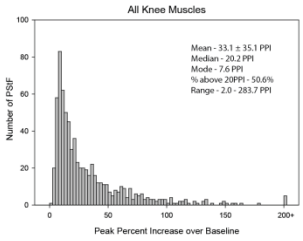

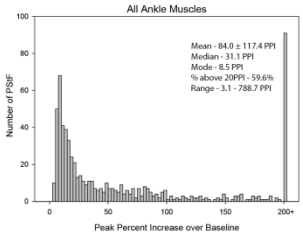

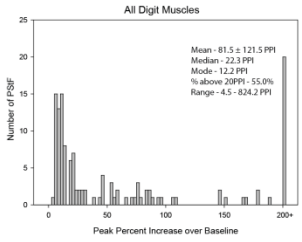

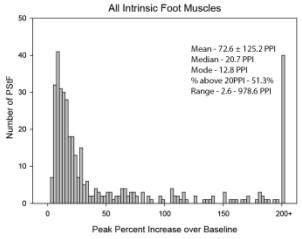

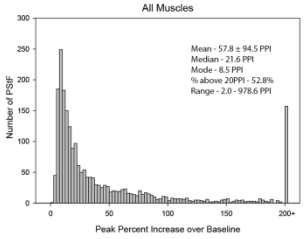

Ipsilateral 120µA

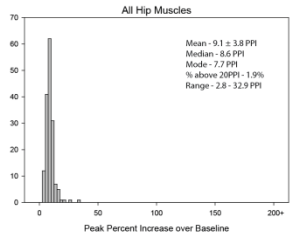

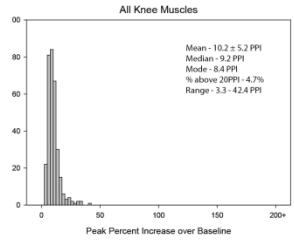

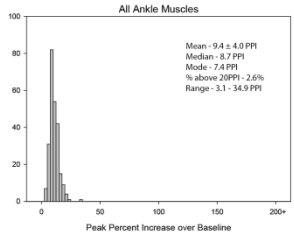

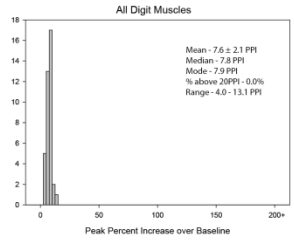

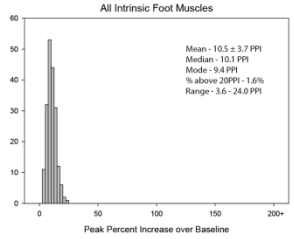

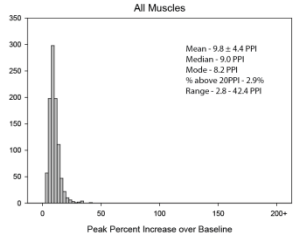

Figure 20. Distribution of PStF magnitudes for all muscles at the hip, knee, ankle, digit, and intrinsic foot joints using 120 μA stimulus in the contralateral and ipsilateral hemisphere for both monkeys. The mean, median, mode, % of effects above 20PPI, and range for each muscle group is also shown.

All Muscles

Total

Contralateral 120µA

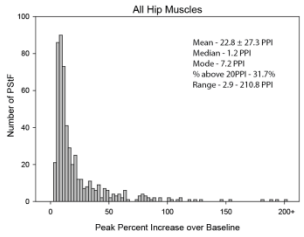

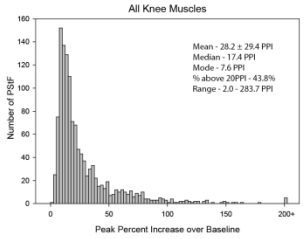

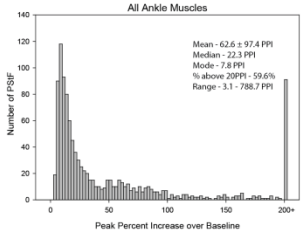

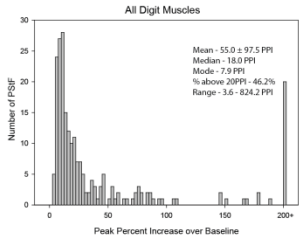

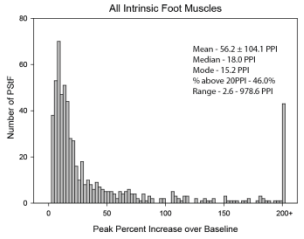

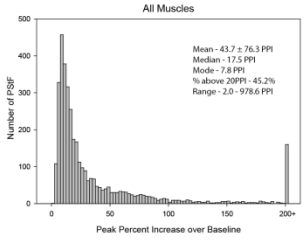

Ipsilateral 120µA

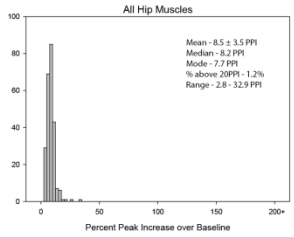

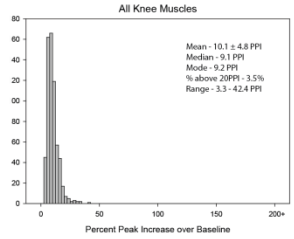

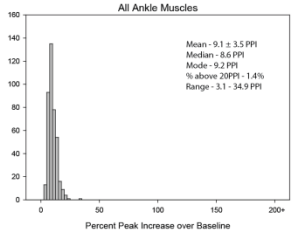

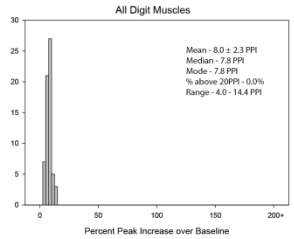

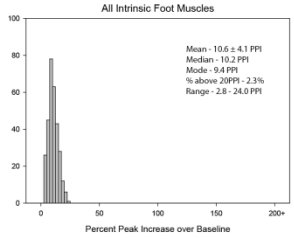

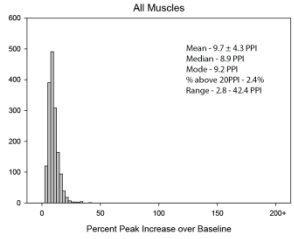

Figure 21. Distribution of PStF onset latencies for hip muscles using 120 μA stimulus in the contralateral and ipsilateral hemisphere for Monkey M. The mean, median, mode, % of latencies longer than 20ms, and range for each muscle group is also shown.

Hip Muscles

Monkey M

Contralateral 120µA

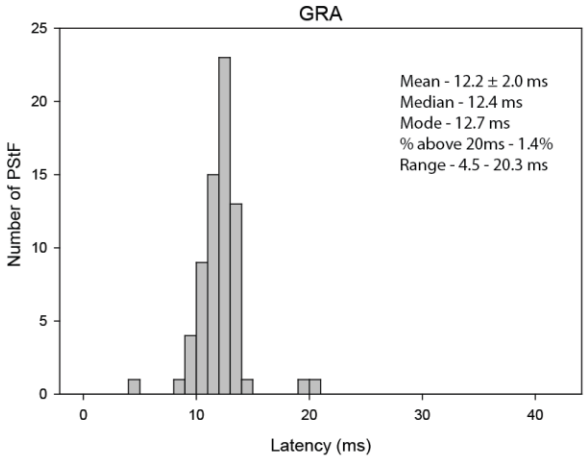

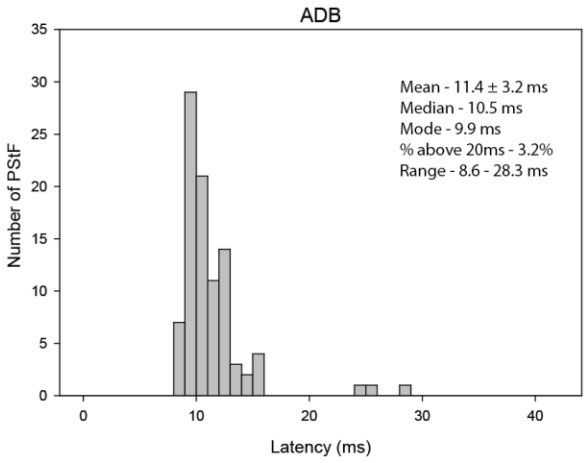

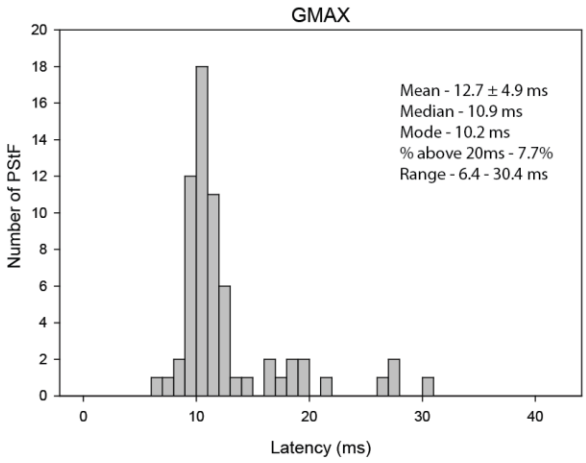

Ipsilateral 120µA

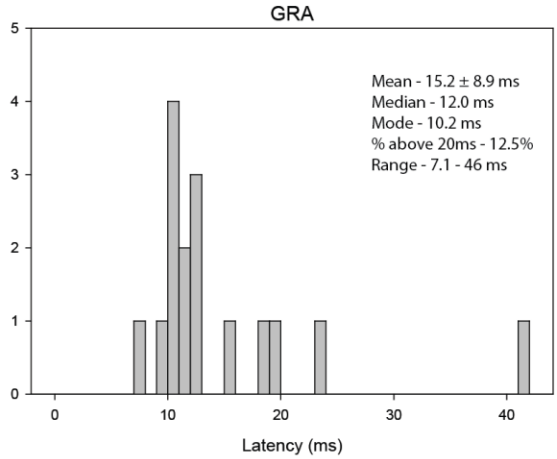

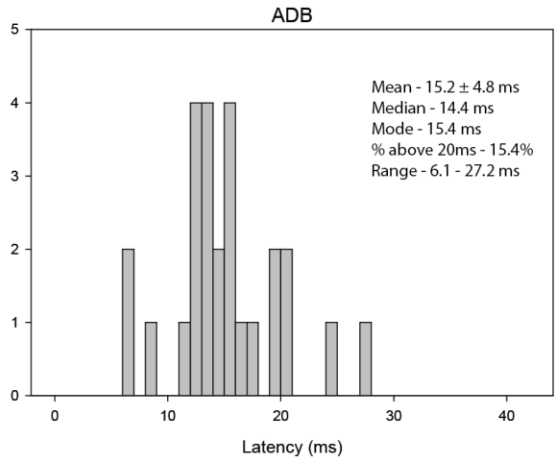

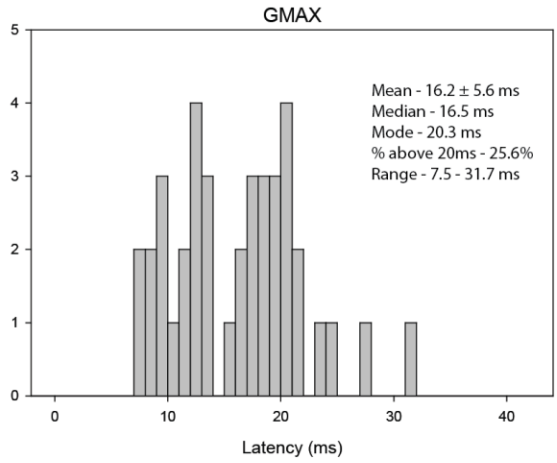

Figure 22. Distribution of PStF onset latencies for hip muscles using 120 μA stimulus in the contralateral and ipsilateral hemisphere for Monkey L. The mean, median, mode, % of latencies longer than 20ms, and range for each muscle group is also shown.

Hip Muscles

Monkey L

Contralateral 120µA

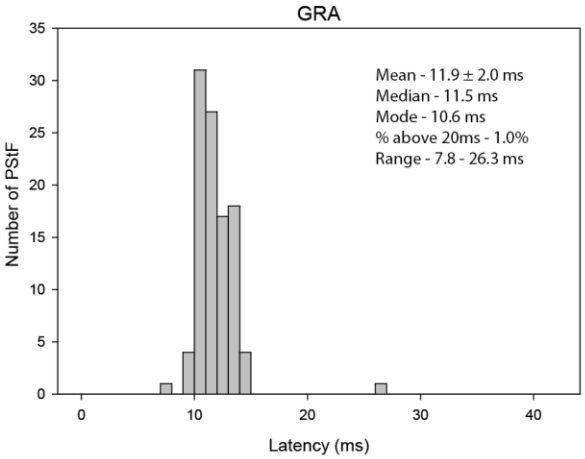

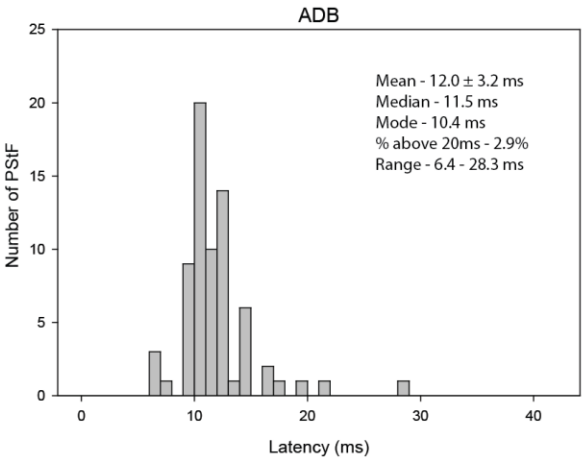

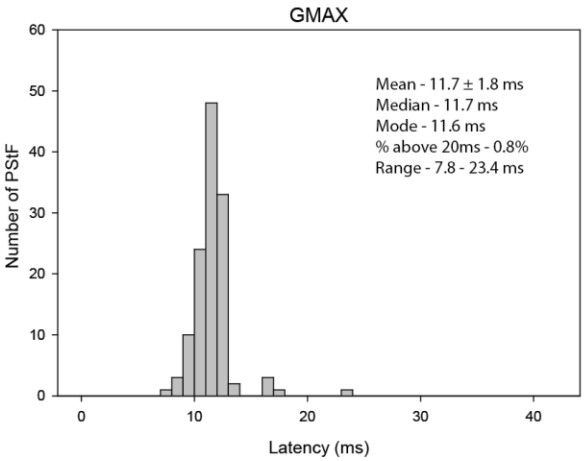

Ipsilateral 120µA

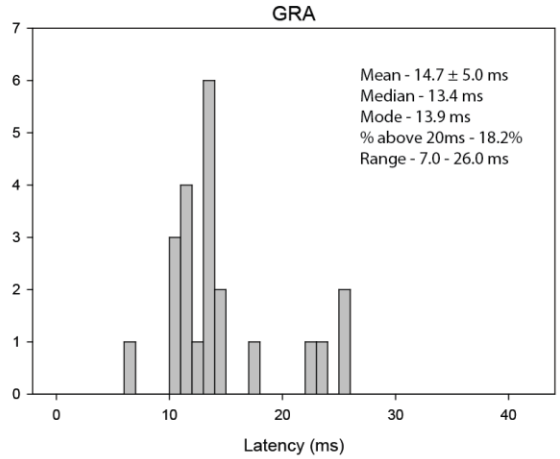

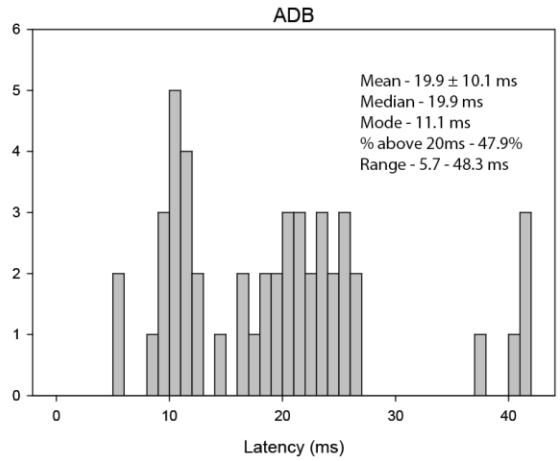

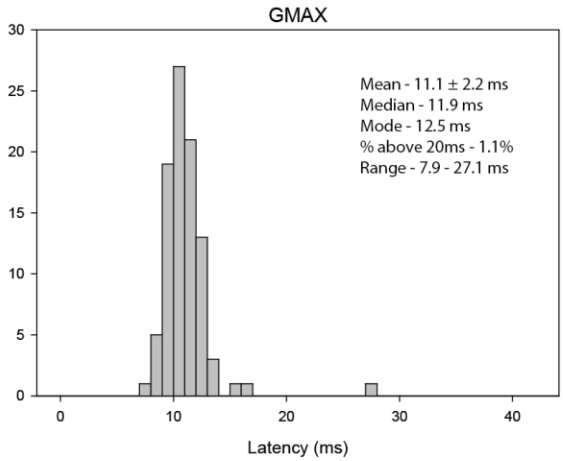

Figure 23. Distribution of PStF onset latencies for hip muscles using 120 μA stimulus in the contralateral and ipsilateral hemisphere for both monkeys. The mean, median, mode, % of latencies longer than 20ms, and range for each muscle group is also shown.

Hip Muscles

Total

Contralateral 120µA

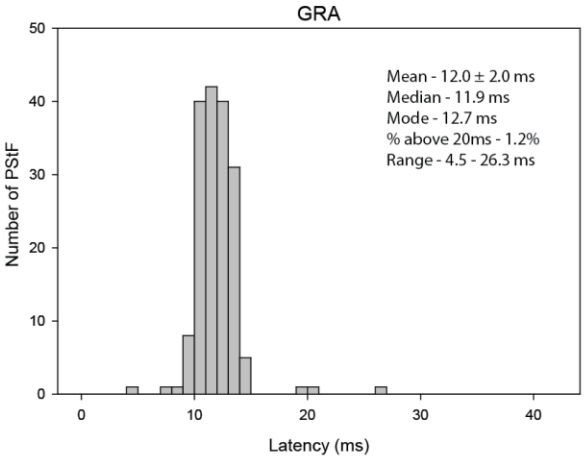

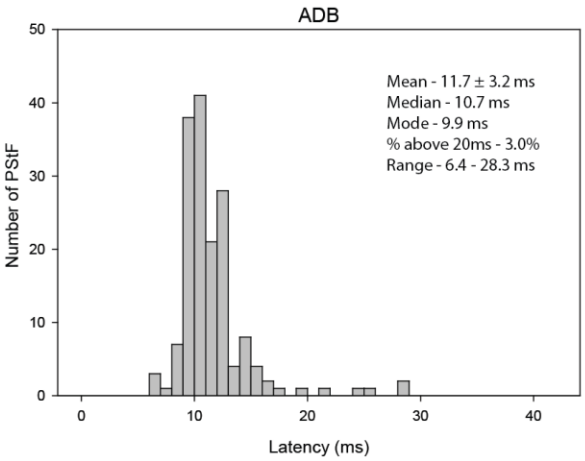

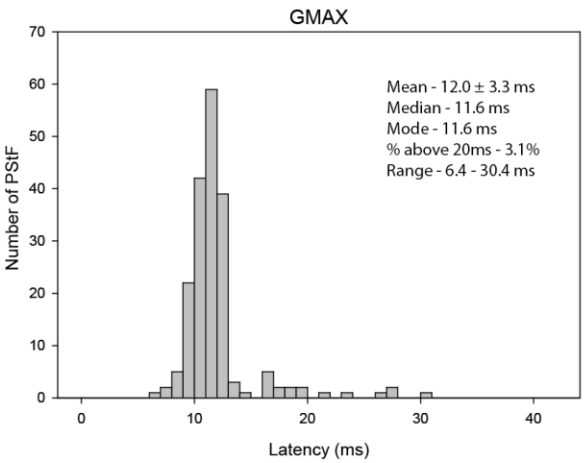

Ipsilateral 120µA

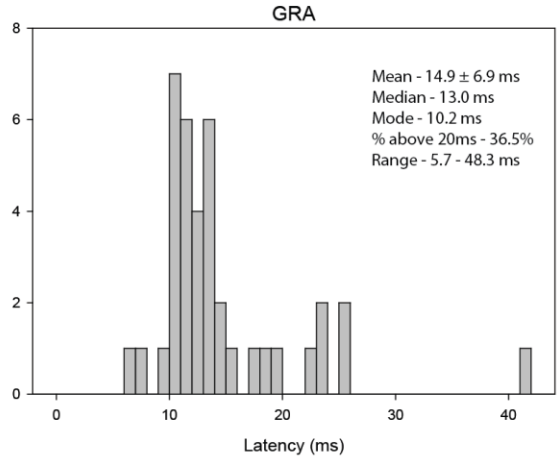

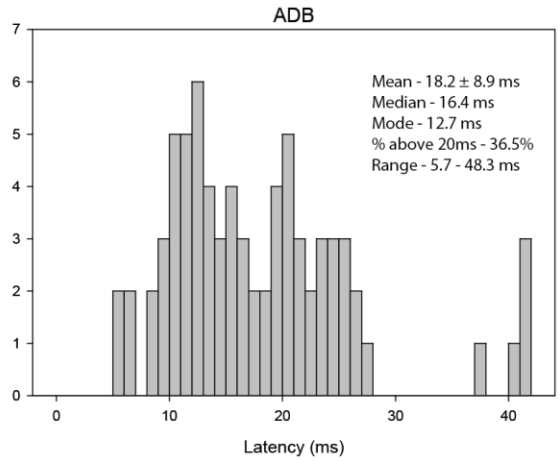

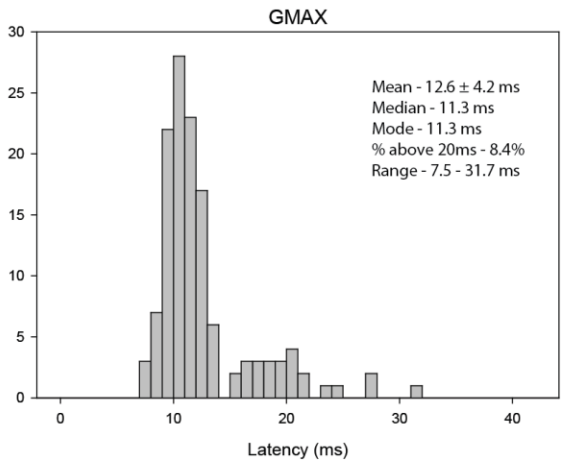

Figure 24. Distribution of PStF onset latencies knee for muscles using 120 μA stimulus in the contralateral and ipsilateral hemisphere for Monkey M. The mean, median, mode, % of latencies longer than 20ms, and range for each muscle group is also shown.

Knee Muscles

Monkey M

Contralateral 120µA

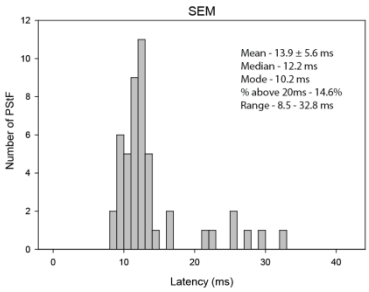

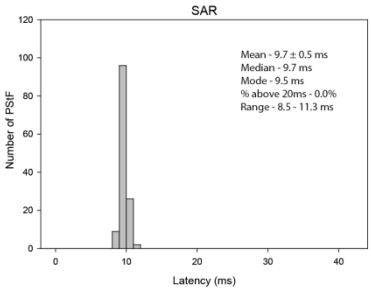

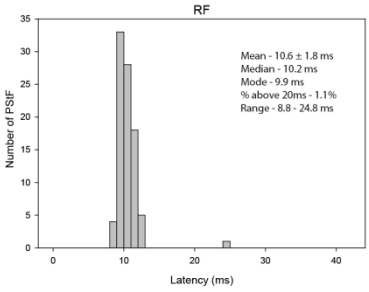

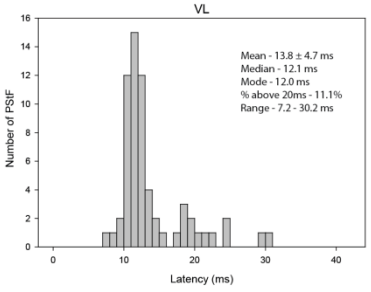

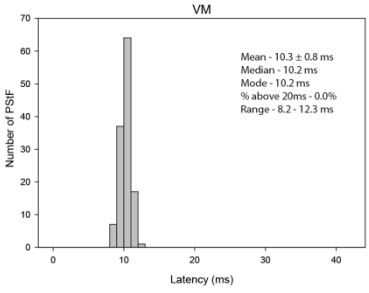

Ipsilateral 120µA

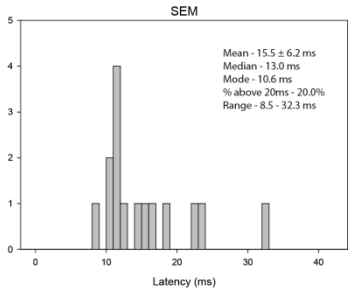

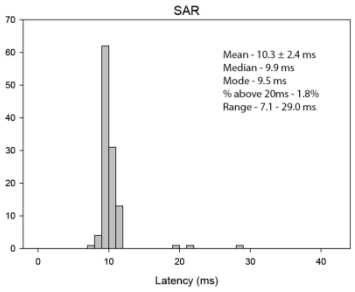

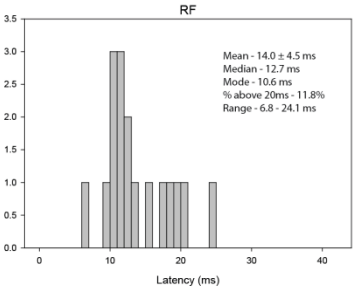

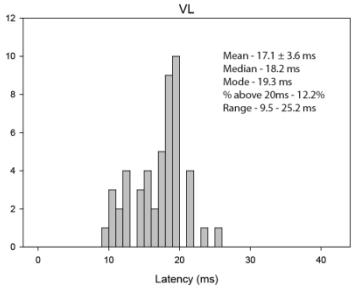

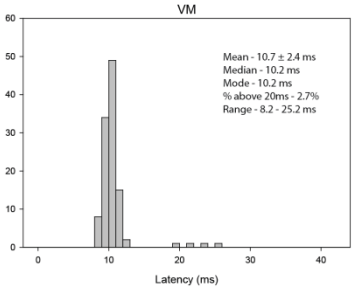

Figure 25. Distribution of PStF onset latencies for knee muscles using 120 μA stimulus in the contralateral and ipsilateral hemisphere for Monkey L. The mean, median, mode, % of latencies longer than 20ms, and range for each muscle group is also shown.

Knee Muscles

Monkey L

Contralateral 120μA

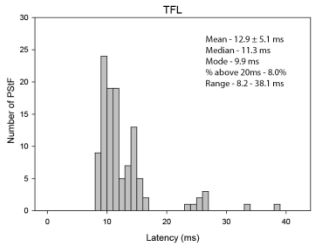

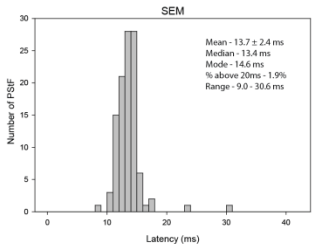

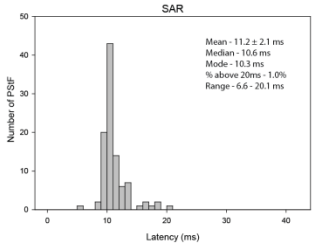

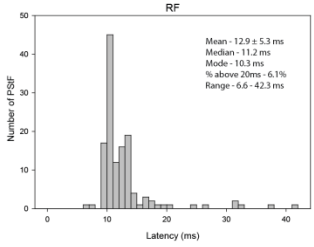

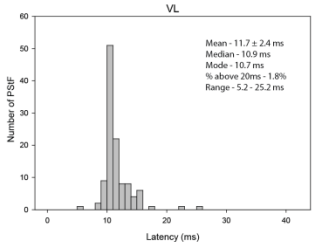

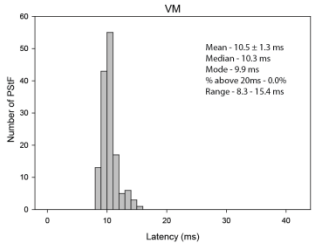

Ipsilateral 120μA

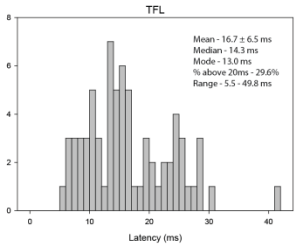

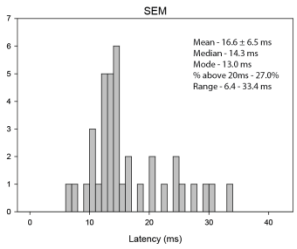

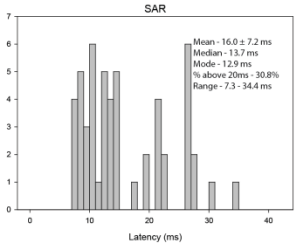

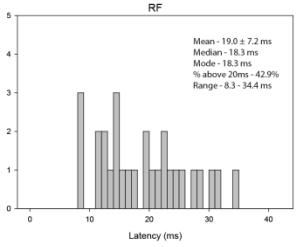

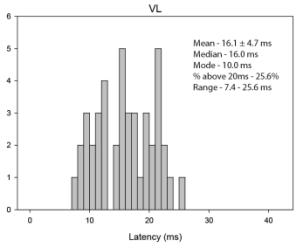

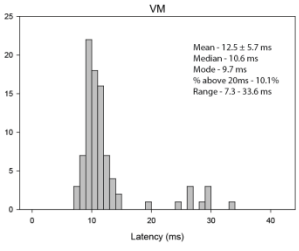

Figure 26. Distribution of PStF onset latencies for knee muscles using 120 μA stimulus in the contralateral and ipsilateral hemisphere for both monkeys. The mean, median, mode, % of latencies longer than 20ms, and range for each muscle group is also shown.

Knee Muscles

Total

Contralateral 120μA

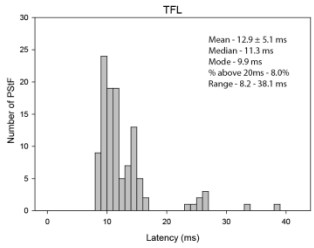

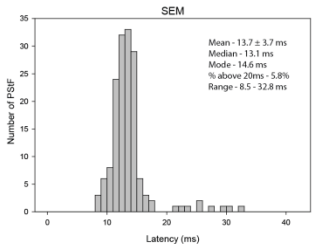

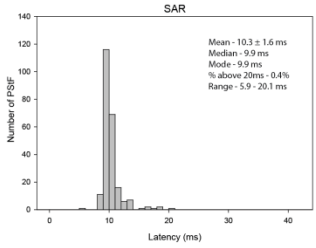

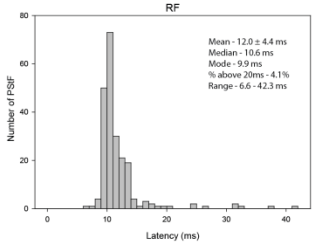

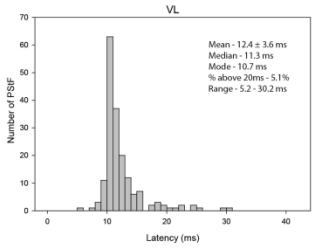

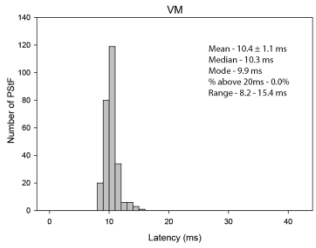

Ipsilateral 120μA

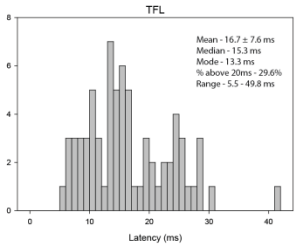

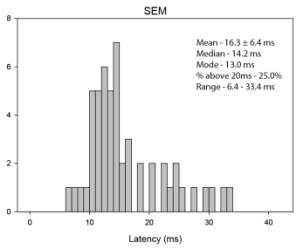

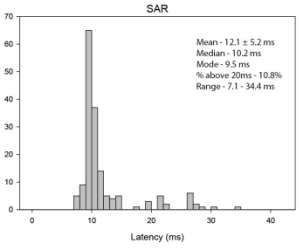

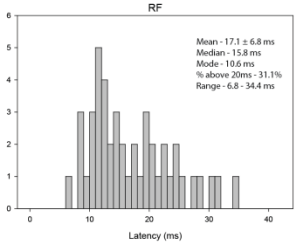

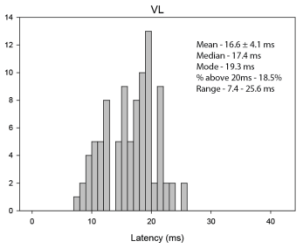

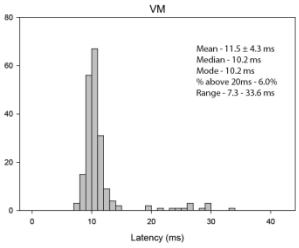

Figure 27. Distribution of PStF onset latencies for ankle muscles using 120 μA stimulus in the contralateral and ipsilateral hemisphere for Monkey M. The mean, median, mode, % of latencies longer than 20ms, and range for each muscle group is also shown.

Ankle Muscles

Monkey M

Contralateral 120µA

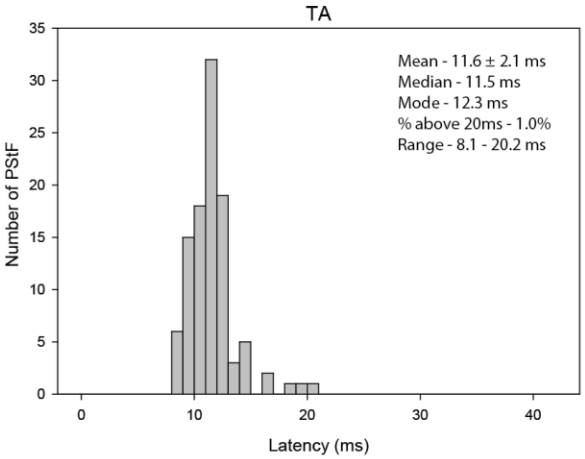

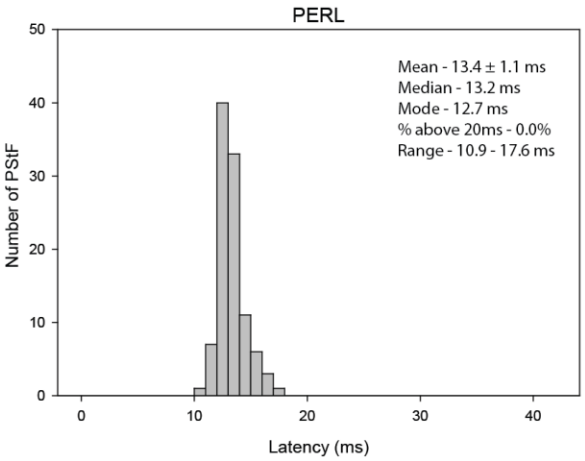

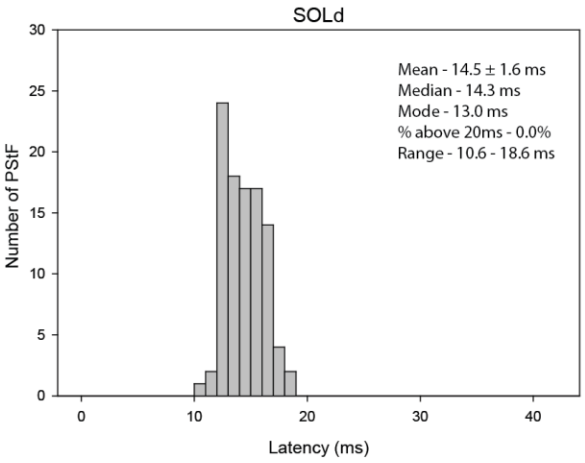

Ipsilateral 120µA

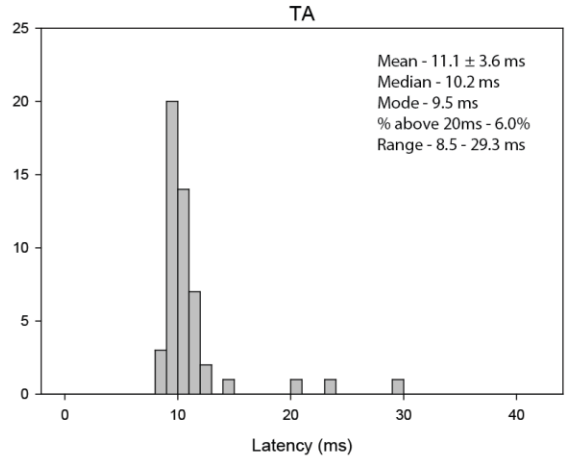

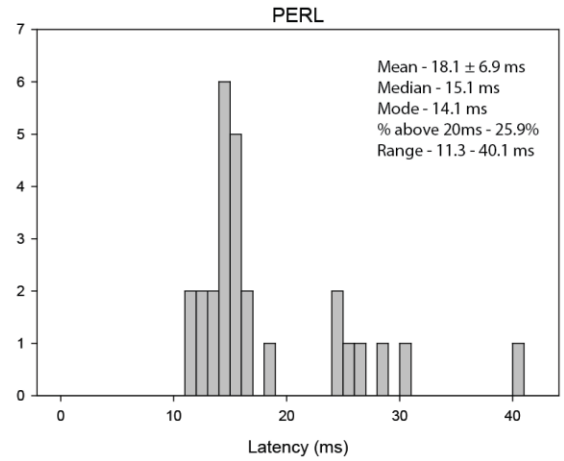

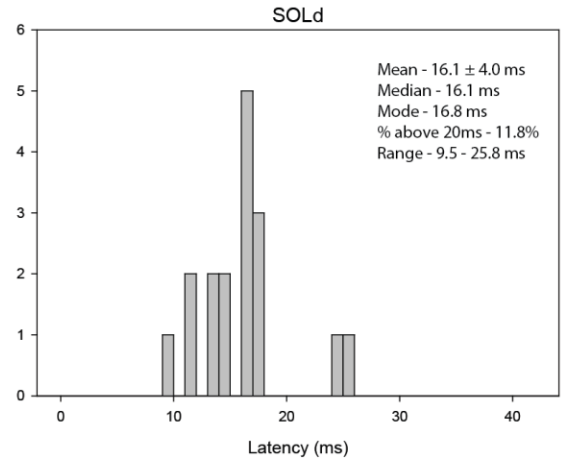

Figure 28. Distribution of PStF onset latencies for ankle muscles using 120 μA stimulus in the contralateral and ipsilateral hemisphere for Monkey L. The mean, median, mode, % of latencies longer than 20ms, and range for each muscle group is also shown.

Ankle Muscles

Monkey L

Contralateral 120µA

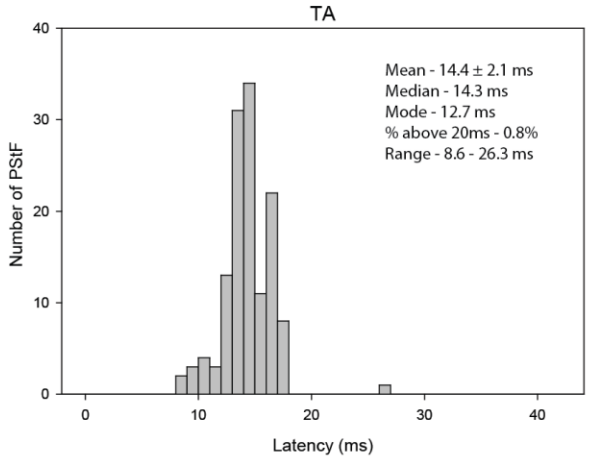

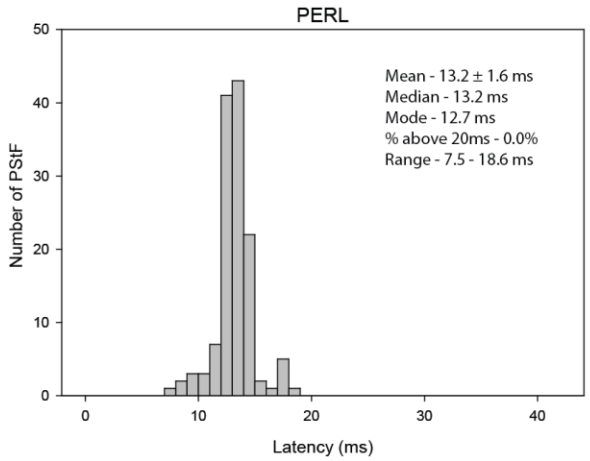

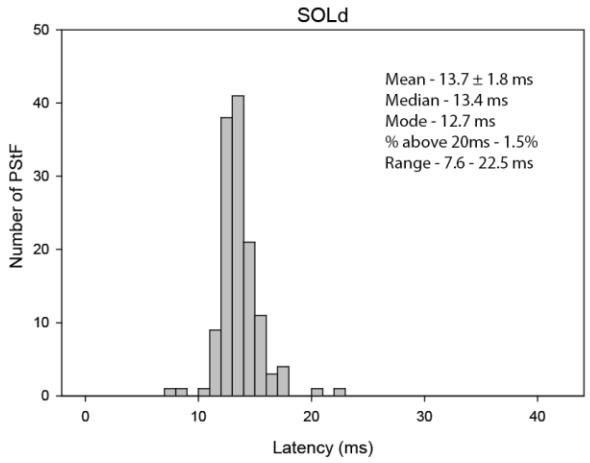

Ipsilateral 120µA

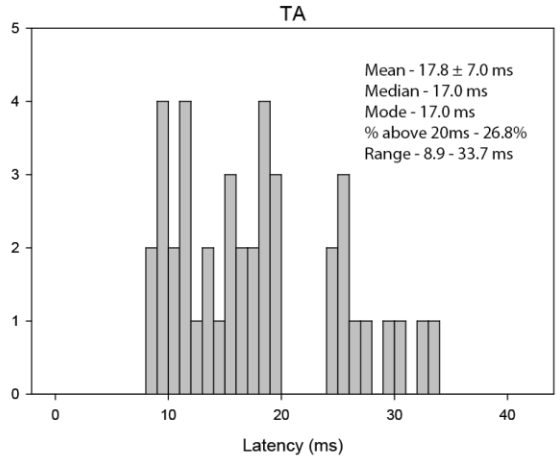

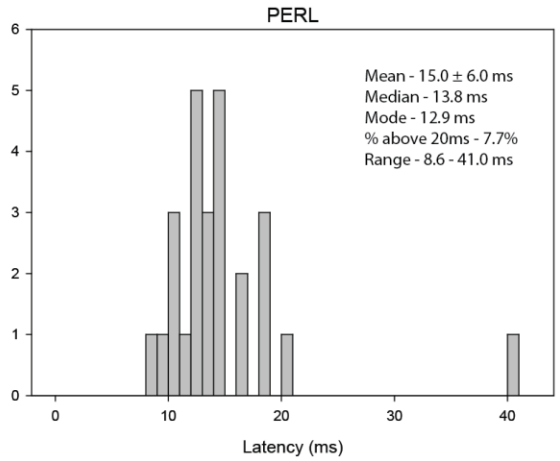

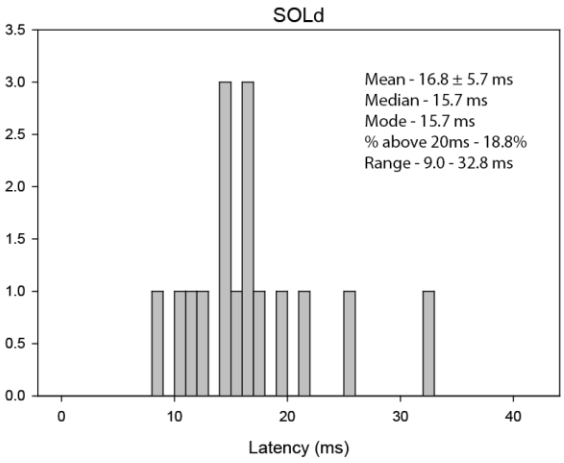

Figure 29. Distribution of PStF onset latencies for ankle muscles using 120 μA stimulus in the contralateral and ipsilateral hemisphere for both monkeys. The mean, median, mode, % of latencies longer than 20ms, and range for each muscle group is also shown.

Ankle Muscles

Total

Contralateral 120µA

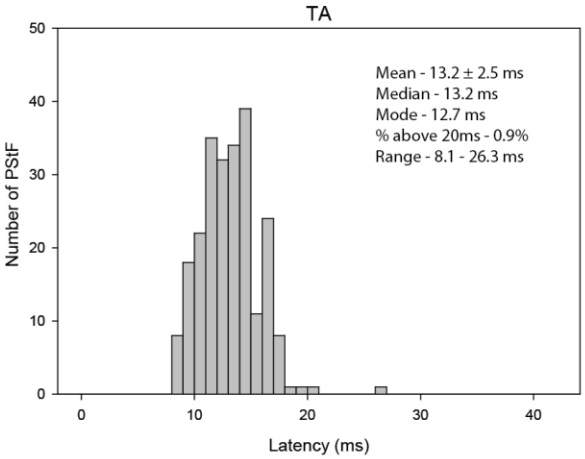

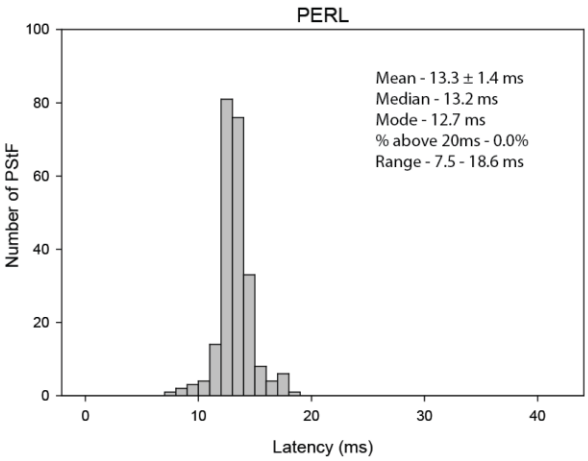

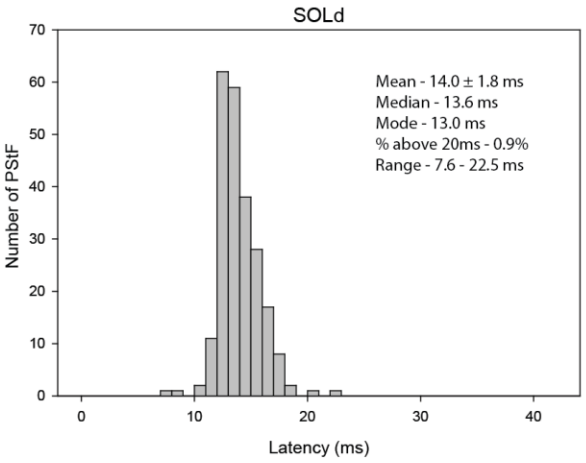

Ipsilateral 120µA

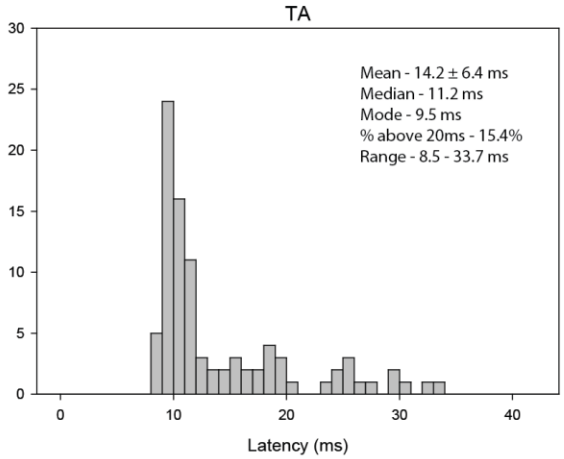

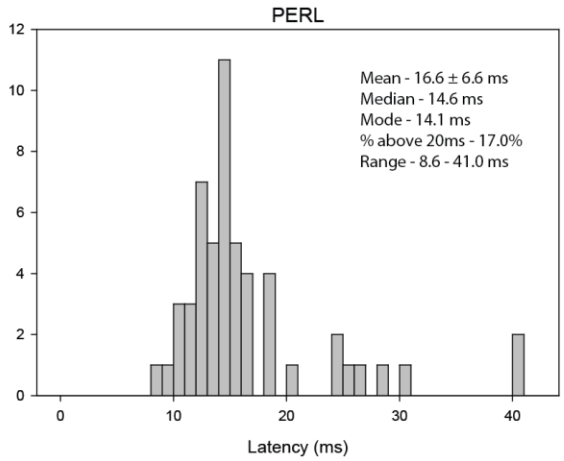

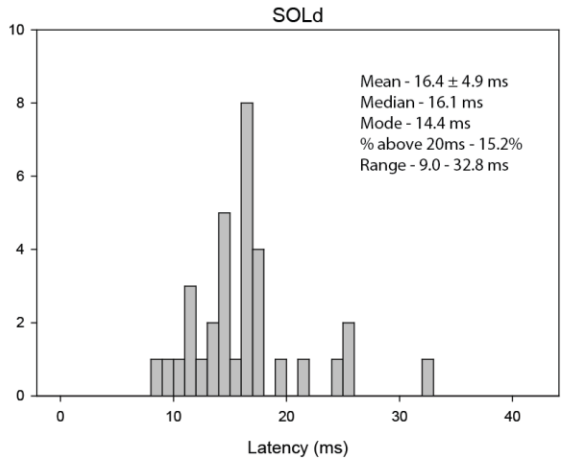

Figure 30. Distribution of PStF onset latencies for digit and intrinsic foot muscles using 120 μA stimulus in the contralateral and ipsilateral hemisphere for Monkey M. The mean, median, mode, % of latencies longer than 20ms, and range for each muscle group is also shown.

Digit Muscles

Monkey M

Contralateral 120µA

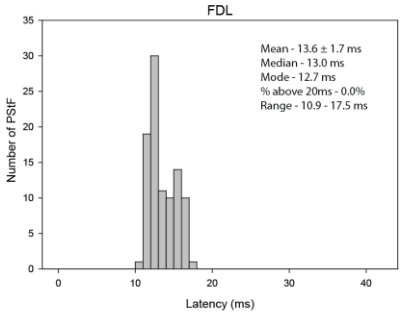

Ipsilateral 120µA

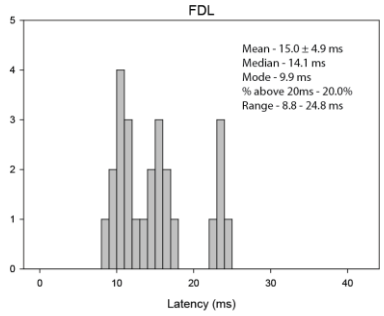

Intrinsic Foot Muscles

Monkey M

Contralateral 120µA

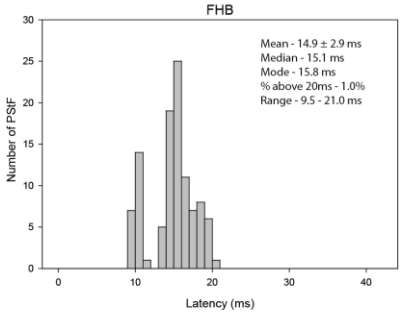

Ipsilateral 120µA

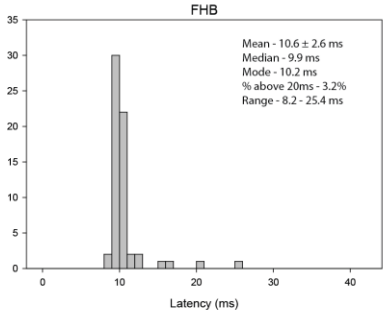

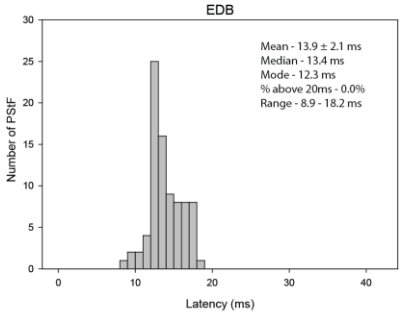

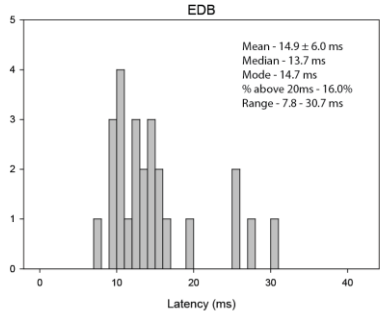

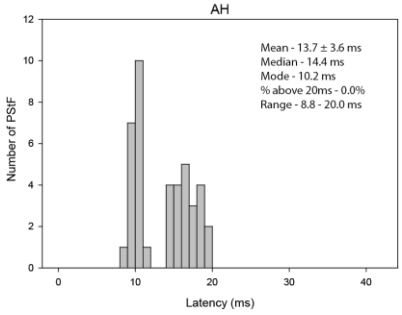

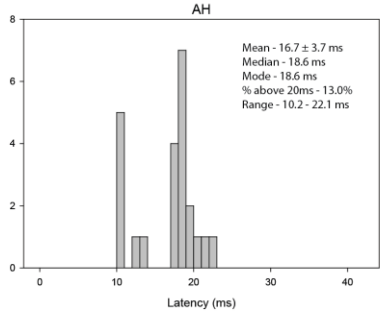

Figure 31. Distribution of PStF onset latencies for digit and intrinsic foot muscles using 120 μA stimulus in the contralateral and ipsilateral hemisphere for Monkey L. The mean, median, mode, % of latencies longer than 20ms, and range for each muscle group is also shown.

Digit Muscles

Monkey L

Contralateral 120µA

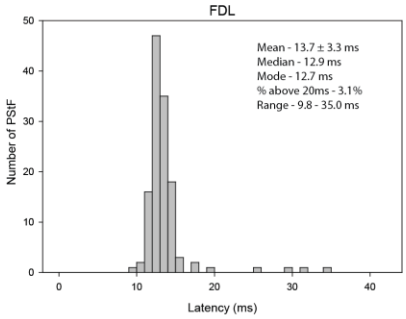

Ipsilateral 120µA

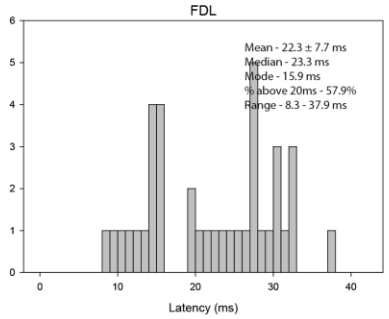

Intrinsic Foot Muscles

Monkey L

Contralateral 120µA

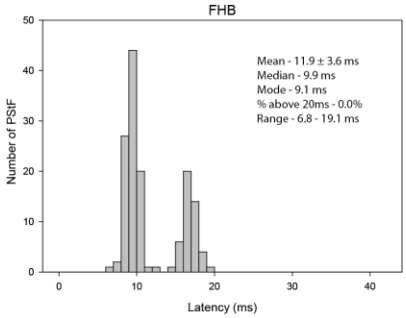

Ipsilateral 120µA

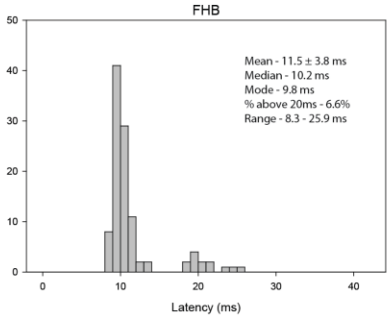

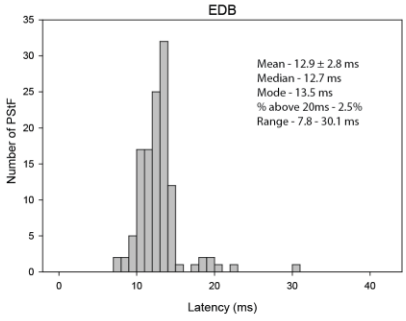

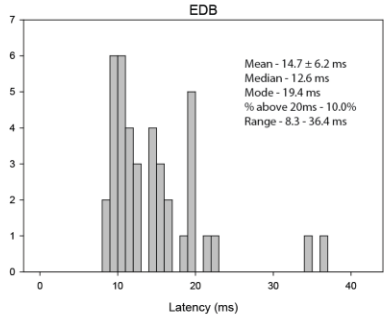

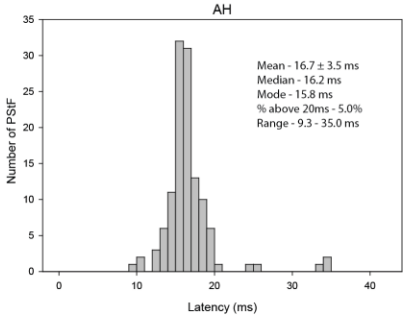

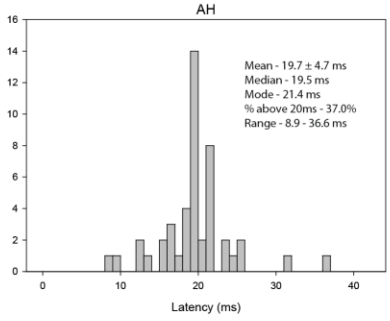

Figure 32. Distribution of PStF onset latencies for digit and intrinsic foot muscles using 120 μA stimulus in the contralateral and ipsilateral hemisphere for both monkeys. The mean, median, mode, % of latencies longer than 20ms, and range for each muscle group is also shown.

Digit Muscles

Total

Contralateral 120μA

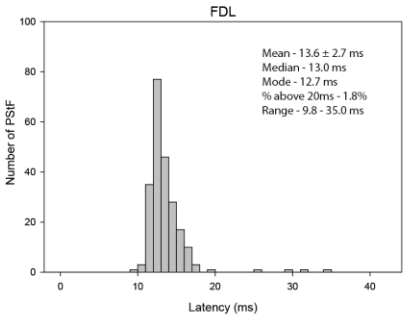

Ipsilateral 120μA

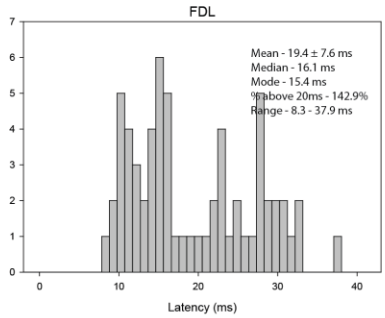

Intrinsic Foot Muscles

Total

Contralateral 120μA

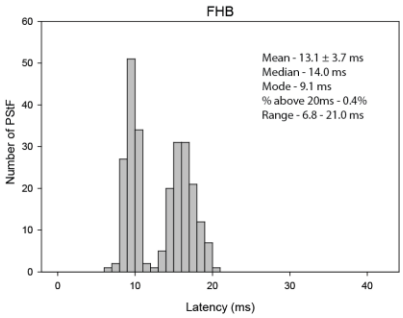

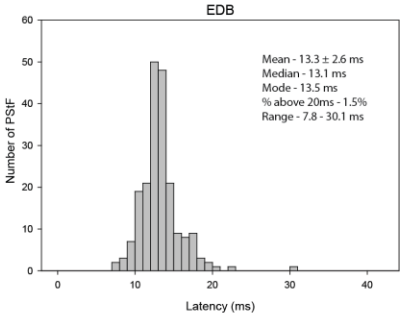

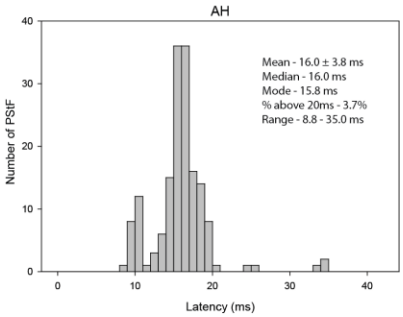

Ipsilateral 120μA

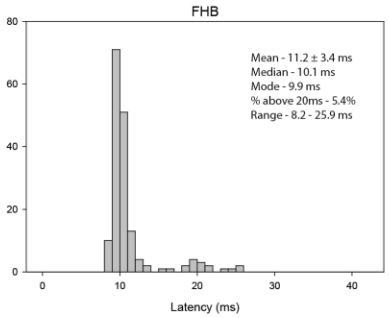

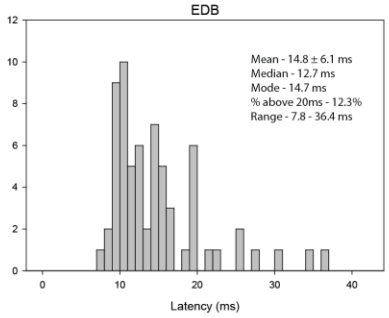

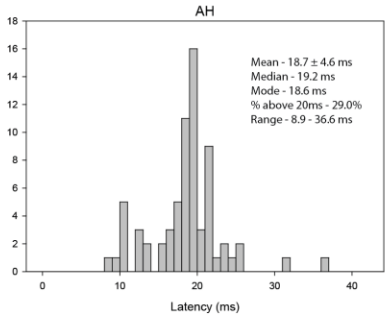

Figure 33. Distribution of PStF onset latencies for muscles at the hip, knee, ankle, digit, and intrinsic foot joints using 120 μA stimulus in the contralateral and ipsilateral hemisphere for monkey M. The mean, median, mode, % of latencies longer than 20ms, and range for each muscle group is also shown.

All Muscles

Monkey M

Contralateral 120μA

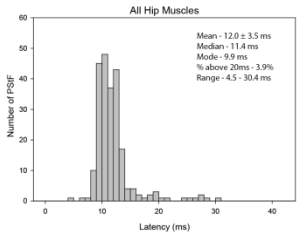

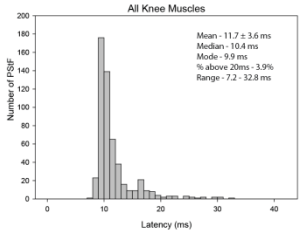

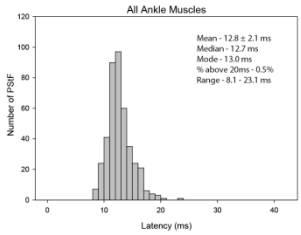

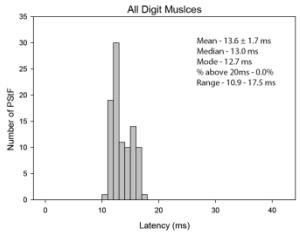

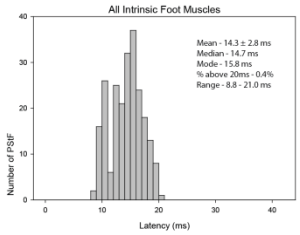

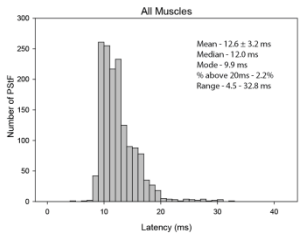

Ipsilateral 120μA

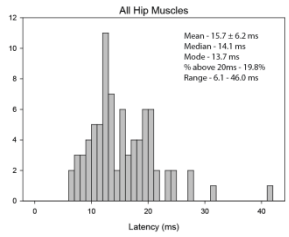

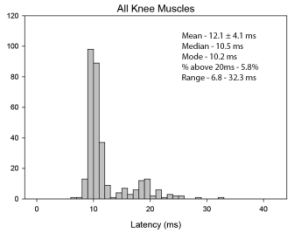

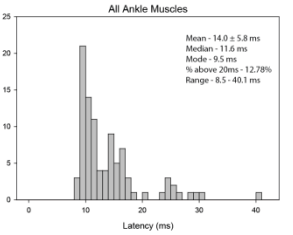

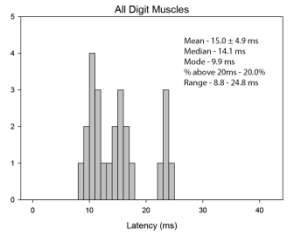

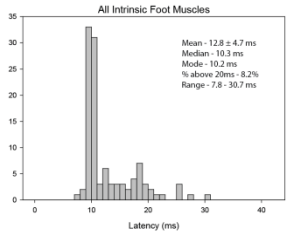

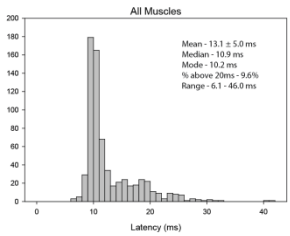

Figure 34. Distribution of PStF onset latencies for muscles at the hip, knee, ankle, digit, and intrinsic foot joints using 120 μA stimulus in the contralateral and ipsilateral hemisphere for monkey L. The mean, median, mode, % of latencies longer than 20ms, and range for each muscle group is also shown.

All Muscles

Monkey L

Contralateral 120μA

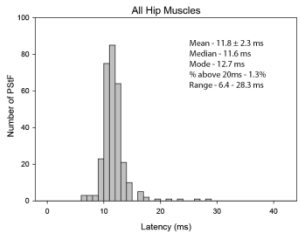

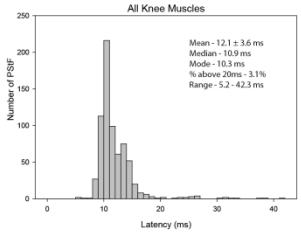

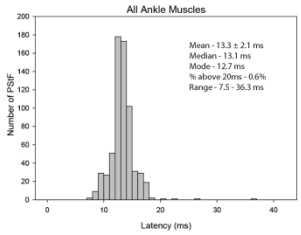

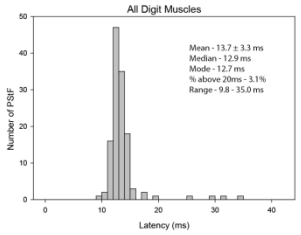

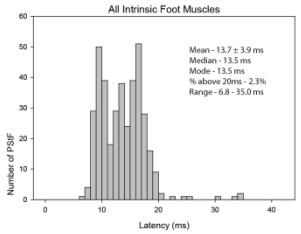

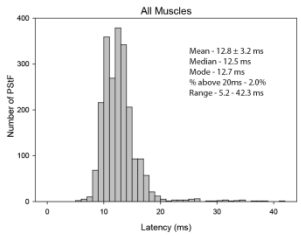

Ipsilateral 120μA

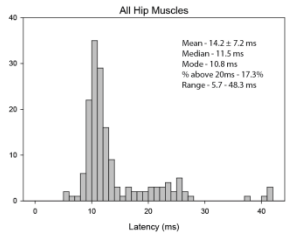

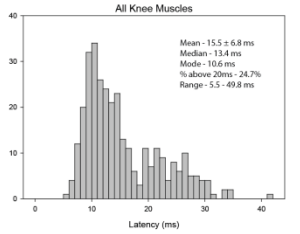

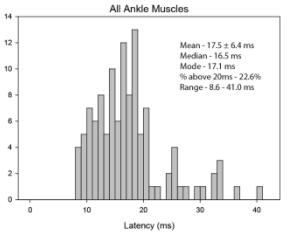

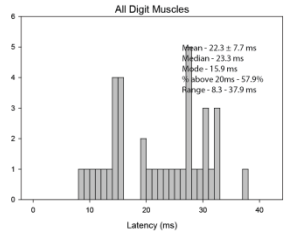

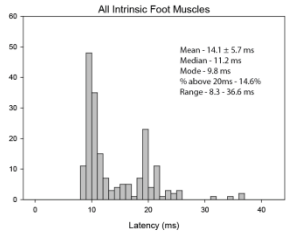

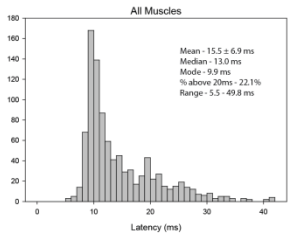

Figure 35. Distribution of PStF onset latencies for muscles at the hip, knee, ankle, digit, and intrinsic foot joints using 120 μA stimulus in the contralateral and ipsilateral hemisphere for both monkeys. The mean, median, mode, % of latencies longer than 20ms, and range for each muscle group is also shown.

All Muscles

Total

Contralateral 120μA

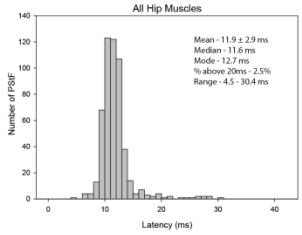

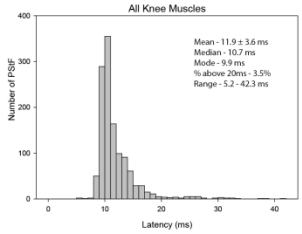

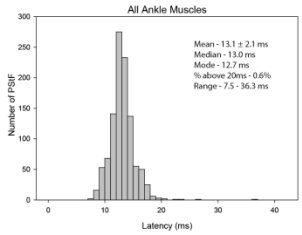

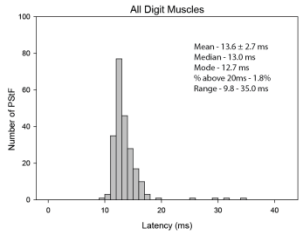

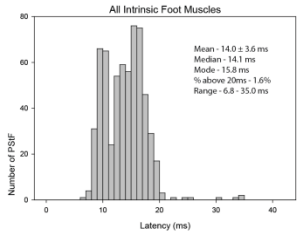

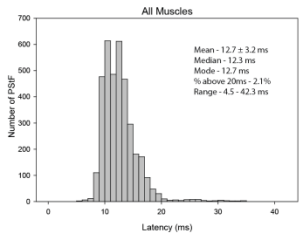

Ipsilateral 120μA

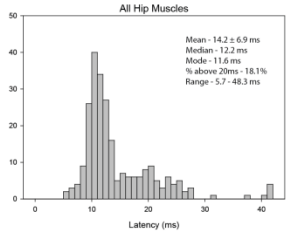

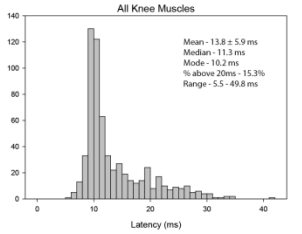

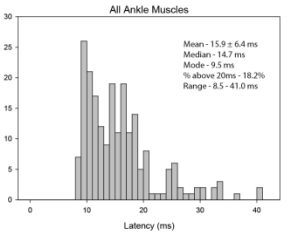

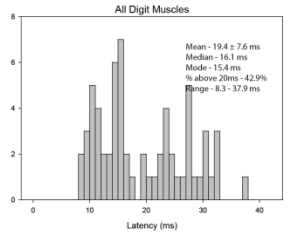

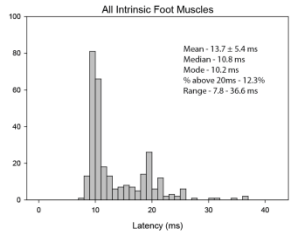

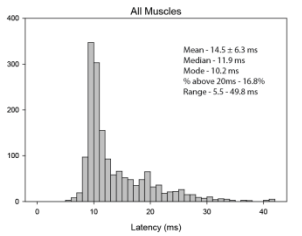

Figure 36. 2D contour map plotting the magnitudes of PStF for muscles at the hip joint using 120 μA stimulus in the contralateral and a two pulse train of 120 μA stimulus separated by 3ms in the ipsilateral hemisphere. The vertical y-axis corresponds to the superior sagittal sinus and the dashed line corresponds to the central sulcus. The x and y axis are on a 1mm x 1mm scale.

Hip Muscles

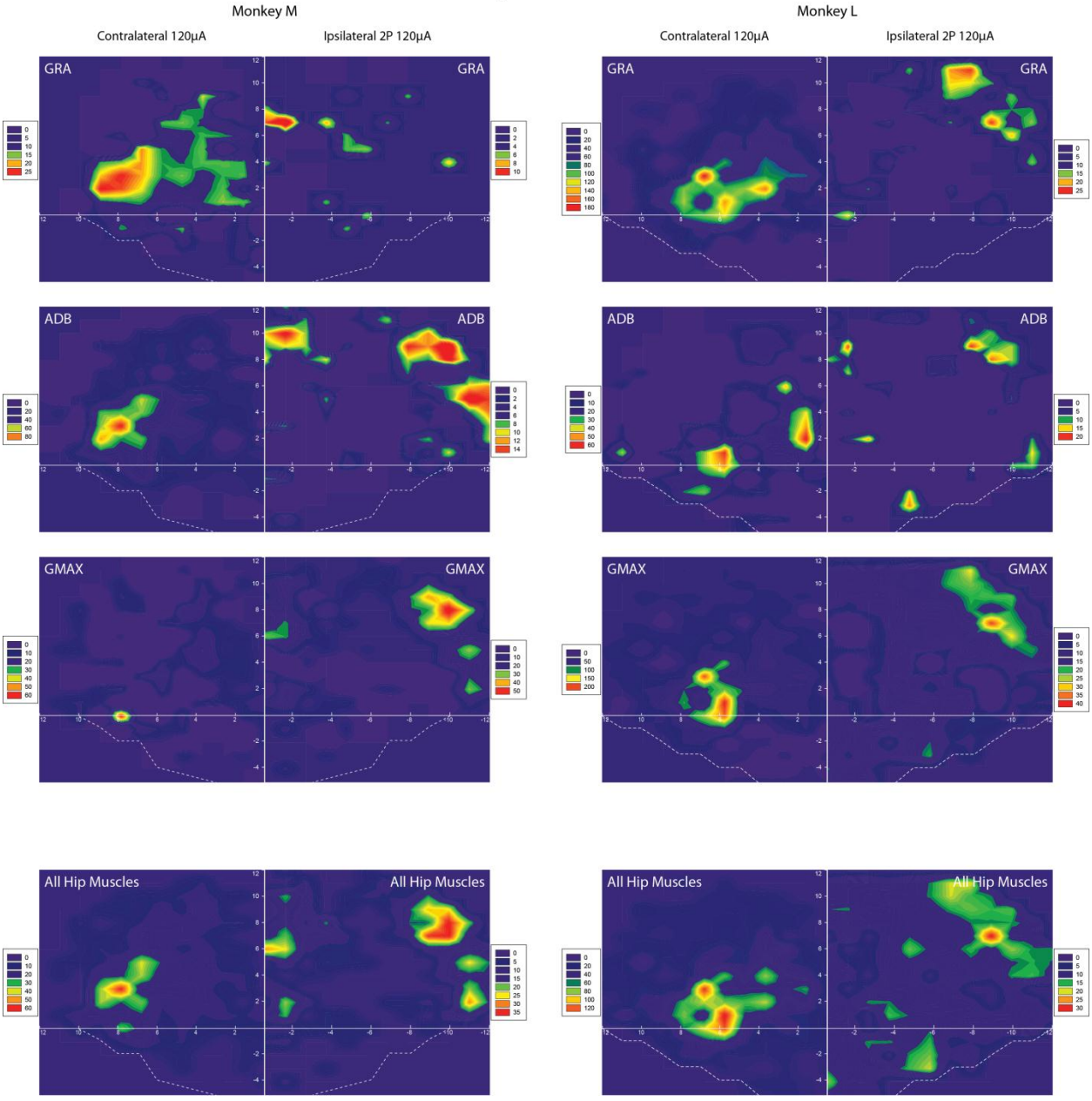
Monkey M
Contralateral 120µA
Ipsilateral 2P 120µA
Monkey L
Contralateral 120µA
Ipsilateral 2P 120µA
GRA
GRA
GRA
GRA
ADB
ADB
ADB
ADB
GMAX
GMAX
GMAX
GMAX
All Hip Muscles
All Hip Muscles
All Hip Muscles
All Hip Muscles

Figure 37. 2D contour map plotting the magnitudes of PStF for muscles at the knee joint using 120 μA stimulus in the contralateral and a two pulse train of 120 μA stimulus separated by 3ms in the ipsilateral hemisphere. The vertical y-axis corresponds to the superior sagittal sinus and the dashed line corresponds to the central sulcus. The x and y axis are on a 1mm x 1mm scale.

Knee Muscles

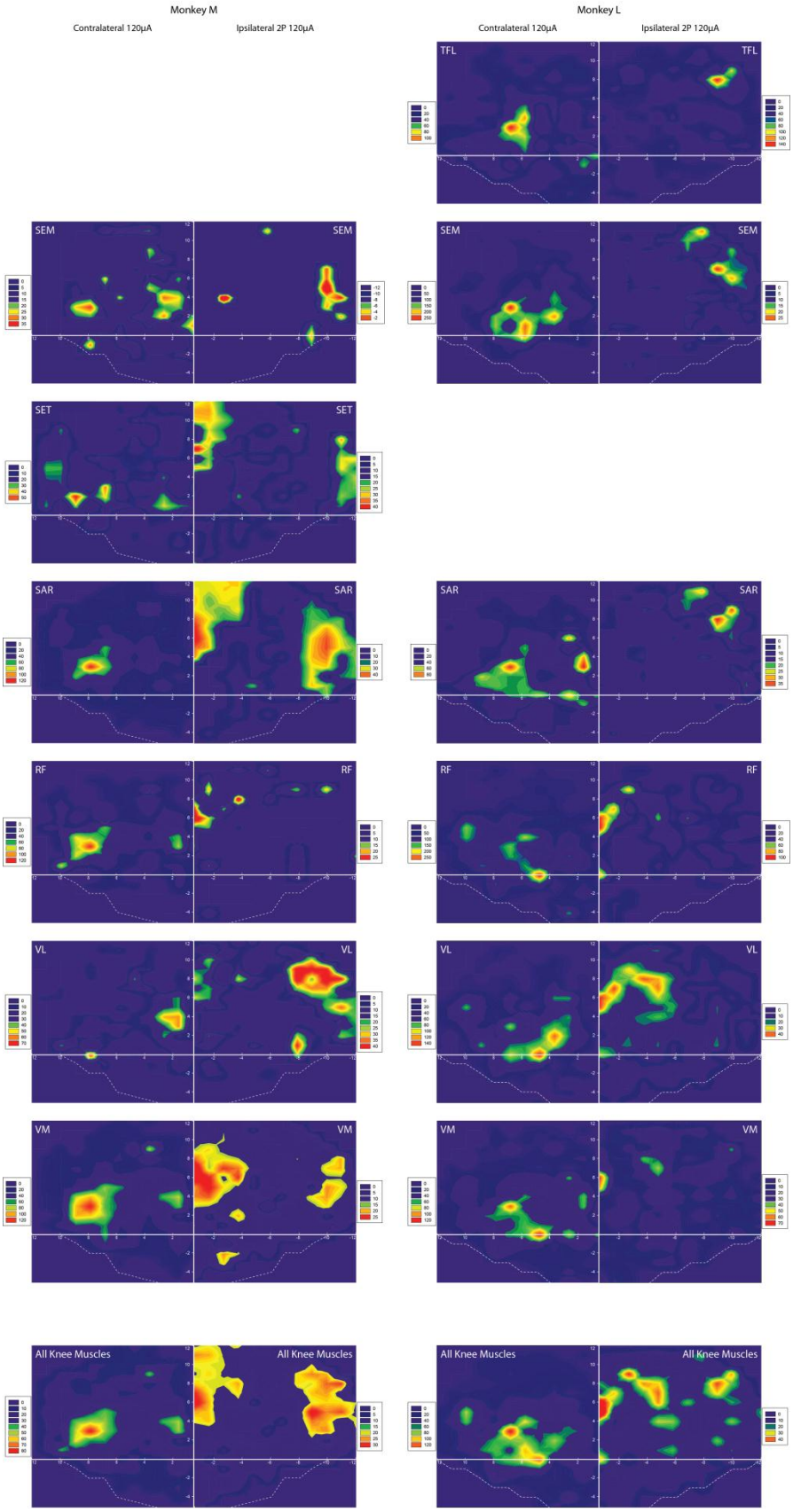

Figure 38. 2D contour map plotting the magnitudes of PStF for muscles at the ankle joint using 120 μA stimulus in the contralateral and a two pulse train of 120 μA stimulus separated by 3ms in the ipsilateral hemisphere. The vertical y-axis corresponds to the superior sagittal sinus and the dashed line corresponds to the central sulcus. The x and y axis are on a 1mm x 1mm scale.

Ankle Muscles

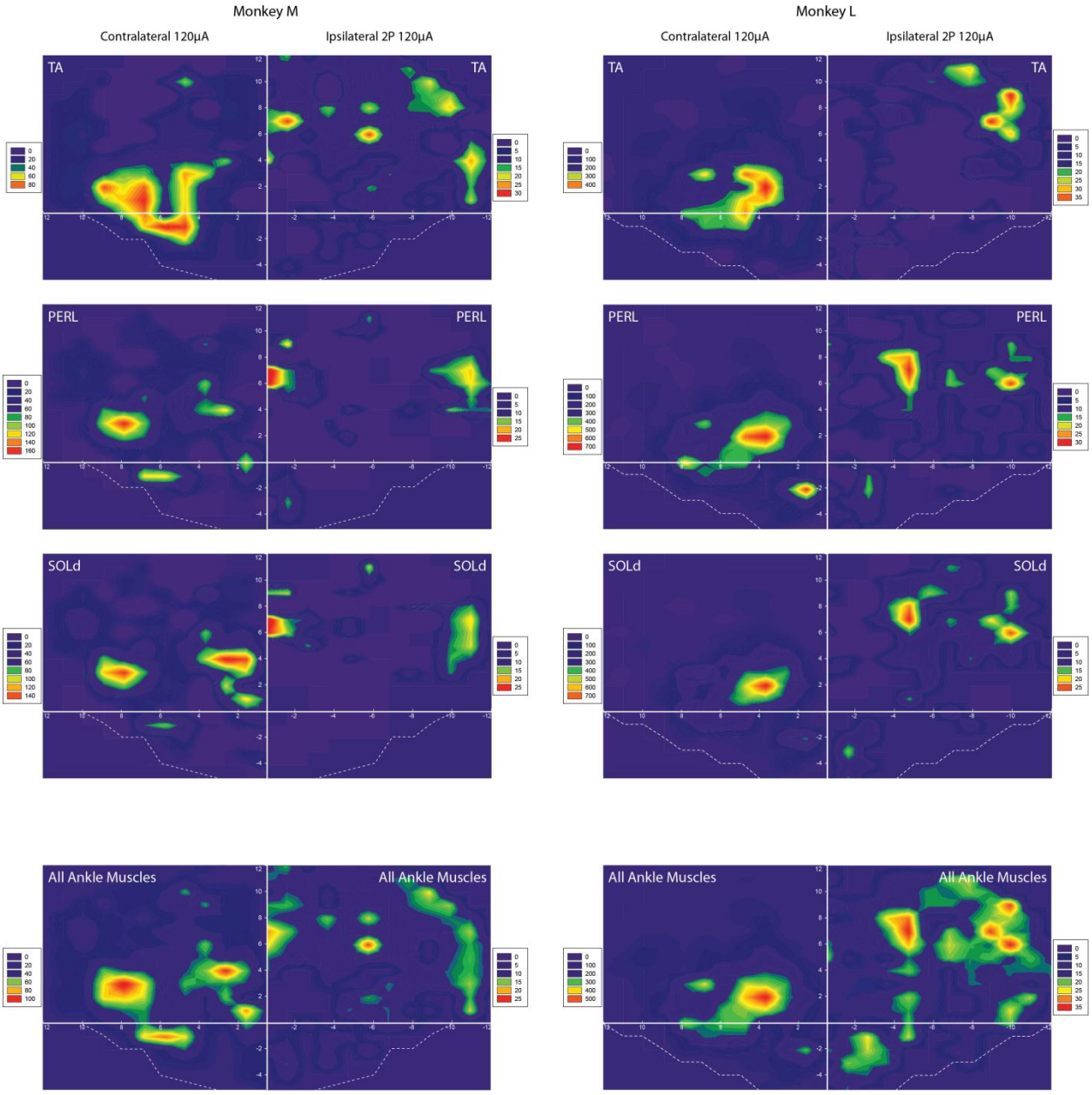

Figure 39. 2D contour map plotting the magnitudes of PStF for muscles at the digit and intrinsic foot joints using 120 μA stimulus in the contralateral and a two pulse train of 120 μA stimulus separated by 3ms in the ipsilateral hemisphere. The vertical y-axis corresponds to the superior sagittal sinus and the dashed line corresponds to the central sulcus. The x and y axis are on a 1mm x 1mm scale.

Digit Muscles

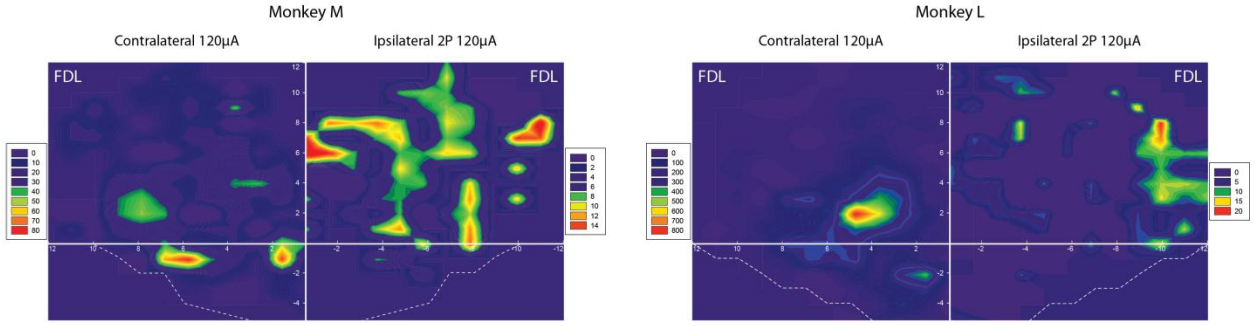

Intrinsic Foot Muscles

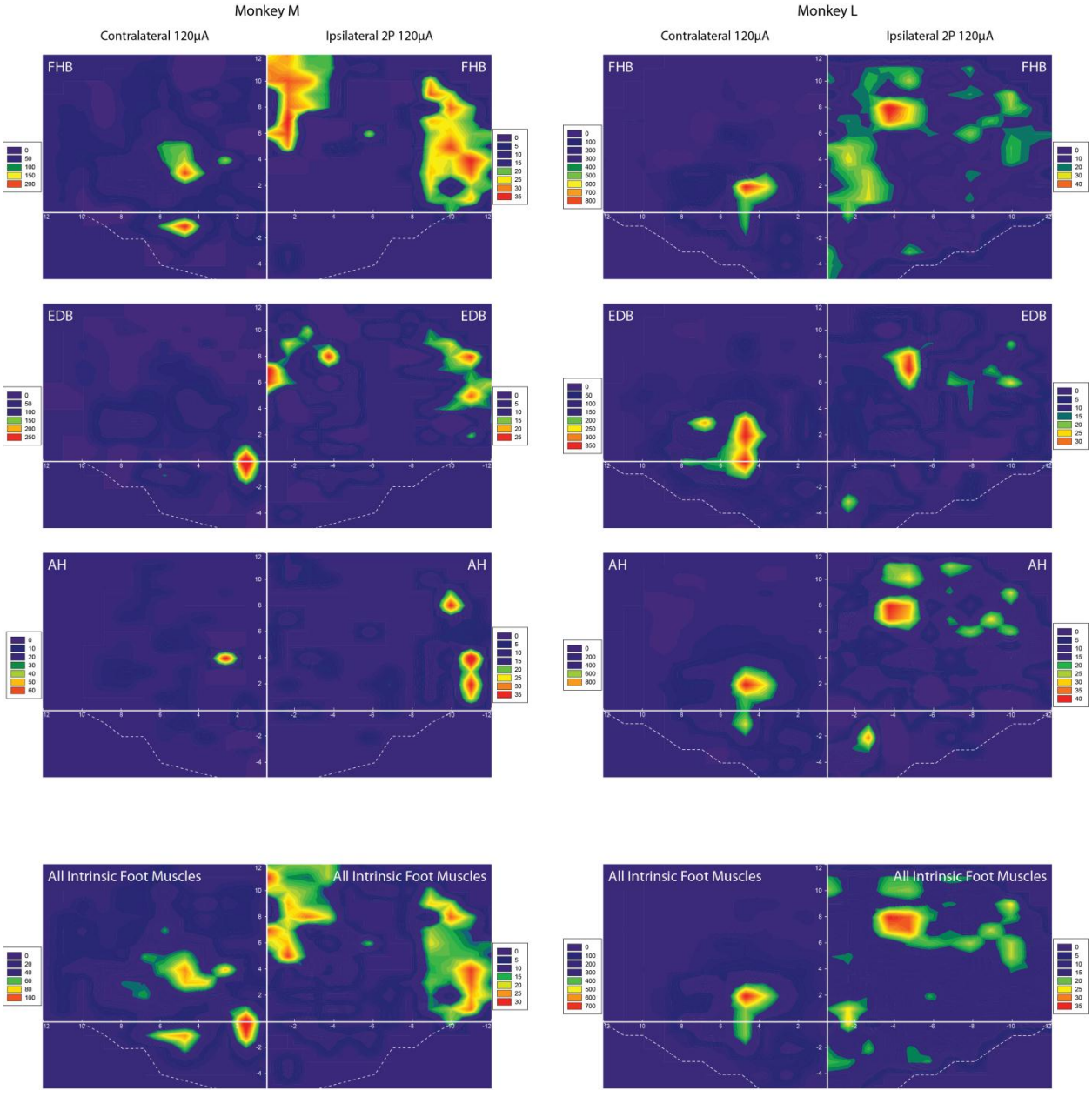

Figure 40. 2D contour map plotting the magnitudes of PStF for muscles at the hip, knee, ankle, digit, and intrinsic foot joints using 120 μA stimulus in the contralateral and a two pulse train of 120 μA stimulus separated by 3ms in the ipsilateral hemisphere. The vertical y-axis corresponds to the superior sagittal sinus and the dashed line corresponds to the central sulcus. The x and y axis are on a 1mm x 1mm scale.

All Muscle Groups

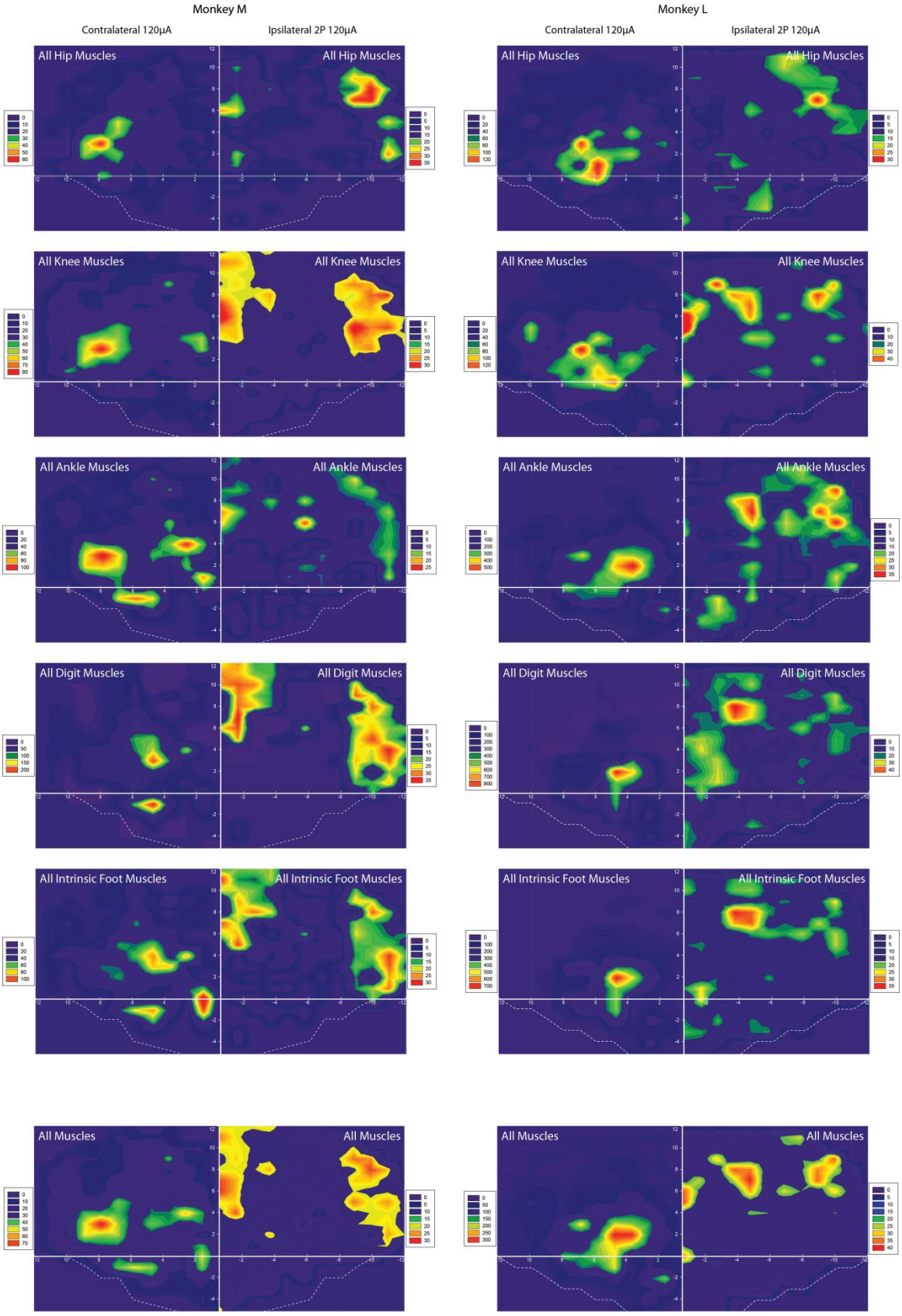

CHAPTER 4

MOTOR CORTICAL MUSCIMOL INJECTION DISRUPTS HINDLIMB MOVEMENT IN FREELY MOVING MACAQUE MONKEYS

INTRODUCTION

A major role of the primary motor cortex (M1) is the execution of movements and especially the fractionation of digit movements, for instance, the ability to move digits independently. When M1 is damaged, voluntary movements in the affected body parts become weak and slow, and ability to produce highly fractionated movements of the digits is lost. It is known that neurons using γ-aminobutyric acid (GABA) are ubiquitous throughout the cortex and have potent inhibitory effects on target neurons (Hendry et al. 1987; Matsumura et al. 1991). Injection of muscimol, a potent GABA receptor agonist, has been widely used to produce localized reversible inactivation of cortical areas (Martin 1991). Numerous studies have taken advantage of this fact to investigate the function of specific cortical areas.

When muscimol is injected into the cortex, the discharge of neurons in the vicinity of the injection, including movement related neurons decreases or completely ceases (Matsumura et al. 1992; Schieber and Poliakov 1998). Local injections of muscimol into the forelimb representation of primary motor cortex in primates leads to significant motor deficits (Matsumura et al. 1991; Schieber and Poliakov 1998). In addition to marked contralateral deficits, both movement time and reaction time of the ipsilateral hand were also prolonged (Kubota 1996). Our results with spike and stimulus triggered averaging demonstrate substantially weaker effects from hindlimb M1 cortex on muscle activity compared to forelimb M1. These results suggest the possibility that the overall functional contribution of M1 cortex to hindlimb movement execution and control might be less significant than its contribution to forelimb movement. To test this we made muscimol injections into the left cortex of three adult rhesus male monkeys with the goal of inactivating all of the hindlimb representation. We compared the effects of hindlimb M1 cortex to those reported by others (Kubota 1996; Schieber

and Poliakov 1998) for similar injections into forelimb M1 cortex. We predicted that injecting the GABA-A agonist muscimol into the hindlimb representation of primary motor cortex in rhesus macaques would produce serious functional impairments but potentially less severe than those reported for the forelimb (Kubota 1996; Schieber and Poliakov 1998; Brochier et al. 1999).

MATERIALS AND METHODS

Methods for the behavioral task, surgical procedure, cortical chamber implant, surgical follow up, and recording are found in Chapter 2. Methods unique to this study are given below.

Identification of the M1 hindlimb area

Stimulus triggered averages were collected with spatial resolution of 1 x 1mm from the left cortices of three awake, behaving rhesus macaque monkeys. Sites yielding hindlimb muscle facilitation in stimulus triggered averages were used to identify physiologically the M1 hindlimb area for each monkey.

Experimental sessions

Reversible inactivation of the hindlimb representation of M1 was produced by intracortical injection of the GABA-A agonist, muscimol. Muscimol was injected with a 10 μL Hamilton syringe connected by polyethylene tubing to a cannula mounted on an X-Y positioner previously used for the cortical mapping. A 25 gauge cannula with a 45º beveled tip was lowered through the dura to a depth of 2mm. Once the cannula was positioned it was immobilized with a small set screw on the microdrive set-up. Cortical inactivation was achieved by injecting 1.0 μL of muscimol (5 μg/μL) into nine sites covering the complete hindlimb representation of M1 (Figures 1 & 2). The extent of spread of muscimol from an injection site is always an important issue. Martin reported the spread as a sphere approximately 1.7 mm in radius based on autoradiographic data in the rat and a muscimol concentration of 1 μg/μL. Schieber and Poliakov using a higher concentration (5 μg/μL) in rhesus macaque estimated a similar spread (3mm diameter) of muscimol in the motor cortex (Martin 1991; Schieber and Poliakov 1998).

Behavioral Evaluation

Performance on the push-pull task, bipedal and quadrapedal walking, as well as normal movement around the cage were recorded with a video camera before and after each session of injections. The Gait Assessment Rating Scale (GARS) was adapted to clinically evaluate the deficits seen following muscimol injections and is referred to as the adapted Gait Assessment Rating Scale (aGARS) in Table 1. Changes in use and functions of the affected limb were identified, evaluated and ranked according the aGARS. Frame by frame analysis of the step cycle along with clinical evaluation of the deficits seen was also performed.

RESULTS

Efficacy of muscimol injections

To confirm the efficacy of the muscimol injections, unit recordings were performed at the same cortical site 1mm away from the injection site both before administering the muscimol injections and after all the injections were finished. Figure 3 shows the neural activity at two tests sites located 1mm away from two of the injection sites. At both sites, the muscimol injections nearly eliminated all neuronal activity.

Muscimol effect on performance of a skilled task

The two initial injections of muscimol into the M1 hindlimb representation had little to no effect on the monkey's ability to perform the push-pull task. With injection at the third and fourth sites, the monkey began to lose the ability to grip the manipulandum with its foot during the pull phase of the push-pull task. At this point, the monkey was still able to push the manipulandum using its proximal muscles during the push phase of the task. By the injection into the sixth site, all three of the monkeys were no longer able to perform the push-pull task, often times letting their affected leg dangle out in front of them.

Muscimol effect on free movement

Upon completion of the injections the monkeys were observed during bipedal and quadrapedal walking, and in normal free movement about their cage. During bipedal and quadrapedal locomotion, the monkeys were allowed to walk toward food rewards placed on the floor. Locomotion was guided using a pole and collar system. After injections of muscimol, the monkeys dragged their affected leg over the floor. There was also prominent foot drop typical of

nerve injury, stroke, or neuropathy evident in Figures 4 and 5. This caused the monkey's foot to go into an extended position with the dorsal surface of the foot in contact with the floor. To compensate the limb was flexed at the hip and knee and the limb overall lifted higher than normal. The areas that were most affected were the intrinsic foot muscles and the ankle muscles controlling the foot. Less affected were the more proximal muscles. Upon observation of free movement about the cage, the same deficits were clear. When climbing, the monkeys had little to no control of the intrinsic foot muscles, which prevented gripping with the affected hindlimb. They also had awkward control over their ankle muscles causing them to make a number of missteps when climbing along a narrow perch. To compensate they relied heavily on their unaffected three limbs to hang and move about the cage. Relatively good control of proximal hip muscles, evident in the cage, allowed effective use of the impaired leg for standing as long as refined movement was not required. The deficits seen during the skilled task, bipedal and quadrapedal locomotion, and free movement about their cage were rated on the aGARS in Table 1. Monkey L was unable to do the pole walking behavioral assessment and was evaluated on the ability to perform the skilled task, and free movement about the cage. All three monkeys showed marked deficits on the aGARS (Monkey M from 0 to 15 post-injection; Monkey L from 1 to 13 post-injection; Monkey E from 4 to 23 post-injection.

The monkeys recovered fully from the muscimol injections within 24-36 hours post injection. Following recovery, they were able to use their hindlimb to grip and climb about their cage showing no lasting deficits from inactivation of cortical cells.

DISCUSSION

In awake monkeys performing a behavioral task, as well as freely moving monkeys, muscimol injection into the hindlimb area of the primary motor cortex resulted in severe impairments of fine motor control of the ankle and foot. During locomotion, severe foot drop was evident typical of that in patients with neuropathies or stroke affecting the lower limb. While robust deficits were seen in the intrinsic foot muscles and ankle muscles, the hip and to some extent the knee muscles were less affected by inactivation of cortical neurons in M1. When trying to grip or climb using the intrinsic foot muscles of the affected limbs the monkeys were unable to make accurate movements and were unable to maintain grip for stabilization purposes. However, when not moving about the cage, monkeys were able to use their proximal anti-gravity muscles to stand upright, showing very little difficulty maintaining balance. What this suggests is that much like forelimb M1, hindlimb M1 plays a major role in movements of distal muscles (ankle and digits), but has less of an effect on the proximal hip and knee muscles used for more stereotyped movement and antigravity stabilization.

Despite the significantly weaker output effects observed with spike and stimulus triggered averaging of EMG activity, muscimol inactivation of hindlimb M1 cortex led to impairments that seemed equally as severe as those reported for inactivation of forelimb M1 cortex. Muscimol injections into forelimb M1 had pronounced effects on the individuated finger movements needed to perform a skilled task (Schieber and Poliakov 1998), and as a result, in freely behaving monkeys, compensatory mechanisms involving the unaffected limb become evident (Kubota 1996). We observed the same phenomenon following muscimol injection into hindlimb M1. The injections had pronounced effects on the skilled intrinsic foot muscles needed to perform a skilled push-pull task, and when allowed to move around freely the monkeys

demonstrated heavy compensation by the unaffected limb. By its nature, the strength of output effects with spike and stimulus triggered averaging is heavily dependent on the synaptic linkage with monosynaptic effects producing the strongest effects. The weaker postspike and poststimulus effects from hindlimb M1 reported in this study compared to the forelimb most likely reflect a less direct synaptic linkage with fewer monosynaptic linkages (Jankowska et al. 1975). However, the fact that muscimol had equally severe effects on the hindlimb and forelimb demonstrates that the functional importance of M1 neurons to voluntary movement is not dependent on the directness of the synaptic linkage. The natural output from motor cortex can exert effects through oligosynaptic linkages that are just as powerful as those through monosynaptic linkages.

Table 1. Adapted Gait Assessment Rating Scale (aGARS) for evaluation of muscimol injections on hindlimb M1

ADAPTED GAIT ASSESSMENT RATING SCALE (aGARS)

1. **Walking Categories**
    a. Variability - a measure of inconsistency and arrhythmicity in steps and arm movements
        0 = Fluid and predictably paced limb movements.
        1 = Occasional interruptions (changes in velocity) approximately < 25% of the time.
        2 = Unpredictability of rhythm of movement > 25% of the time.
        3 = Random timing of limb movements.
    b. Guardedness - hesitancy, slowness, diminished propulsion and lack of commitment stepping and arm swing.
        0 = Good forward momentum and lack of apprehension in propulsion.
        1 = Slight apprehension but still good arm - leg coordination.
        2 = Moderate apprehension and some moderate loss of smooth reciprocation.
        3 = Great tentativeness in stepping and loss of smooth reciprocation.
    c. Weaving - an irregular line of progression.
        0 = Straight line of progress on frontal view.
        1 = Single deviation from straight line of progression.
        2 = Two to three deviations from straight line of progression.
        3 = Four or more deviations from straight line of progression.

2. **Lower Extremity Categories**
    a. Percent of time in swing - loss of percentage in the gait cycle constituted by the swing phase.
        0 = Approximately 3:2 ratio of stance:swing.
        1 = 1:1 or less ratio of stance:swing.
        2 = Markedly prolonged stance phase but with some obvious swing time remaining.
        3 = Barely perceptible portion of cycle spent in swing phase.
    b. Foot Contact - the degree to which the heel strikes the ground before the forefoot.
        0 = Very obvious angle of impact of heel on ground.
        1 = Barely visible contact of heel before forefoot.
        2 = Entire foot lands on ground.
        3 = Anterior aspect of foot strikes ground before heel.

3. **Behavioral Specific Movement**
    a. Degree of compensation
        0 = Equal use of both limbs for gripping and moving about the cage.
        1 = Use of unaffected limb to stabilize standing with slight impairment in ability to grip in unaffected limb when moving about the cage.
        2 = Ability to grip with unaffected limb completely impaired, but maintains ability to stand using affected limb for support when moving about the cage.
        3 = Total absence of use of unaffected limb in standing or moving about the cage.

b. Movement hesitation - latency between presentation of food reward and start of movement toward the reward.
   0 = No hesitation in moving toward a food reward.
   1 = Slight hesitation in moving toward a food reward.
   2 = Long hesitation or lack of movement toward a food reward.
c. Performance of behavioral task
   0 = No impairment in ability to perform a behavioral task.
   1 = Delay in ability to perform a behavioral task.
   2 = Inability to perform a behavioral task.
d. Staggering - sudden and unexpected laterally directed partial losses of balance when standing on a perch.
   0 = No losses of balance to side.
   1 = One to two misstep to the side in 30sec period.
   2 = Three to five missteps to the side in a 30sec period.
   3 = Five or more missteps to the side in a 30sec period.

Table 2. aGARS scores pre-injection and post-injection for three monkeys.

	Monkey M		**Monkey L**		**Monkey E**	
	Pre-Injection	Post-Injection	Pre-Injection	Post-Injection	Pre-Injection	Post-Injection
1a	0	1	-	-	1	2
1b	0	1	-	-	0	3
1c	0	2	-	-	0	2
2a	0	1	-	-	1	3
2b	0	3	0	3	2	3
3a	0	2	0	3	0	3
3b	0	0	1	2	0	2
3c	0	2	0	2	0	2
3d	0	3	0	3	0	3
Total	0	15	1	13	4	23

Figure 1. 3D reconstruction of Monkey M's MRI showing a superimposed 30mm diameter chamber and the sites and spread of muscimol injections. The hindlimb representation of M1 confirmed using stimulus triggered averaging is shown with the closed black circles. Cortical inactivation was achieved by injecting 1.0 μL of muscimol (5 μg/μL) into nine sites covering the complete hindlimb representation of M1. The sites of injection of the GABA-A agonist, muscimol and its relative spread (assuming a 3mm diameter spread) are shown with the yellow circles. The red arrows point to the two test sites used to test the efficacy of the muscimol injections.

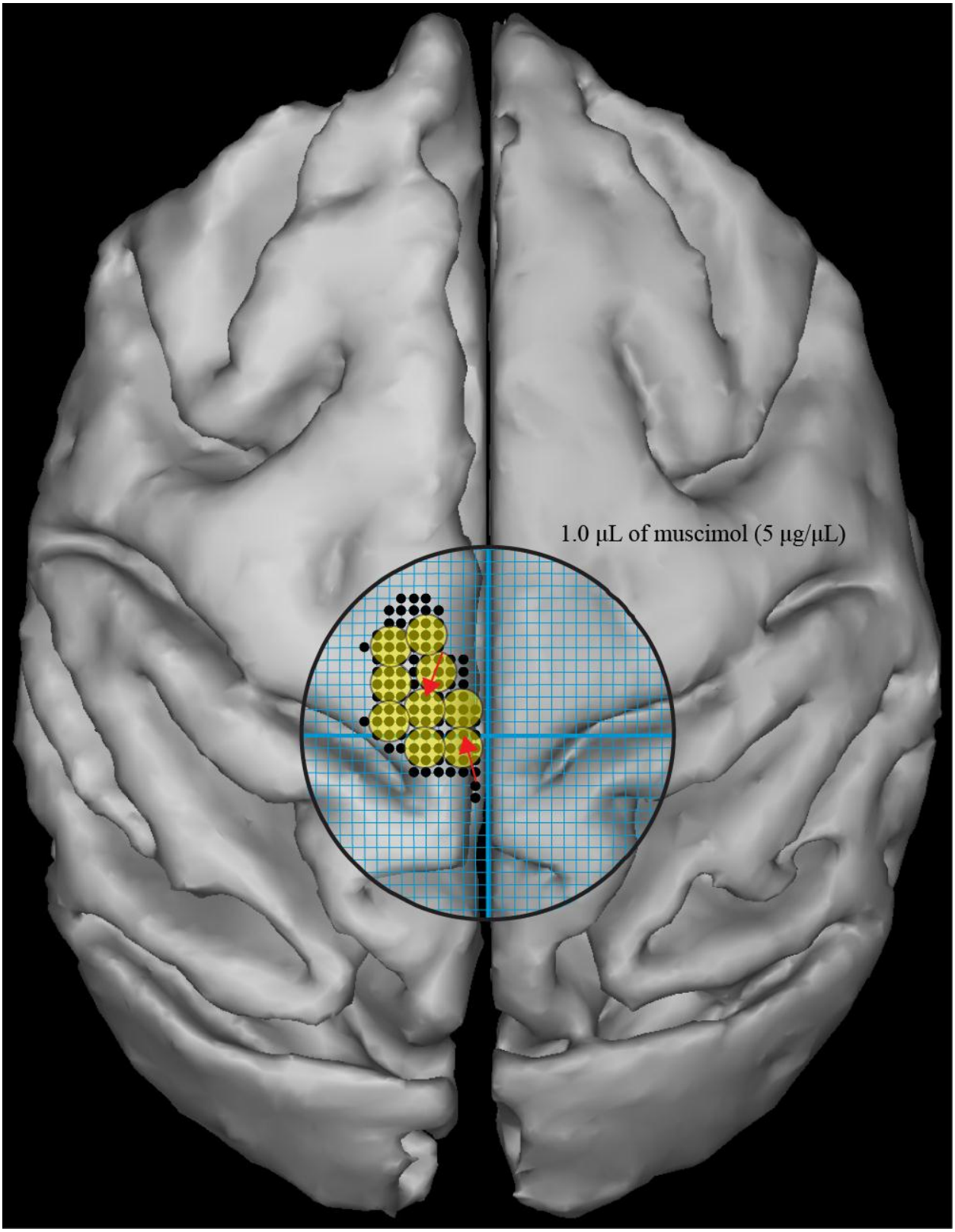
1.0 µL of muscimol (5 µg/µL)

Figure 2. 3D reconstruction of Monkey L's MRI showing a superimposed 30mm diameter chamber and the sites and spread of muscimol injections. The hindlimb representation of M1 confirmed using stimulus triggered averaging is shown with the closed black circles. Cortical inactivation was achieved by injecting 1.0 μL of muscimol (5 μg/μL) into nine sites covering the complete hindlimb representation of M1. The sites of injection of the GABA-A agonist, muscimol and its relative spread (assuming a 3mm diameter spread) are shown with the yellow circles. The red arrows point to the two test sites used to test the efficacy of the muscimol injections.

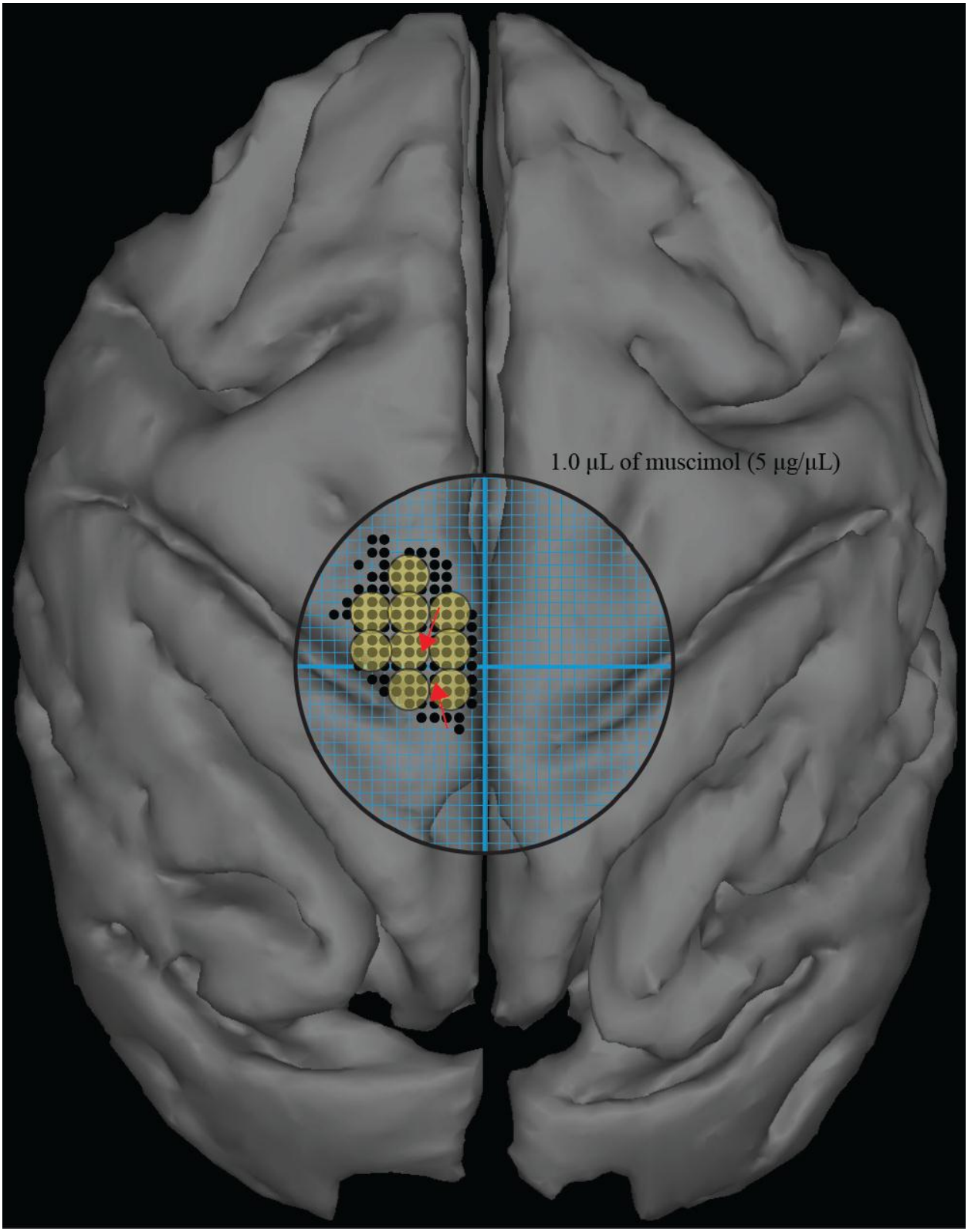
1.0 µL of muscimol (5 µg/µL)

Figure 3. Unit recording from layer 5 of M1 at two sites 1mm from sites of muscimol injection. The left panel shows the activity of the two sites before the administration of muscimol. The right panel shows the activity of the same two sites following administration of muscimol. The two test sites show that neural activity was virtually eliminated following muscimol injection. Cortical inactivation was achieved by injecting 1.0 μL of muscimol (5 μg/μL) into nine sites covering the complete hindlimb representation of M1.

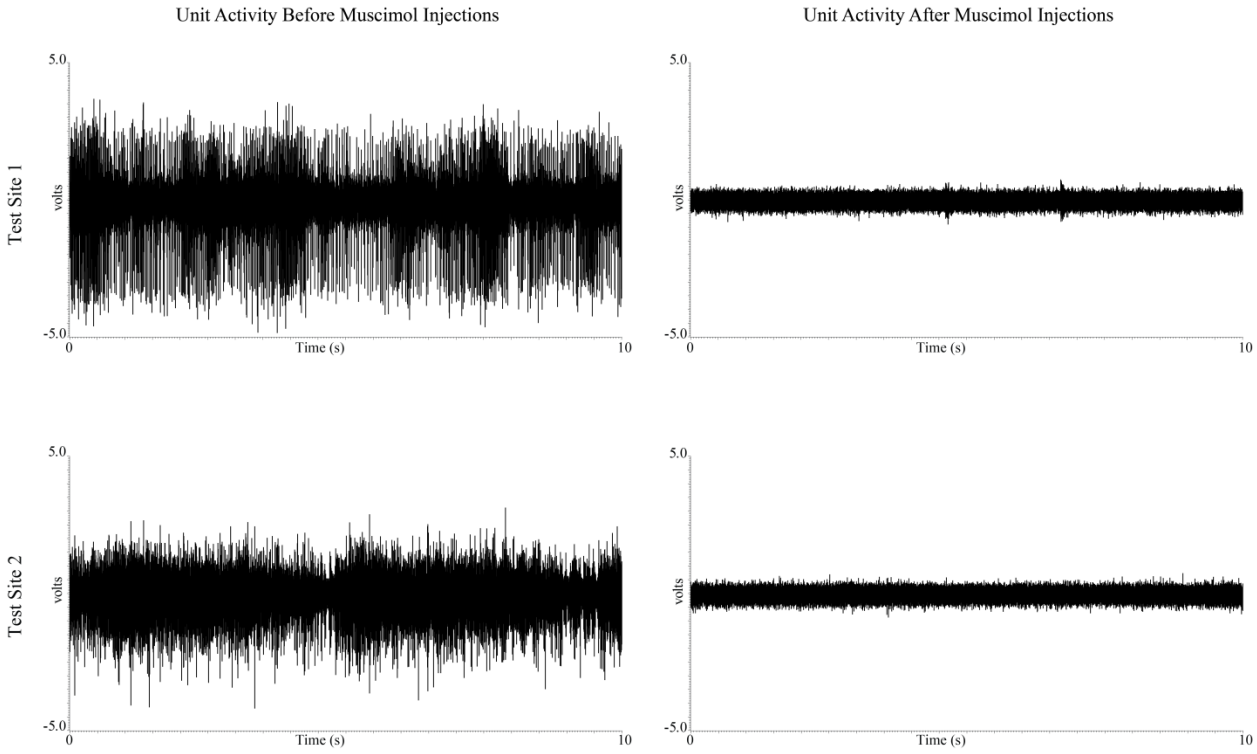
Unit Activity Before Muscimol Injections
Unit Activity After Muscimol Injections
Test Site 1
Test Site 2
5.0
-5.0
volts
0
Time (s)
10

Figure 4. Breakdown of stepping for Monkey M pre-injection and post-injection. Panel A shows a single stepping cycle of Monkey M before injections of muscimol into hindlimb M1. Panel 1A shows the initial stance phase of the stepping cycle. Monkey M then pushes off with the anterior aspect of his foot in 2A. During the swing phase of stepping cycle in 3A, Monkey M raises the anterior aspect of his foot and extends his knee to prepare for contact. In 4A, Monkey M makes contact with the posterior aspect of his foot before finishing a single step cycle in 5A. Panel B shows a single stepping cycle of Monkey M after injection of muscimol into hindlimb M1. To compensate for decreased muscle control, Monkey M flexes the hip and knee to stabilize himself during the stance phase in 1B. Decreased control of the intrinsic foot and ankle muscles makes pushing off difficult in 2B and 3B. To compensate Monkey M flexes the knee to lift the foot off the ground. The anterior aspect of the foot is the first to strike the ground in 4B, and without fine control, the foot slips backwards in 5B.

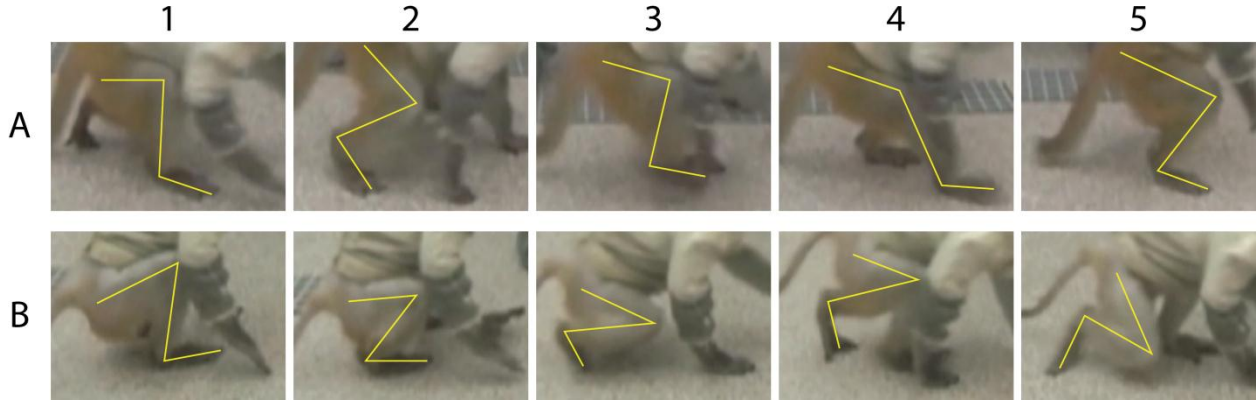
1
2
3
4
5
A
B

Figure 5. Breakdown of stepping for Monkey E pre-injection and post-injection. Panel A shows a single stepping cycle of Monkey E before injections of muscimol into hindlimb M1. Panel 1A shows the initial stance phase of the stepping cycle. Monkey E then pushes off with the anterior aspect of his foot in 2A. During the swing phase of stepping cycle in 3A, Monkey E raises the anterior aspect of his foot and extends his knee to prepare for contact. In 4A, Monkey E makes contact with the anterior aspect of his foot before finishing a single step cycle in 5A. Panel B shows a single stepping cycle of Monkey E after injection of muscimol into hindlimb M1. With no control over the distal muscles of the leg Monkey E is unable to support a single leg stance with the affected leg during the stepping cycle. Decreased control of the intrinsic foot and ankle muscles makes pushing off difficult in 2B and 3B. Monkey E is forced to drag the affected limb and use the proximal muscles to swing it forward while hopping with the unaffected leg.

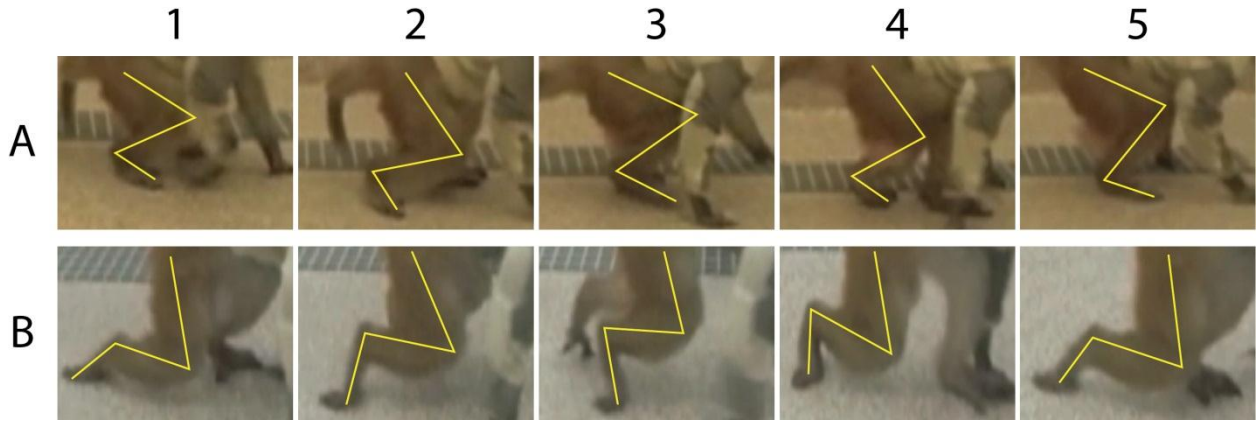
1
2
3
4
5
A
B

CHAPTER 5

CONCLUSION

A detailed knowledge of the corticospinal tract is important because "its structure and organization serve as a guide to understanding what the output from the cortex means for the motor apparatus of the limb (Porter and Lemon 1993)." To this end we set out to better characterize the structure and organization of the hindlimb portion of the primary motor cortex (M1). We employed three unique methods to achieve this aim. To evaluate the basic organizational units of the motor cortex, pyramidal corticospinal cells, we used spike triggered averaging of EMG activity. To elucidate the role that ipsilateral primary motor cortex plays in hindlimb movements, we used stimulus triggered averaging, which allows the output effects of small populations of corticospinal cells to be identified and quantified. Finally to test the role the primary cortex plays in skilled and stereotyped movement, we selectively inactivated neurons in the primary motor cortex with the GABA-A agonist, muscimol.

Evidence of monosynaptic connections demonstrated by intracellular recordings and anatomical labeling led us to attempt to characterize these connections using spike triggered averaging. Spike triggered averaging has the potential to reveal the synaptic linkages between the trigger cell and motoneurons of the recorded muscles. We were successful in detecting postspike effects in EMG records of hindlimb muscles. Comparing these effects to previous work from our laboratory on forelimb M1 revealed clear differences between the hindlimb and forelimb representations. Unlike in the forelimb, the magnitudes of hindlimb PSpF effects were much weaker and did not increase when going from proximal to distal muscles. The more stereotyped movements of the hindlimb correlates with a much smaller muscle field size for hindlimb cells compared to forelimb cells. With less direct synaptic linkages and much more prominent synchronous effects, we have demonstrated fundamental differences in the properties of output from hindlimb M1 compared to forelimb M1.

With approximately 10% of corticospinal axons descending anatomically to make connections to motoneurons in the spinal cord and growing evidence suggesting the important role of the ipsilateral primary motor cortex in recovery from injury, we wanted to study the cortical output effects and their role in normal control of movement. A cortical chamber mounted along the superior sagittal sinus provided an opportunity to evaluate both the contralateral and ipsilateral cortices in an awake monkey. Using stimulus triggered averaging we were able to collect definitive data on the properties (sign, strength, latency, and distribution) of ipsilaterally descending corticospinal neurons and compare them with contralaterally descending corticospinal neurons. We were able to detect clear effects in ipsilateral muscles using stimulus triggered averaging. These effects were weaker, but shared similar properties to their contralateral counterparts. Although the average latency of effects from ipsilateral cortex was slightly longer than contralateral cortex, it is particularly significant that the shortest latency effects were as short as those from contralateral cortex. The simplest explanation of this result is that ipsilateral cortex has a connection to motoneurons that is as direct as the connection from contralateral cortex. We also found that the ipsilateral representation was not located in the mirror image position of the contralateral representation. Rather the ipsilateral representation was present in a largely non-overlapping region of cortex at the periphery of the contralateral representation. Given the brain's plasticity, these functional connections might be exploited and possibly expand their representation following a lesion to the contralateral cortex to aid in recovery of lost function.

Lastly, we wanted to evaluate the effect of selectively and reversibly inactivating the hindlimb M1 representation. Inactivation was accomplished using a series of nine muscimol injections done during the same test session. Deficits in the distal muscles were clearly evident

and the monkeys lost the ability to perform any skilled task with the affected limb. In addition, the inability to grip and stabilize themselves with the affected foot led to severe deficits not only in performance of a skilled task, but also in bipedal and quadrapedal locomotion, and their ability to freely move about their environment. Our results demonstrate the importance of hindlimb M1 in the execution of skilled movement of the ankle and foot, as well as its importance in the movement repertoire of the primate.

The three studies summarized above provide a clear picture of the importance of the primary motor cortex to hindlimb movements as well as clear differences from forelimb cortex. The relatively sparse and weak postspike effects are in contrast to forelimb M1 and suggest fundamental differences in the synaptic linkage to motoneurons. Although evidence exists from intracellular recording studies of monosynaptic connections to motoneurons from hindlimb cortex, our results from spike triggered averaging suggest a very modest to non-existent monosynaptic linkage. Does this mean that the hindlimb cortex is less important for the control of movement than forelimb cortex? We tested this using muscimol injections to inactivate hindlimb cortex. Without corticospinal output, highly skilled hindlimb tasks as well as locomotion are severely impacted. The deficits appear to be as severe as those reported for muscimol injections into forelimb M1 cortex. This result emphasizes the importance and robustness of non-monosynaptic inputs for natural performance of movements. Although our methods did not focus on optimizing sensitivity, no clear deficits were observed in the ipsilateral limb from muscimol injections. However, using stimulus triggered averaging of EMG activity we were able to identify and quantify for the first time, clear effects from hindlimb M1 cortex on motoneurons of muscles at all joints of the ipsilateral limb. This ipsilateral linkage is spared

following injury to the opposite hemisphere and may undergo plasticity to aid in recovery of motor function.

REFERENCES

Aizawa, H., H. Mushiake, et al. (1990). "An output zone of the monkey primary motor cortex specialized for bilateral hand movement." Exp Brain Res **82**(1): 219-221.

Asanuma, H., J. Fernandez, et al. (1974). "Characteristics of projections from the nucleus ventralis lateralis to the motor cortex in the cats: an anatomical and physiological study." Exp Brain Res **20**(4): 315-330.

Asanuma, H. and H. Sakata (1967). "Functional Organization of a Cortical Efferent System Examined with Focal Depth Stimulation in Cats." J Neurophysiol **30**(1): 35-&.

Bortoff, G. A. (1990). Termination of corticospinal efferents within the cervical cord fo New World primates. Society of Neuroscience Abstract.

Boudrias, M. H., A. Belhaj-Saif, et al. (2006). "Contrasting properties of motor output from the supplementary motor area and primary motor cortex in rhesus macaques." Cereb Cortex **16**(5): 632-638.

Broca, P. M. (1999). "[The discovery of cerebral localization]." Rev Prat **49**(16): 1725-1727.

Brochier, T., M. J. Boudreau, et al. (1999). "The effects of muscimol inactivation of small regions of motor and somatosensory cortex on independent finger movements and force control in the precision grip." Exp Brain Res **128**(1-2): 31-40.

Brus-Ramer, M., J. B. Carmel, et al. (2007). "Electrical stimulation of spared corticospinal axons augments connections with ipsilateral spinal motor circuits after injury." J Neurosci **27**(50): 13793-13801.

Bucy, P. C., J. E. Keplinger, et al. (1964). "Destruction of the "Pyramidal Tract" in Man." J Neurosurg **21**: 285-298.

Buys, E. J., R. N. Lemon, et al. (1986). "Selective facilitation of different hand muscles by single corticospinal neurones in the conscious monkey." J Physiol **381**: 529-549.

Campbell, A. W. (1905). Histological studies on the localisation of cerebral function. Cambridge,, University Press.

Caramia, M. D., M. G. Palmieri, et al. (2000). "Ipsilateral activation of the unaffected motor cortex in patients with hemiparetic stroke." Clin Neurophysiol **111**(11): 1990-1996.

Chen, R., C. Gerloff, et al. (1997). "Involvement of the ipsilateral motor cortex in finger movements of different complexities." Ann Neurol **41**(2): 247-254.

Cheney, P. D., A. Belhaj-Saif, et al. (2004). Principles of corticospinal system organization and function. Handbook of Clinical Neurophysiology. A. Eisen. New York, NY, Elsevier. **Vol. 4:** 59-96.

Cheney, P. D. and E. E. Fetz (1985). "Comparable patterns of muscle facilitation evoked by individual corticomotoneuronal (CM) cells and by single intracortical microstimuli in primates: evidence for functional groups of CM cells." J Neurophysiol **53**(3): 786-804.

Chollet, F., V. DiPiero, et al. (1991). "The functional anatomy of motor recovery after stroke in humans: a study with positron emission tomography." Ann Neurol **29**(1): 63-71.

Clough, J. F., D. Kernell, et al. (1968). "The distribution of monosynaptic excitation from the pyramidal tract and from primary spindle afferents to motoneurones of the baboon's hand and forearm." J Physiol **198**(1): 145-166.

Colebatch, J. G. and S. C. Gandevia (1989). "The distribution of muscular weakness in upper motor neuron lesions affecting the arm." Brain **112 (Pt 3)**: 749-763.

Coulter, J. D. and E. G. Jones (1977). "Differential distribution of corticospinal projections from individual cytoarchitectonic fields in the monkey." Brain Res **129**(2): 335-340.
Cramer, S. C., S. P. Finklestein, et al. (1999). "Activation of distinct motor cortex regions during ipsilateral and contralateral finger movements." J Neurophysiol **81**(1): 383-387.
Davidson, A. G., R. O'Dell, et al. (2007). "Comparing effects in spike-triggered averages of rectified EMG across different behaviors." J Neurosci Methods **163**(2): 283-294.
DeFelipe, J., M. Conley, et al. (1986). "Long-range focal collateralization of axons arising from corticocortical cells in monkey sensory-motor cortex." J Neurosci **6**(12): 3749-3766.
Dum, R. P. and P. L. Strick (1991). "The origin of corticospinal projections from the premotor areas in the frontal lobe." J Neurosci **11**(3): 667-689.
Dum, R. P. and P. L. Strick (1996). "Spinal cord terminations of the medial wall motor areas in macaque monkeys." J Neurosci **16**(20): 6513-6525.
Evarts, E. V. (1964). "Temporal Patterns of Discharge of Pyramidal Tract Neurons during Sleep and Waking in the Monkey." J Neurophysiol **27**: 152-171.
Evarts, E. V. (1966). "Pyramidal tract activity associated with a conditioned hand movement in the monkey." J Neurophysiol **29**(6): 1011-1027.
Eyre, J. A., S. Miller, et al. (1991). "Constancy of central conduction delays during development in man: investigation of motor and somatosensory pathways." J Physiol **434**: 441-452.
Ferrier, D. (1874). "On the Localisation of the Functions of the Brain." Br Med J **2**(729): 766-767.
Fetz, E. E. (1990). Neural network models of the primate motor system. Advanced neural computers. R. Eckmiller. Amsterdam, Elsevier**:** 43-50.
Fetz, E. E. and P. D. Cheney (1980). "Postspike facilitation of forelimb muscle activity by primate corticomotoneuronal cells." J Neurophysiol **44**(4): 751-772.
Feydy, A., R. Carlier, et al. (2002). "Longitudinal study of motor recovery after stroke: recruitment and focusing of brain activation." Stroke **33**(6): 1610-1617.
Fisher, C. M. (1992). "Concerning the mechanism of recovery in stroke hemiplegia." Can J Neurol Sci **19**(1): 57-63.
Fritsch, G. and E. Hitzig (2009). "Electric excitability of the cerebrum (Uber die elektrische Erregbarkeit des Grosshirns)." Epilepsy Behav **15**(2): 123-130.
Goldring, S. and R. Ratcheson (1972). "Human motor cortex: sensory input data from single neuron recordings." Science **175**(29): 1493-1495.
Griffin, D. M., H. M. Hudson, et al. (2009). "Stability of output effects from motor cortex to forelimb muscles in primates." J Neurosci **29**(6): 1915-1927.
Griffin, D. M., H. M. Hudson, et al. (2008). "Do corticomotoneuronal cells predict target muscle EMG activity?" J Neurophysiol **99**(3): 1169-1986.
Heffner, R. S. and R. B. Masterton (1983). "The role of the corticospinal tract in the evolution of human digital dexterity." Brain Behav Evol **23**(3-4): 165-183.
Hendry, S. H., H. D. Schwark, et al. (1987). "Numbers and proportions of GABA-immunoreactive neurons in different areas of monkey cerebral cortex." J Neurosci **7**(5): 1503-1519.
Hudson, H. M., D. M. griffin, et al. (2011). "Representation of hindlimb muscles in primary motor cortex of rhesus macaques." Society for Neurosciene **Annual Meeting** 591.519/MM527.
Hudson, H. M., D. M. Griffin, et al. (2010). "Methods for chronic recording of EMG activity from large numbers of hindlimb muscles in awake rhesus macaques." J Neurosci Methods **189**(2): 153-161.
Hudson, H. M., D. M. Griffin, et al. (2010). Muscle synergies represented in the output of hindlimb M1 in comparison to forelimb M1 of the rhesus macaque. Program No. 494.25/HHH15_2010 Neuroscience Meeting Planner. San Diego, CA, Society for Neuroscience. **494.25/HHH15:** Online.

Huntley, G. W. and E. G. Jones (1991). "Relationship of intrinsic connections to forelimb movement representations in monkey motor cortex: a correlative anatomic and physiological study." J Neurophysiol **66**(2): 390-413.
Hutchins, K. D., A. M. Martino, et al. (1988). "Corticospinal projections from the medial wall of the hemisphere." Exp Brain Res **71**(3): 667-672.
Jackson, J. H. (1873). "On the Anatomical Investigation of Epilepsy and Epileptiform Convulsions." Br Med J **1**(645): 531-533.
Jankowska, E., Y. Padel, et al. (1975). "Projections of pyramidal tract cells to alpha-motoneurones innervating hind-limb muscles in the monkey." J Physiol **249**(3): 637-667.
Jankowska, E., Y. Padel, et al. (1976). "Disynaptic inhibition of spinal motoneurones from the motor cortex in the monkey." J Physiol **258**(2): 467-487.
Jones, E. G. (1984). Laminar distribution of cortical efferent cells. Cerebral cortex. A. Peters and E. G. Jones. Plenum, New York. **Vol. 1:** 521-553.
Kasser, R. J. and P. D. Cheney (1985). "Characteristics of corticomotoneuronal postspike facilitation and reciprocal suppression of EMG activity in the monkey." J Neurophysiol **53**(4): 959-978.
Kubota, K. (1996). "Motor cortical muscimol injection disrupts forelimb movement in freely moving monkeys." Neuroreport **7**(14): 2379-2384.
Kuypers, H. G. (1962). "Corticospinal connections: postnatal development in the rhesus monkey." Science **138**: 678-680.
Kuypers, H. G. and J. Brinkman (1970). "Precentral projections to different parts of the spinal intermediate zone in therhesus monkey." Brain Res **24**(1): 29-48.
Lacroix, S., L. A. Havton, et al. (2004). "Bilateral corticospinal projections arise from each motor cortex in the macaque monkey: a quantitative study." J Comp Neurol **473**(2): 147-161.
Lawrence, D. G., R. Porter, et al. (1985). "Corticomotoneuronal synapses in the monkey: light microscopic localization upon motoneurons of intrinsic muscles of the hand." J Comp Neurol **232**(4): 499-510.
Lemon, R. N. and J. Griffiths (2005). "Comparing the function of the corticospinal system in different species: organizational differences for motor specialization?" Muscle Nerve **32**(3): 261-279.
Lemon, R. N., J. A. Hanby, et al. (1976). "Relationship between the activity of precentral neurones during active and passive movements in conscious monkeys." Proc R Soc Lond B Biol Sci **194**(1116): 341-373.
Lemon, R. N., G. W. Mantel, et al. (1986). "Corticospinal facilitation of hand muscles during voluntary movement in the conscious monkey." J Physiol **381**: 497-527.
Lewis, R. and G. S. Brindley (1965). "The extrapyramidal cortical motor map." Brain **88**(2): 397-406.
Leyton, A. S. F. and C. S. Sherrington (1917). "Observations on the excitable cortex of the chimpanzee, orangutan, and gorilla." Experimental Physiology **11**: 135-222.
Martin, J. H. (1991). "Autoradiographic estimation of the extent of reversible inactivation produced by microinjection of lidocaine and muscimol in the rat." Neurosci Lett **127**(2): 160-164.
Matsumura, M., T. Sawaguchi, et al. (1992). "GABAergic inhibition of neuronal activity in the primate motor and premotor cortex during voluntary movement." J Neurophysiol **68**(3): 692-702.
Matsumura, M., T. Sawaguchi, et al. (1991). "Behavioral deficits induced by local injection of bicuculline and muscimol into the primate motor and premotor cortex." J Neurophysiol **65**(6): 1542-1553.
Matsunami, K. and I. Hamada (1978). "Precentral neuron activity associated with ipsilateral forelimb movements in monkeys." J Physiol (Paris) **74**(3): 319-322.
McKiernan, B. J., J. K. Marcario, et al. (1998). "Corticomotoneuronal postspike effects in shoulder, elbow, wrist, digit, and intrinsic hand muscles during a reach and prehension task." J Neurophysiol **80**(4): 1961-1980.

Mountcastle, V. B. (1978). An organizing principle for cerebral function: the unit model and the distributed system. The mindful brain. G. Edelman and V. B. Mountcastle. Cambridge, Massachusetts, MIT Press**:** 7-50.
Park, M. C., A. Belhaj-Saif, et al. (2000). "Chronic recording of EMG activity from large numbers of forelimb muscles in awake macaque monkeys." J Neurosci Methods **96**(2): 153-160.
Park, M. C., A. Belhaj-Saif, et al. (2001). "Consistent features in the forelimb representation of primary motor cortex in rhesus macaques." J Neurosci **21**(8): 2784-2792.
Penfield, W. and E. Boldrey (1937). "Somatic motor and sensory representation in the cerebral cortex of man as studied by electrical stimulation." Brain **60**: 389-443.
Penfield, W. and T. Rasmussen (1950). The cerebral cortex of man; a clinical study of localization of function. New York,, Macmillan.
Phillips, C. G. and R. Porter (1977). "Corticospinal neurones. Their role in movement." Monogr Physiol Soc(34): v-xii, 1-450.
Porter, R. and R. Lemon (1993). Corticospinal function and vountary movement, Clarendon Press.
Ramon y Cajal, S. (1911). "Histologie du systeme nerveux de l'Homme et des vertebres." Maloine, Paris.
Rosenzweig, E. S., J. H. Brock, et al. (2009). "Extensive spinal decussation and bilateral termination of cervical corticospinal projections in rhesus monkeys." J Comp Neurol **513**(2): 151-163.
Schieber, M. H. and A. V. Poliakov (1998). "Partial inactivation of the primary motor cortex hand area: effects on individuated finger movements." J Neurosci **18**(21): 9038-9054.
Schieber, M. H. and G. Rivlis (2005). "A spectrum from pure post-spike effects to synchrony effects in spike-triggered averages of electromyographic activity during skilled finger movements." J Neurophysiol **94**(5): 3325-3341.
Soteropoulos, D. S., S. A. Edgley, et al. (2011). "Lack of evidence for direct corticospinal contributions to control of the ipsilateral forelimb in monkey." J Neurosci **31**(31): 11208-11219.
Tanji, J., K. Okano, et al. (1988). "Neuronal activity in cortical motor areas related to ipsilateral, contralateral, and bilateral digit movements of the monkey." J Neurophysiol **60**(1): 325-343.
Tehovnik, E. J., A. S. Tolias, et al. (2006). "Direct and indirect activation of cortical neurons by electrical microstimulation." J Neurophysiol **96**(2): 512-521.
Ward, N. S. (2005). "Mechanisms underlying recovery of motor function after stroke." Postgrad Med J **81**(958): 510-514.
Yarosh, C. A., D. S. Hoffman, et al. (2004). "Deficits in movements of the wrist ipsilateral to a stroke in hemiparetic subjects." J Neurophysiol **92**(6): 3276-3285.